Critical Evaluation of the Pitfalls in the PVT Behavior Arising from Hard-Sphere Chain and Association Theories

BY

Yousef A. Al-Sunni

A Thesis Presented to the

DEANSHIP OF GRADUATE STUDIES

KING FAHD UNIVERSITY OF PETROLEUM & MINERALS

DHAHRAN, SAUDI ARABIA

In Partial Fulfillment of the

Requirements for the Degree of

MASTER OF SCIENCE

In

Chemical Engineering

April 2016

KING FAHD UNIVERSITY OF PETROLEUM & MINERALS

DHAHRAN- 31261, SAUDI ARABIA

DEANSHIP OF GRADUATE STUDIES

This thesis, written by **Yousef A. Al-Sunni** under the direction his thesis advisor and approved by his thesis committee, has been presented and accepted by the Dean of Graduate Studies, in partial fulfillment of the requirements for the degree of **MASTER OF SCIENCE IN CHEMICAL ENGINEERING.**

Dr. Nayef M. Al-Saifi

(Advisor)

Dr. Mohammed Ba-Shammakh
Department Chairman

Dr. Nadhir A. H. Al-Baghli
(Member)

Dr. Salam A. Zummo
Dean of Graduate Studies

Dr. Housam Binous

(Member)

15/5/16

Date

DEDICATION

Dedicated to my dear parents,

To my sister,

and

To my family

ACKNOWLEDGEMENTS

I would like to express my sincere appreciation to my advisor Dr. Nayef Al-Saifi for the continuous support of my master's study for his patient, supportive, encouraging and immense knowledge. His guidance helped me in my research and writing of this thesis.

Besides my advisor, I would like to thank the rest of my thesis committee: Dr. Housam Binous and Dr. Nadhir Al-Baghli for their encouragement and support in this thesis.

I also want to give thanks to my friend and co-worker Mr. Mohammed Al-Khater for his support during the master's program.

I would like to thank my closest friend Mr. Nayef Jalkhaf for his moral support.

I am grateful to the King Fahd University of Petroleum & Minerals for offering me the master's program in chemical engineering.

TABLE OF CONTENTS

LIST OF TABLES

LIST OF FIGURES

NOMENCLATURE

A	Helmholtz free energy
AAD	average absolute deviation
B_n	n^{th} virial coefficient
d	effective hard sphere dimeter
g(d)	pair correlation function at contact
k	Boltzmann's constant
M	number of association sites
m	segment number
N_{Av}	Avogadro's number
P	pressure
R	ideal gas constant
T	temperature
T_R	reduced temperature
u^0	temperature independent square-well depth
V	volume
v^*	closed-packed molar volume of a segment
v^{00}	volume in a closed-packed arrangement
v_s	molar volume of a hard sphere segment
X^A	fraction of association sites A that are not bonded
Z	compressibility factor

Greek letters

Δ^{AB}	association strength
η_c	closest packing fraction
κ^{AB}	volume of interaction between association sites A and B
ρ^*	reduced density
ϵ^{AB}	association energy
σ	temperature independent diameter
η	packing fraction
ξ	packing fraction ratio
ρ	molar density
ϵ	Lennard-Jones intermolecular energy

Subscripts

DB	hard dumbbell
HD	hard dimer
HS	hard sphere

Superscripts

assoc	association
disp	dispersion
GFD	generalized Flory dimer theory
hs	hard sphere
res	residual

THESIS ABSTRACT

Name: Yousef Abdulrahman Al-Sunni

Title: Critical Evaluation of the Pitfalls in the PVT Behavior Arising from Hard-Sphere Chain and Association Theories

Degree: Master of Engineering Since

Major Field: Chemical Engineering

Date of Degree: April 2016

The hard-sphere chain theories have become a major component in most practical theory-based models. Although the hard-sphere chain theories have improved the accuracy in theory-based models, various problems have appeared such as high number of multiple volume roots and multiple phase separation regions. These problems are usually attributed to the added dispersion term. However, the influence of the mathematical formulations of the hard-spheres theories is always ignored.

In this thesis, the role of mathematical forms of the hard sphere chain theory (HSC), the first order thermodynamic perturbation theory (TPT1), the thermodynamic perturbation dimer theory (TPT-D) and the generalized Flory dimer theory (GFD) is critically investigated for the existence of the non-physical behavior that might arise in pressure-volume-temperature (PVT) behavior. Because the hard-sphere chain theories are based on hard sphere models, several hard sphere models are considered in this study including Carnahan and Starling (CS) (1969), Kolafa (Boublík, 1986), Khoshbarchi and Vera (1997), Yelash and Kraska (2001) and Rambaldi et al. (2006) hard-sphere models.

In order to accomplish the study of pressure-temperature-volume behavior, the arc-length continuation method was utilized to generate the bifurcation diagrams, which illustrate how the compressibility factor (Z) roots vary with temperature at a specified pressure. It was found that different mathematical forms of the hard sphere and the chain terms could influence the number of non-physical volume roots. The role of utilizing different dispersion terms with various hard sphere models was also studied and it was found that with specific combination of the hard sphere, chain, dispersion and association terms, one could obtain a PVT behavior that is free from the multiple non-physical volume roots and the artificial two-phase separation region.

Masters of Engineering Science Degree

King Fahd University of Petroleum & Minerals

Dhahran, Saudi Arabia

ملخص الرسالة

الاسم: يوسف بن عبدالرحمن السني

عنوان الرسالة: تقييم نقدي للعثرات في سلوك دالة الحجم -الناتجة عن حل المعادلات النظرية لحالة المادة- الناشئة عن نظريات سلسة الكرات المصمتة ونظرية الترابط

الدرجة: ماجستير في العلوم الهندسية

التخصص: هندسة كيميائية

التاريخ: إبريل 2016

نظريات سلسة الكرات المصمتة المتنافرة هي المكون الرئيس لكثير من المعادلات النظرية التي تصف حالة المادة، وعلى الرغم مما أضفت هذه النظرية من زيادة في الدقة عند استخدامها في الحسابات المتعلقة بحالات المادة إلا أنها أظهرت بعض المشاكل كالتنبؤ بوجود حالتين فزيائيتين مختلفتين لمركب واحد نقي عند نفس الضغط ودرجة الحرارة، وكذلك تعدد حلول المعادلة بالنسبة للحجم مما يتطلب اختبار جميع الحلول لمعرفة الحلول ذات الدلالة المنطقية، وقد ساد اعتقاد عند العلماء بأن هذه المشاكل ناتجة عن أحد حدود المعادلة النظرية والذي يطلق عليه حد التشتت بالرغم من وجود حدود أخرى في المعادلة قد لا تقل في تعقيدها الرياضي عن حد التشتت، فالمعادلة النظرية تحتوي على حد تنافر الكرات المصمتة وحد سلسة الكرات المصمتة وحد التشتت بالإضافة إلى حد الترابط الخاص ببعض المركبات الكيميائية المترابطة، لذلك قام هذا البحث بدراسة الحدود الأخرى في المعادلة لمعرفة مدى تأثيرها على نتائج المعادلة النظرية.

في هذه الرسالة تم دراسة أربعة من نظريات سلسة الكرات المصمتة: النظرية المبسطة لسلسة الكرات المصمتة ونظرية الاضطراب الأولى ونظرية الاضطراب الثانية ونظرية فلوري العامة، وبما أن حد سلسة الكرات المصمتة يعتمد في اشتقاقه على حد تنافر الكرات المصمتة؛ فقد تم اختيار خمسة نماذج لحد تنافر الكرات المصمتة مختلفة في شكلها الرياضي وذلك لاستكشاف مدى التأثير على سلوك دالة الحجم الناتجة عن حل المعادلة النظرية.

في هذا البحث تم رسم معامل الانضغاط -عوضاً عن الحجم- بدلالة درجة الحرارة عند ثبوت الضغط باستخدام ما يسمى بالرسوم البيانية التشعبية، وقد تم استخدام طريقة رياضية عددية تدعى بطريقة طول القوس للاستمرار العددي، وقد أثبت بالفعل أن لحدي تنافر الكرات المصمتة وسلسة الكرات المصمتة دور في تعدد الحلول الغير منطقية، كذلك تم دراسة تأثير تغيير حد التشتت مع حدود مختلفة من الكرات المصمتة المتنافرة وسلسة الكرات المصمتة وقد وجد أنه يمكن معالجة مشكلة تعدد الحلول الغير منطقية ومشكلة التنبؤ بوجود حالتين فزيائيتين مختلفتين لمركب واحد نقي عند نفس الضغط ودرجة الحرارة وذلك عند توافر شروط محددة في الشكل الرياضي للحدود المختلفة في المعادلة النظرية، أي أن هذه المشاكل ناتجة عن تأثير جميع الحدود مجتمعة وليست مستقلة بحد واحد فقط.

درجة الماجستير في العلوم الهندسية

جامعة الملك فهد للبترول والمعادن

CHAPTER 1

INTRODUCTION

1.1. Motivation

The study of the Pressure-Volume-Temperature (PVT) behavior of fluids has always been a subject of interest due to thermodynamic needs for calculating thermo-physical properties and phase equilibrium. The accurate PVT behavior is obtained by experimental measurements, which are expensive and time consuming. This is why the development of theoretical models has gained significant interest over the past years. Although many models have been proposed in the literature, an exact model has not been found. In fact, the theory-based models are still far from being exact. However, significant effort has been paid to develop successful theories to describe fluid behavior. The most successful models are those that are based on hard sphere theories.

Since the pioneering work of Verlet (1968), Barker and Henderson (1971) and Week et al. (1971), it became evident that the harsh repulsive forces dominate the structure of simple fluids. This is why the subject of hard sphere systems has gained significant interest in the study of liquid theories. To give accurate representation of the repulsive forces, various hard sphere models have been proposed and improved over the years. The development of these models has mainly been attributed to the use of molecular simulation data and statistical mechanical theories. For instance, Carnahan and Starling (1969) and Kolafa (Boublík, 1986) were examples of hard sphere models that are capable to describe the hard sphere system with good accuracy. An excellent review for hard sphere models was given by Mulero et al. (2008).

The success of hard sphere models made it possible to extend the study to account for the repulsive forces in large molecules. For this purpose, the concept of hard-sphere chain was introduced using statistical-mechanical theories based on hard sphere models. Extensive research has directed to develop hard-sphere chain theories such as those proposed by Honnell and Hall (1989), Chapman et al. (1988), Chiew (1990), Song et al. (1994b; 1994a), Chang and Sandler (1994) and Sadus (1995; 1999). The compressibility factor obtained from these theories compare well with simulation data. They were utilized as practical theory-based equations of state when a mean field term has been added. The most commonly utilized hard-sphere chain theories are the first order Wertheim's perturbation theory (TPT1) (Wertheim, 1984a; Wertheim, 1986b), thermodynamic perturbation dimer theory (TPT-D) (Ghonasgi & Chapman, 1994; Chang & Sandler, 1994), hard sphere chain theory (HSC) (Chiew, 1990; Song, et al., 1994a; Song, et al., 1994b) and generalized Flory dimer theory (GFD) (Dickman & Hall, 1986; Honnell & Hall, 1989).

These chain theories contributed to the calculation of phase equilibria and thermodynamic properties for various types of molecules such as small, large, polar and associating molecules. They have been utilized in the vapor-liquid-equilibrium (VLE) calculations for alkanes, alcohols and acids (Huang & Radosz, 1990; Walsh, et al., 1992; Chen, et al., 1998; Huang & Radosz, 1991a; Gregg, et al., 1993; Hasch, et al., 1994; Byun, et al., 1996; Pan & Radosz, 1998; Blas & Vega, 1998; McCabe, et al., 1998a). In addition, these theories have been adapted for VLE calculation for fluorohydrocarbons and refrigerants (Clements, et al., 1997; Galindo, et al., 1997; Galindo, et al., 1998; McCabe, et al., 1998b). Moreover, Button and Gubbins (1999) applied the hard-sphere

chain theories for VLE calculations of aqueous alkanolamine solutions. Hard-sphere chain theories could also be utilized in the liquid-liquid-equilibrium (LLE) calculations for hydrocarbons, alcohols, solvating mixtures (Gregg, et al., 1993; Yu & Chen, 1994; Suresh & Beckman, 1994). Furthermore, Pan and Radosz (Pan & Radosz, 1999) utilized hard-sphere chain theories in solid-liquid-equilibrium (SLE) calculation for naphthalene, alkane and polyethylene solutions.

In addition to the previous applications, the hard-sphere chain theories have extensively been utilized in the calculation of fluid phase equilibria of aqueous mixtures (Economou & Donohue, 1992; Kuespert & Donohue, 1993; Suresh & ElliottJr., 1992; Kraska & Gubbins, 1996a; Kraska & Gubbins, 1996b; Galindo, et al., 1996), aqueous ionic fluids (Liu, et al., 1999), critical micellar concentrations of aqueous surfactant solution (Li , et al., 1998) and aspheltene-oil equilibria (Wu, et al., 1998). Moreover, these theories have been used in the calculation of phase behavior of reservoir fluids, bitumen and petroleum pitch (Huang & Radosz, 1991b; Yu, et al., 1994; Bolaños & Thies, 1996). Likewise, these theories have been utilized in the calculation of phase behavior and solubility of polymer solutions and blends (Wu & Chen, 1994; Suresh, et al., 1994; Xiong & Kiran, 1995; Hasch & McHugh, 1995; Sadowski, et al., 1997; Koak, et al., 1999b). The hard-sphere chain theories have been further utilized in the field of polymers such as the calculation of cloud points of polymer and copolymer solutions (Byun, et al., 1996; Lee, et al., 1996; Han, et al., 1997; Garcia-Lisbona, et al., 1998). The hard-sphere chain theories have also been applied in the calculation of supercritical fluid extraction (Economou, et al., 1992; Gregg & Radosz, 1993; Pfohl & Brunner, 1998; Behme, et al., 1999).

Although the previous theories have shown good accuracy in the calculations of phase behavior and thermodynamic properties, some of these theories experience some pitfalls. For example, some versions of the statistical association fluid theories (SAFT) that utilize TPT1 has shown artificial two-phase separation regions (Yelash, et al., 2005; Privat, et al., 2010), unrealistic thermodynamic properties (Polishuk, 2011; Polishuk & Mulero, 2011) and multiple non-physical volume roots (Koak, et al., 1999a; Lucia & Luo, 2002; Privat, et al., 2010). All of these pitfalls could be explored by analyzing the PVT behavior since all thermodynamic properties are related to the PVT calculation. These problems could arise from various reasons including the formulation of the mathematical equations, accuracy of dispersion term and the empirical approximations. The reasons behind most of the problems associated with these theory-based models were assumed to be related to the dispersion term.

In this study, the problems of exhibiting artificial two-phase separation regions and obtaining multiple non-physical volume roots is explored by studying how the PVT behavior could be affected by other factors other than dispersion terms. Thus, focus is given to the role of the repulsive term on the PVT behavior. Unlike the previous studies that utilized Carnahan and Starling (1969) hard sphere term, various hard sphere terms that have different mathematical forms are utilized in a complete EOS to investigate their influence on the PVT behavior. Likewise, various chain theories and dispersion terms are studied to explore their contribution on the PVT behavior. The role of adding the association term in the EOS is also considered. **Figure 1.1** describes the physical meaning of the various terms in the theory based EOS. The study of the PVT behavior is accomplished by utilizing an uncommon tool to the thermodynamic community known as

bifurcation diagrams. This tool has been extensively utilized for dynamic systems such as reaction kinetics (Mie, 2013; Mangold & Gilles , 2012). Numerical techniques called continuation methods (Allgower & Georg, 1990) are utilized to generate the bifurcation diagrams. This study utilizes arc-length continuation method (Binous & Shaikh, 2015) to generate the bifurcation diagrams.

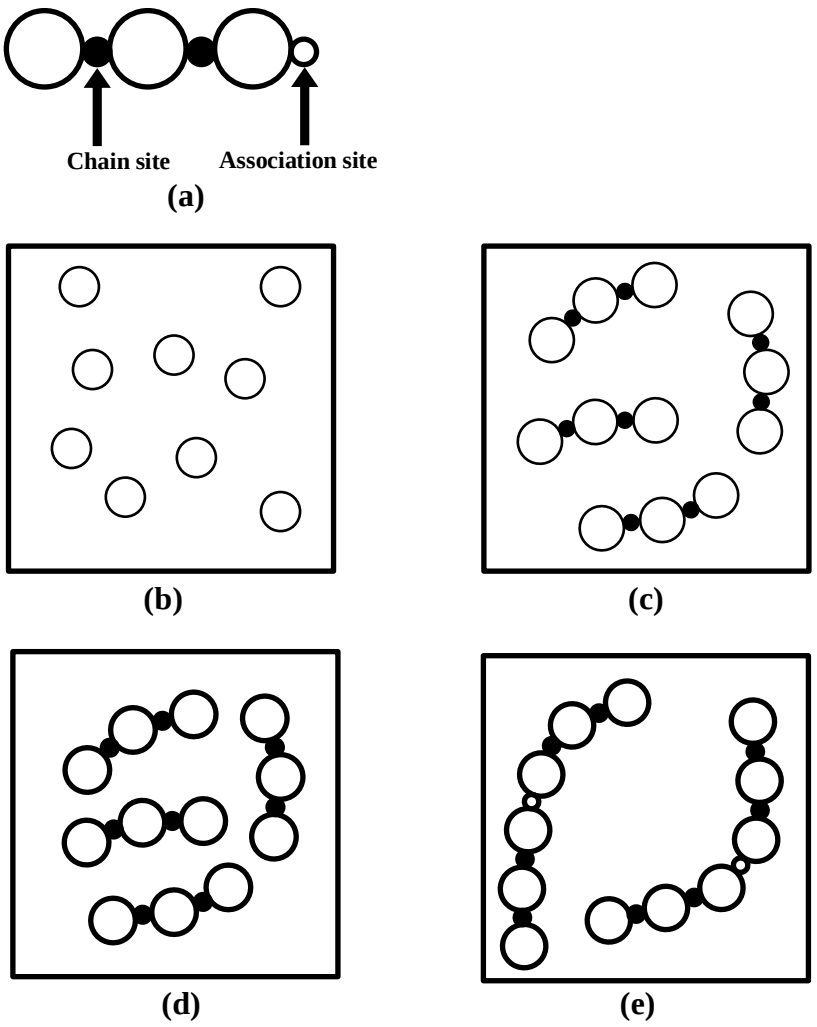

Figure 1.1: Physical interpretation of the various terms in the theory-based EOS. (a) Proposed molecule. (b) Initially the fluid is composed of hard spheres (c) Chain sites are added to form chain molecules. (d) Dispersion forces are added. (e) Association sites are added to form association complexes.

1.2. Objectives of the study

- To investigate the solution behavior of theory-based equations of state using bifurcation diagrams
- To study the role of the hard sphere term on the PVT behavior by selecting various hard sphere modes
- To study the influence of utilizing various hard-sphere chain theories on the PVT behavior
- To demonstrate how the PVT behavior could be influenced by using different dispersion terms
- To study the role of adding an association term on the PVT behavior
- To propose a new model that is applicable for associating and non-associating components and is free from exhibiting artificial two-phase separation regions and multiple non-physical volume roots

1.3. Approach

Any theory-based equation of state must contain hard sphere, chain, dispersion, and association terms. The chain and the association terms depend on the form of the hard sphere term. The association term could be eliminated if non-associating components are considered. Thus, this study will first consider non-associating components. First, the effect of utilizing various hard sphere terms while fixing the other terms in the EOS will be explored. After that, the chain term will be derived according to the various hard sphere models that were utilized in order to study the integrated effect of

both terms and to explore their influence on the PVT behavior. Then, various chain theories will be utilized to derive the chain term and then their effect on the PVT behavior will be explored. After that, different dispersion term will be utilized with the various hard sphere models and their corresponding chain terms. After getting clear picture of the role of the hard sphere, chain and dispersion terms on the EOS and their integrated effect on the PVT behavior, a new model for non-associating fluid that is free from exhibiting artificial two-phase separation regions and multiple non-physical volume roots will be proposed. Finally, a proper association term will be added to the proposed model in order to make it applicable for associating components.

1.4. Scope of the work

The theory-based EOSs are not attractive for practice implementation into process simulators. This is due to the existence of multiple volume roots at specific pressure and temperature. This study explored the role of each term on the theory-based EOS and proposed a model that is simple and free from non-physical behavior including the existence of non-physical multiple volume roots. Thus, the proposed model could practically be implemented into process simulators since its PVT behavior is similar to cubic EOS.

1.5. Thesis organization

In **Chapter 2**, a description of hard sphere theory and some proposed models with their accuracy will be given.

Chapter 3 shows some important chain theories that were proposed to describe non-simple molecules.

Chapter 4 gives the basic theory behind bifurcation diagram which is a powerful tool that is utilized in this study to explore the solution behavior of any equation of state.

Chapter 5 is devoted to explore the role of the hard sphere term on the solution behavior of a complete equation of state.

Chapter 6 explores the role of the different chain theories of the solution behavior.

In **Chapter 7**, the role of the dispersion and the association interaction is studied. The study presents an approach to resolve the problem of getting multiple roots in solving the equations of state.

CHAPTER 2

EQUATIONS OF STATE FOR HARD SPHERES

2.1. Introduction

As indicated in Chapter 1, the harsh repulsive forces play a major role in the determination of the structure and thermodynamic properties of simple fluids. Therefore, an accurate hard sphere model is a crucial factor in the development of any fluid theory. The simplicity of the hard sphere (HS) models is also another important factor because it would allow quick calculations and simple derivations if needed for all thermodynamic properties. Various hard sphere models have been proposed over last decades. The developments of these models have mainly been attributed to the adjustment of molecular simulation data and/or from the knowledge of the virial coefficients. In recent years, the HS models are extensively utilized in the development of perturbation theories. This chapter is devoted to present some of the hard sphere models that have been proposed over the past years.

2.2. Hard sphere models

Before shedding light on the different HS models, it would be beneficial to introduce the main variables that will be utilized in the mathematical representation of the hard sphere models. The hard sphere model is given by a compressibility factor (Z) as the dependent variable while the packing fraction (η) as the independent variable. The packing fraction is defined as:

$$\eta = \frac{\pi \rho^*}{6} \tag{2.1}$$

where ρ^* is the reduced density. The compressibility factor may also be obtained as a function of the packing fraction ratio (ξ) which is defined as:

$$\xi = \frac{\eta}{\eta_c} \tag{2.2}$$

where η_c is the maximum η value which is corresponding to the closest packing fraction ($\eta_c = \pi\sqrt{2}/6$). For instance, the repulsive term in the van der Waals equation of state is given in terms of Z and packing fraction by:

$$Z = \frac{1}{1 - 4\eta} \tag{2.3}$$

Several hard sphere models have been proposed after van der Waals's repulsive term. The model of van der Waals has extensively been utilized in the famous cubic equations of state. However, this model is not accurate when it is compared with molecular simulation data. Enormous effort has been spent in developing and improving the accuracy of the hard sphere models. The following subsections will briefly describe some common hard sphere models. These models will be given in chronological order.

2.2.1 Carnahan and Starling's hard sphere model

Carnahan and Starling (CS) (1969) obtained their well-known expression by approximating the first virial coefficients to their nearest integer and then re-summing the virial series. The resulted expression was:

$$Z = \frac{1 + \eta + \eta^2 - \eta^3}{(1 - \eta)^3} \tag{2.4}$$

This expression is very accurate in the low-density region (Baus & Colot, 1987). It is the most common HS EOS and it has been widely used in the statistical association fluid theory (SAFT). However, this expression fails to reproduce the exact virial coefficients beyond the third.

2.2.2 Kolafa's hard sphere model

Kolafa (Boublík, 1986) introduced an expression that is almost equivalent in simplicity to CS equation:

$$Z = \frac{1 + \eta + \eta^2 - \frac{2}{3}(\eta^3 + \eta^4)}{(1 - \eta)^3} \tag{2.5}$$

This expression is better that CS in producing the virial coefficients. In addition, it gives excellent results compared to Erpenbeck and Wood's (1984) simulation data.

2.2.3 Goldman and White's hard sphere model

Goldman and White (1988) obtained their expression by interpolating between close packed and gas configurations:

$$Z = \frac{1 + 2.649526\eta + 4.598102\eta^2 + 4.860055\eta^3 + 3.498\eta^4}{1 - \xi} \tag{2.6}$$

This equation has a pole at the closed packed limit as could be noticed from the denominator. The constants in the nominator resulted from the numerical adjustment.

2.2.4 Solana's hard sphere model

The expression that was proposed by Solana (Mulero, et al., 2008) has the same format as CS equation:

$$Z = \frac{1 + \eta + \eta^2 - 0.6352\eta^3}{(1-\eta)^3} \tag{2.7}$$

This equation was developed to calculate the virial coefficients up to the fourth. However, this expression predicts compressibility factor values less accurate than those of CS.

The author proposed another expression that could reproduce seven virial coefficients. Nevertheless, its prediction of the compressibility factor is similar to the previous one. The expression is given by:

$$Z = \frac{1 - \eta - 1.6352\eta^3 + 1.4005\eta^4 + 1.1764\eta^5}{(1-\eta)^5} \tag{2.8}$$

2.2.5 Khoshbarchi and Vera's hard sphere model

Although the packing fraction has a specified maximum limit, most hard sphere models do not predict the correct packing fraction value. Khoshbarchi and Vera (1997) developed an expression that is volume dependent and has the correct limit for the packing fraction. Their proposed expression is given by:

$$Z = \frac{1 - \frac{1}{25}\xi - \frac{2}{5}\xi^2 - \frac{5}{4}\xi^3 + \frac{9}{50}\xi^5 + \frac{71}{50}\xi^{12}}{(1-\xi)^3} \tag{2.9}$$

This expression is accurate in predicting the first eight virial coefficients and reproducing the computer simulation data of Alder and Wainwright (1960) and of Erpenbeck and Wood (1984).

2.2.6 Malijevsky and Veverka's hard sphere model

By approximating the first seven virial coefficients, Malijevsky and Veverka (1999) proposed the following form:

$$Z = \frac{1 + 1.056\,\eta + 1.6539\,\eta^2 + 0.3262\,\eta^3}{(1-\eta)^3(1 + 0.056\,\eta + 0.5979\,\eta^2 + 0.3076\,\eta^3)} \tag{2.10}$$

The values of the compressibility factor obtained from this equation were compared to the computer simulation data of Barosova (1996) and found to have a good agreement.

2.2.7 Yelash and Kraska's hard sphere model

Yelash and Kraska (2001) proposed an equation of the form:

$$Z = \frac{3 + 8\eta + 14\eta^2 + 14\eta^3 + \frac{40}{3}\eta^4}{3 - 4\eta} \tag{2.11}$$

This expression can accurately reproduce the first ten virial coefficients. In addition, it is in good agreement with the computer simulation data generated by Barker and Henderson (1971).

2.2.8 Ghotbi and Vera's hard sphere model

Ghotbi and Vera (2001) proposed two expressions that have the correct packing fraction limit:

$$Z = 1 + 2.9619\xi + 5.4831\xi^2 + 7.4564\xi^3 + 8.4856\xi^4 + \frac{8.85\xi^5}{1-\xi} - \frac{0.62\xi^7}{(1-\xi)^2} + \frac{0.04\xi^{10}}{(1-\xi)^3} \tag{2.12}$$

$$Z = 1 + 2.9619\xi + 5.4831\xi^2 + 7.4564\xi^3 + 8.4856\xi^4 + \frac{8.9\xi^5 - 2.8\xi^8}{1 - \xi} \quad (2.13)$$

These two equations include the first five virial coefficients in its mathematical form (Kratky, 1977). Ghotbi and Vera (2001) concluded that equation 2.13 has a good agreement with the first eight virial coefficient values.

2.2.9 Wang's hard sphere model

Wang (2002) established the following equation from the first ten virial coefficients:

$$Z = \frac{8.8854}{1 - \frac{\eta}{\eta c}} - 7.8854 - 8\eta - 6.2057\eta^2 - 3.52\eta^3 - 1.3312\eta^4 + 2.048\eta^6 \quad (2.14)$$

This equation does not agree well with the simulation data at high densities (Mulero, et al., 2008). However, Wang emphasized that the most important feature of this equation is that it can be a valuable guide to treat complex interaction potentials.

2.2.10 Rambaldi et al.'s hard sphere model

Rambaldi et al. (2006) proposed a simple model given by:

$$Z = 1 + \frac{4\eta}{1 - 2.5\eta + 1.658808\eta^2} \quad (2.15)$$

This model could be considered as an extension of the work of Hoover an Alder (1967). The coefficients in the above equation were determined based on new computer simulation data.

2.2.11 Miandehy et al.'s hard sphere model

Miandehy et al. (2006) developed an expression of the form:

$$Z = \frac{1}{(1-\xi)^2}(1 + 0.9619\xi + 0.5593\xi^2 - 0.5499\xi^3 - 0.9415\xi^4 - 0.647\xi^5 - 0.7324\xi^7) \tag{2.16}$$

This expression is capable to reproduce the first eight virial coefficients. Moreover, it was used in the perturbation theory of Leonard–Henderson–Barker (Miandehy, et al., 2006) in order to obtain excess properties of mixtures.

2.2.12 Liu's hard sphere model

Liu (Mulero, et al., 2008) developed an expression that is valid for the entire metastable and stable regions:

$$Z = 1 + \frac{3.68584\eta}{1 - 2.5848\eta + 1.9499\eta^2 - 0.17228\eta^3 - 0.16012\eta^4} + \frac{0.31416\eta}{1 - 1.573357\eta} + 4.1637 \times 10^{10}\eta^{40} - 2.3452 \times 10^{11}\eta^{42} + 3.6684 \times 10^{11}\eta^{44} \tag{2.17}$$

2.3. Comparison of hard sphere model with molecular simulation data

The compressibility factors predicted from the previous HS expressions are compared with molecular simulation data in Table 2.1. The simulation data were obtained from Erpenbeck & Wood (1984) except the last three values that were taken from Henderson & Barker (1971). The HS models that are listed in Table 2.1 are in the same sequence as presented in section 2.2. The data clearly indicate that all expressions provide accurate predictions compared to the simulation data especially at low packing fraction values.

Table 2.1: Comparison of the compressibility factor from various hard-sphere models with simulation data

η	z_{sim}	Carnahan and Starling	Kolafa	Goldman and White	Solana	Solana	Khoshbarchi and Vera	Malijevsky and Veverka
0.02962	1.1278	1.1277	1.1278	1.1278	1.1278	1.1278	1.1277	1.1278
0.04114	1.1828	1.1828	1.1828	1.1828	1.1828	1.1828	1.1827	1.1828
0.07405	1.3594	1.3593	1.3594	1.3594	1.3595	1.3594	1.3591	1.3594
0.14809	1.8884	1.8872	1.8884	1.8884	1.8891	1.8885	1.8868	1.8885
0.18512	2.2436	2.2418	2.2442	2.2440	2.2461	2.2443	2.2415	2.2443
0.24682	3.0316	3.0256	3.0315	3.0302	3.0384	3.0320	3.0262	3.0315
0.37024	5.8502	5.8319	5.8495	5.8473	5.9060	5.8682	5.8378	5.8511
0.41138	7.4304	7.4088	7.4290	7.4398	7.5333	7.4828	7.4122	7.4343
0.43558	8.6003	8.5794	8.5991	8.6312	8.7470	8.6963	8.5763	8.6091
0.46280	10.195	10.1779	10.1937	10.2752	10.4111	10.3788	10.1600	10.2125
0.47124	10.79	10.7461	10.7597	10.8655	11.0044	10.9850	10.7221	10.7824
0.48435	11.72	11.7084	11.7170	11.8727	12.0107	12.0221	11.6742	11.7472

Yelash and Kraska	Ghotbi and Vera	Ghotbi and Vera	Wang	Rambaldi et al.	Miandehy et al.	Liu
1.1277	1.1278	1.1278	1.1277	1.1278	1.1278	1.1278
1.1828	1.1828	1.1828	1.1828	1.1828	1.1828	1.1829
1.3593	1.3594	1.3594	1.3594	1.3595	1.3594	1.3595
1.8872	1.8884	1.8885	1.8884	1.8893	1.8885	1.8885
2.2417	2.2443	2.2443	2.2443	2.2465	2.2444	2.2443
3.0245	3.0314	3.0317	3.0326	3.0399	3.0325	3.0316
5.8209	5.8482	5.8486	5.8745	5.9074	5.8691	5.8498
7.3952	7.4284	7.4272	7.4922	7.5225	7.4764	7.4295
8.5694	8.6007	8.5980	8.7066	8.7169	8.6776	8.5999
10.1848	10.2014	10.1977	10.3874	10.3357	10.3306	10.1953
10.7632	10.7708	10.7671	10.9921	10.9069	10.9222	10.7620
11.7482	11.7353	11.7330	12.0251	11.8676	11.9290	11.7215

To quantify the agreement with simulation data, the average absolute deviation (AAD) was determined for the compressibility factors predicted by the various models. The average absolute deviation is defined as:

$$AAD = \frac{1}{N}\sum_{i=1}^{N}\left|\frac{Z_{sim} - Z_{theory}}{Z_{sim}}\right| \tag{2.18}$$

where N is the number of data points. The AAD (%) are summarized in Table 2.2.

Table 2.2: Percentage average absolute deviation (%AAD) of the calculated compressibility factor compared with molecular simulation data

Carnahan and Starling	Kolafa	Goldman and White	Solana	Solana	Khoshbarchi and Vera	Malijevsky and Veverka
0.157	0.034	0.283	0.918	0.698	0.208	0.057
Yelash and Kraska	**Ghotbi and Vera**	**Ghotbi and Vera**	**Wang**	**Rambaldi et al.**	**Miandehy et al.**	**Liu**
0.193	0.040	0.041	0.743	0.646	0.521	0.030

Table 2.2 evidently shows that all of the HS models that were tested have an excellent agreement with the simulation data. Liu model, which is the most recent model among the others, has the least value of AAD. In general, all models tend to overestimate the compressibility factor especially at high density.

To sum up, all of the listed HS models accurately predict the compressibility factor. Therefore, one needs additional criteria in addition to the accuracy of compressibility factor to judge on the most convenient model for perturbation theories.

CHAPTER 3

EQUATIONS OF STATE FOR HARD SPHERE CHAINS

3.1. Introduction

If a hard sphere model is combined with a mean field term, the combination of the two terms could satisfactorily describe phase equilibria and thermodynamic properties of simple fluids such as noble gases and low molecular weight alkanes. However, several classes of substances such as polymers, proteins, high molecular weight hydrocarbons and surfactants cannot accurately be described with such combination due to incapability of the resulted model to account for the molecular size. . Therefore, the molecular size of these compounds must be taken into consideration. One way to account for the molecular size is to approximate it with hard-chain models, which consists of hard spherical segments connected with covalent bonds.

Many theories have been proposed over the years to describe the hard sphere chain systems. This chapter sheds light on the most popular theories.

3.2. Hard sphere-chain theories

3.2.1. Hard sphere chain theory (HSC)

Chiew (1990) proposed simple hard-sphere chain theory. This theory was utilized in a complete equation of state by Song et al. (1994a; 1994b). The approach is referred to as the perturbed hard sphere chain theory since it considers the complete equation of state with the attractive forces among molecules. The hard-sphere chain term of Chiew (1990)

and Song et al. (1994a; 1994b) et al. is referred to the hard sphere chain (HSC) and it can be represented by the following equation:

$$Z = 1 + m(Z_{HS} - 1) + (m - 1)\big(1 - g_{HS}(d)\big) \tag{3.1}$$

where m is the number of spherical segments in the chain, Z_{HS} is the hard-sphere compressibility factor and $g_{HS}(d)$ is the pair correlation function at contact of the monomers which describes how two molecules are different apart where one of the molecules is in the first shell. The first term on the right hand side is the ideal gas term. The second term represents the repulsive forces among monomers, which could be given by any hard sphere model. The third term is the bonding contribution, the chain term. The pair correlation function at contact $g_{HS}(d)$ is obtained from statistical mechanics by:

$$g_{HS}(d) = \frac{Z_{HS} - 1}{4\eta} \tag{3.2}$$

The expression of the pair correlation function at contact must satisfy the ideal gas limit:

$$\lim_{\eta \to 0} g_{HS(d)} = 1 \tag{3.3}$$

3.2.2. First order thermodynamic perturbation theory (TPT1)

Wertheim (1984a; 1984b; 1986a; 1986b) developed a thermodynamic perturbation theory (TPT) that accounts for the covalent bonding and the intermolecular association between spherical segments within molecular chains. The theory was extended by Chapman et al. (1988) and given by:

$$Z = 1 + m(Z_{HS} - 1) + (1 - m)\left(\eta \frac{\partial \ln g_{HS}(d)}{\partial \eta}\right) \tag{3.4}$$

This model gives accurate results when compared with molecular simulation data. This model was utilized as the basis of the statistical associating fluid theory (SAFT) (Chapman, et al., 1990).

3.2.3. Thermodynamic perturbation dimer theory (TPT-D)

Ghonasgi & Chapman (1994) and Chang & Sandler (1994) improved TPT1 equation to incorporate structural information for the diatomic fluid molecules. They derived a general expression for the thermodynamic perturbation dimer theory (TPT-D):

$$Z = m\,Z_{HS} - \frac{m}{2}\left[1 + \eta\frac{\partial \ln g_{HS}(d)}{\partial \eta}\right] - \left(\frac{m}{2} - 1\right)\left[1 + \eta\frac{\partial \ln g_{HD}(d)}{\partial \eta}\right] \tag{3.5}$$

It is clear from the last term that this equation needs the intermolecular site-site hard-dimer pair correlation function at contact $g_{HD}(d)$. Several relations were proposed for $g_{HD}(d)$ with the aid of molecular simulation data or theoretical approaches (Ghonasgi & Chapman, 1994; Chiew, 1991; Chang & Sandler, 1994). Yethiraj and Hall (1990) found that the dimer site-site pair correlation function could be obtained as a linear function of the hard-sphere site-site pair correlation function by the following relation:

$$g_{HD}(d) = g_{HS}(d) \times (\alpha\,\eta + c) \tag{3.6}$$

where α and c are adjustable parameters that could be obtained by fitting molecular simulation data. Substituting this equation into equation (3.5) results in the following expression for the compressibility factor:

$$Z = 1 + m(Z_{HS} - 1) + (1 - m)\eta\frac{\partial \ln g_{HS}(d)}{\partial \eta} + \frac{\alpha\,\eta(2 - m)}{2(\alpha\,\eta + c)} \tag{3.7}$$

The first three terms in the right hand side of equation (3.7) are identical to TPT1 theory. The difference is only in the fourth term which contains two adjustable parameters. This equation is more accurate than TPT1 when compare to the molecular simulation data as will be shown in section 3.3.

3.2.4. Generalized Flory dimer theory (GFD)

During the 1980s, Hall and coworkers proposed the generalized Flory dimer theory (GFD) (Dickman & Hall, 1986; Honnell & Hall, 1989). Their theory was developed by expressing the compressibility factor in terms of the probability of inserting a single chain of m segments into a bulk fluid consisting of chains of length m. The key feature in this theory is the choice of insertion probability expression that depends on the molecular structure. Hall and coworkers (Honnell & Hall, 1989; Gulati & Hall, 1998) developed a suitable insertion probability expression that could be utilized to yield the following expression:

$$Z = (Y^m + 1)Z_{DB} - Y^m Z_{HS} \tag{3.8}$$

where Z_{DB} is hard-dumbbell fluid compressibility factor that could be accurately expressed by Tildesley-Streett equation (Tildesley & Streett, 1980):

$$Z_{DB} = \frac{1 + 2.45696\eta + 4.10386\eta^2 - 3.75503\eta^3}{(1-\eta)^3} \tag{3.9}$$

Y^m is given by:

$$Y^m = \begin{cases} 0.95926 + 0.95926\,(m-3) & 2 \le m \le 8 \\ 12.22789 + 0.92715\,(m-15) & m > 8 \end{cases} \tag{3.10}$$

Thus, equation (3.8) could be used with a suitable expression for Z_{HS}.

3.3. Comparison with molecular simulation data

In this analysis, the HS term will be fixed to CS to evaluate the effect of varying the chain theories on the accuracy. The compressibility factors are calculated from HSC, TPT1, TPT-D and GFD and then compared with molecular simulation data in Table 3.1. The comparison is given for segment numbers of 4, 8, 16, 32, 51 and 201.. The simulation data for $m \leq 16$ and $m = 32$ were taken from Chang and Sandler (1994) and Denlinger and Hall (1990), respectively. The values for the 51-mer and 201-mer chains were obtained by Gao and Weiner (1989).

Table 3.1: Comparison of compressibility factor from HSC, TPT1, TPT-D and GFD with molecular simulation data as a function of reduced density ($\rho^* = 6\eta/\pi$)

	Z				
ρ*	**simulation**	**HSC**	**TPT1**	**TPT-D**	**GFD**
			m = 4		
0.1	1.49	1.53	1.54	1.48	1.53
0.2	2.22	2.25	2.33	2.20	2.30
0.3	3.28	3.25	3.45	3.27	3.40
0.4	4.84	4.64	5.04	4.82	4.98
0.5	7.09	6.57	7.31	7.05	7.21
0.55	8.56	7.81	8.79	8.51	8.67
0.6	10.26	9.30	10.57	10.27	10.42
0.65	12.49	11.07	12.71	12.40	12.53
0.7	15	13.20	15.31	14.98	15.07
0.75	18.26	15.78	18.46	18.11	18.15
0.8	22.1	18.91	22.31	21.95	21.91
0.85	27.02	22.75	27.04	26.66	26.52
0.9	32.49	27.47	32.89	32.50	32.22
			m = 8		
0.1	1.76	1.91	1.95	1.75	1.91
0.2	2.99	3.18	3.36	2.98	3.28
0.3	4.91	4.96	5.42	4.89	5.29

0.4	7.75	7.46	8.40	7.74	8.21
0.5	11.95	10.98	12.71	11.92	12.41
0.55	14.83	13.25	15.54	14.70	15.17
0.6	18.26	15.98	18.95	18.06	18.49
0.65	22.32	19.25	23.08	22.14	22.51
0.7	27.14	23.19	28.10	27.11	27.38
0.75	33.34	27.97	34.22	33.18	33.30
0.8	40.85	33.80	41.71	40.63	40.54
0.85	50.64	40.95	50.95	49.83	49.43
0.9	62.03	49.78	62.41	61.25	60.44
			m = 16		
0.1	2.25	2.67	2.75	2.29	2.67
0.2	4.47	5.04	5.42	4.55	5.24
0.3	8.09	8.39	9.36	8.14	9.07
0.4	13.59	13.11	15.12	13.58	14.67
0.5	21.96	19.79	23.50	21.67	22.80
0.55	27.13	24.14	29.03	27.07	28.16
0.6	34.05	29.34	35.72	33.63	34.64
0.65	41.9	35.60	43.83	41.62	42.47
0.7	51.8	43.17	53.69	51.38	51.99
0.75	65.15	52.36	65.74	63.32	63.58
0.8	81.28	63.57	80.53	78.00	77.78
			m = 32		
0.191	7.08	8.28	8.98	7.20	8.63
0.382	23	22.51	26.20	23.01	25.30
0.478	37	34.15	40.90	37.11	39.53
0.573	57.6	50.35	61.78	57.46	59.72
			m = 51		
0.2	11.46	13.18	14.43	11.40	13.82
0.3	23.04	23.37	26.61	22.33	25.59
0.372	34.87	33.25	38.81	33.71	37.39
0.464	56.56	50.11	60.13	54.08	58.03
0.59	101.04	84.36	104.53	97.32	100.90
0.649	130.17	106.74	134.01	126.31	129.28
0.7	160.56	130.58	165.65	157.55	159.67
0.8	238.12	193.81	250.36	241.51	240.72
0.9	346.51	289.53	379.78	370.26	363.88
			m = 201		
0.2	36.8	48.07	53.06	40.74	50.61

0.3	79.44	87.60	100.54	83.15	96.41
0.4	152.11	143.72	170.56	148.64	164.08
0.5	256.2	223.66	273.08	247.11	263.11
0.6	407.16	338.39	423.40	393.78	407.95
0.7	621.54	505.19	645.48	612.56	621.15
0.8	927.79	752.00	978.19	942.26	939.03
0.9	1354.76	1125.88	1486.89	1448.22	1422.38

The comparison in Table 3.1 clearly shows that TPT-D theory is the most accurate in predicting the compressibility factor for all chain lengths, however it becomes progressively less accurate for long chains. This conclusion is also found with other chain theories which are less accurate than TPT-D.

To see the comparison clearly, Table 3.2 gives the average absolute deviation (AAD) for the compressibility factor predicted by the various chain theories

Table 3.2: Percentage Average Absolute Deviation (%AAD) of the Calculated Compressibility of m-Hard-Sphere Chains Compared with Molecular Simulation Data

	AAD (%)			
m	**HSC**	**TPT1**	**TPT-D**	**GFD**
4	9.00	2.57	0.58	1.71
8	11.65	5.33	0.65	3.60
16	13.32	9.04	1.39	6.71
32	9.85	14.63	0.56	10.60
51	13.42	9.26	3.13	5.45
201	16.32	14.06	4.30	9.49
Overall	12.17	7.87	1.66	5.35

As seen in the table, the AAD for the 32-mer chain is inconsistent with the rest of the analysis. This is because the comparison for 32-mer chain is limited to moderate density values. Furthermore, it is obvious that there is a noticeable difference among the various chain theories for all values of hard sphere segments (m). The accuracy of all

chain theories deteriorates substantially for long chains with minimum deterioration in TPT-D theory which provides the best overall agreement with the simulation data.

CHAPTER 4

BIFURCATION DIAGRAMS

4.1. Introduction

The previous two chapters showed that the accuracy of a hard sphere model as well as a hard-sphere chain theory varies from one to another when compared to simulation data. Thus, the construction of a complete equation of state may be sensitive to the selection of any model or theory. However, the question is not only limited to accuracy but also to the pitfalls PVT behavior that might arise from different models. For instance, the mathematical complexity of some of the hard sphere models makes them expensive for mathematical manipulations.

The mathematical combination of different hard sphere models with a dispersion term produces various algebraic models. These algebraic models might cause non-physical multiple volume roots. Previous studies (Koak, et al., 1999; Lucia & Luo, 2002; Privat, et al., 2010) proved that the problem of multiple volume roots in the various versions of the statistical association fluid theory (SAFT), which is based on TPT1, is difficult to handle and resolve. Many techniques that were employed to tackle the problem of the multiple volume roots relied on a reliable solver in order to determine all volume roots at specific temperature and pressure and then to test their physical characteristics and stabilities with an efficient procedure (Koak, et al., 1999; Lucia & Luo, 2002; Xu, et al., 2002; Aslam & Sunol, 2006a; Privat, et al., 2010; Alsaifi & Englezos, 2011). These approaches are tedious and not convenient to investigate the PVT behaviour of many combinations of hard sphere models and hard-chain theories with a

dispersion term. The reason is that the previous approaches give only a snap shot of the whole PVT behaviour since it depends on random selection of temperature and pressure.

In this thesis, the complete loci of volume roots with the variation of temperature and pressure will be studied with an alternative approach. This chapter introduces the method that will be utilized. The approach is based on diagrams called bifurcation diagrams.

4.2. Theory of bifurcation diagrams

The bifurcation diagram is a powerful tool to explore the solution behavior as a bifurcation parameter varies. The bifurcation diagram is usually constructed by utilizing the axis of ordinate to represent the state variable while the axis of abscissas represents the bifurcation parameter. For example, a bifurcation diagram could be generated for the non-liner equation (4.1) by considering x as the state variable while λ represents the bifurcation parameter.

$$F(x, \lambda) = 0 \tag{4.1}$$

The diagram is constructed by plotting x for a wide range of λ. If there are more variables in the equation, one variable is utilized as the bifurcation parameter while the other could be fixed (Seydel, 2009). In this study, the bifurcation parameter (λ) is the temperature and x represents the molar volume (V) while the pressure is fixed. Therefore, the bifurcation diagram could be generated as molar volume versus temperature or compressibility factor (Z) versus temperature.

The bifurcation diagram may exhibit multiple curves. Each separate curve is called branch. The point where the branch changes its direction at specific λ value is called turning point. **Figure 4.1** represents the bifurcation diagram for hexane at 15 atm using Peng-Robinson EOS (Peng & Robinson, 1976). It is clear from the figure that there is only one branch and two turning points that are represented by the solid dots. Thus, there are three maximum volume roots located in the temperature range (433, 484) K. Another example of the bifurcation diagram is given in **Figure 4.2** using simplified SAFT EOS (Fu & Sandler, 1995) for hexane at 15 atm. As shown in the figure, there are three branches with two turning points on the longest branch leading to four maximum volume roots located in the temperature range (422, 496) K.

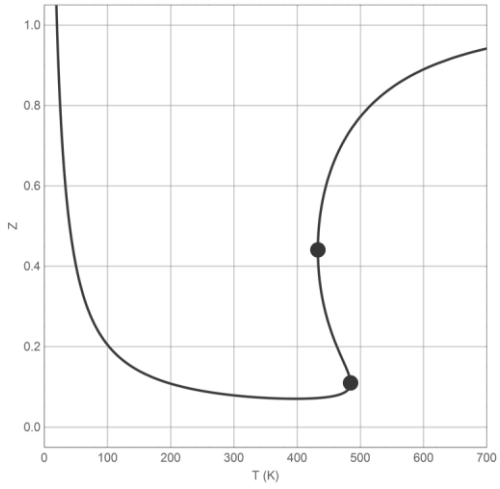

Figure 4.1: Bifurcation diagram for hexane at 15 atm using PR EOS

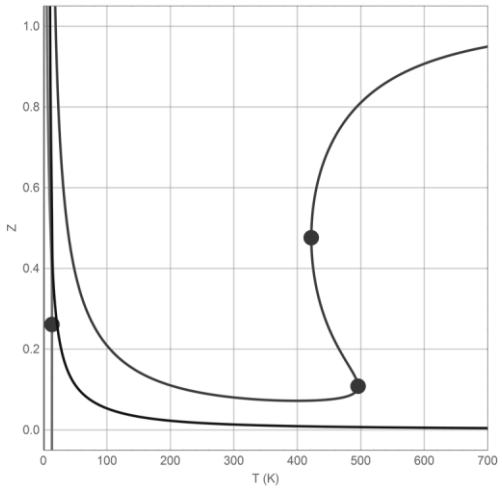

Figure 4.2: Bifurcation diagram for hexane at 15 atm using simplified SAFT EOS

Constructing a complete bifurcation diagram is not a trivial task. The analytical solution is not always possible due to the mathematical complexity of some models. Therefore, it is a common practice to obtain the bifurcation diagrams using numerical techniques such as the continuation methods (Allgower & Georg, 1990). In this work, the

arc-length continuation method (Binous & Shaikh, 2015) is utilized to construct the bifurcation diagrams.

4.3. Arc-length continuation method

The arc-length continuation method is classified as one of the path-following techniques (Allgower & Georg, 1990) that are commonly used to obtain the variation of the solution paths for non-linear equations. The method is a powerful tool to determine available branches in the bifurcation diagram of the non-linear equations. The set of the non-linear algebraic equations can be represented in the form:

$$\boldsymbol{f}(\boldsymbol{x};\lambda) = 0 \tag{4.2}$$

where $\boldsymbol{f}$ and $\boldsymbol{x}$ are vector components given by $\boldsymbol{f} = (f_1, f_2, \dots., f_n)$ and $\boldsymbol{x} = (x_1, x_2, \dots., x_n)$ and λ is an independent variable. A solution path of equation (4.2) is shown by a continuous curve that demonstrates how $\boldsymbol{x}$ varies with λ. To trace the curve that represents the solution path, an initial point on that curve is needed. The initial point should satisfy equation (4.2) leading to:

$$\boldsymbol{f}(\boldsymbol{x_0};\lambda_0) = 0 \tag{4.3}$$

Then, the curve begins from the specified initial point by utilizing a parameter (s) that is called the arc-length segment that assists to trace the solution curve. Thus, equation (4.2) could be rewritten as:

$$\boldsymbol{f}\big(\boldsymbol{x}(s), \lambda(s)\big) = 0 \tag{4.4}$$

Using Pythagorean rule, one can obtain the relationship of λ and x with s:

$$\frac{d\boldsymbol{x}}{ds}.\frac{d\boldsymbol{x}}{ds}+\left(\frac{d\lambda}{ds}\right)^2=1 \tag{4.5}$$

Hence, the non-linear equations (4.2) could be converted to a system of $n+1$ coupled differential equations represented by equations (4.4) and (4.5) with equation (4.3) as an initial guess.

For the PVT calculation, one needs to solve the non-linear equation:

$$f(T,\ V,\ P)=0 \tag{4.6}$$

In order to convert the above equation into a system of differential equations, one could fix the pressure and define the molar volume and temperature in terms of the arc-length segment:

$$f\big(T(s),V(s)\big)=0 \tag{4.7}$$

Hence, the differential equation will be:

$$\left(\frac{dV}{ds}\right)^2+\left(\frac{dT}{ds}\right)^2=1 \tag{4.8}$$

To solve the above differential equation, an initial guess is required:

$$f(T_0,V_0)=0 \tag{4.9}$$

This initial guess could be obtained using any reliable solver.

In this work, NDSolve command in Mathematica© was utilized to solve the differential equations.

The solution of the above equations gives the bifurcation diagram that will be the main tool in the next chapters. Its unique capability to show physical and non-physical

behavior in one diagram makes it a powerful tool to compare theory-based models and to show all PVT pitfalls that might arise from non-physical behavior. This is why it would be a convenient tool for studying my combinations of hard-sphere modes and theories with a dispersion term.

CHAPTER 5

THE ROLE OF VARIOUS HARD SPHERE MODELS ON PVT BEHAVIOR OF NON-ASSOCIATING FLUID: BIFURCATION ANALYSIS

5.1. Introduction

Various hard sphere models and their accuracies were investigated in **Chapter 2**. All of the investigated hard sphere models showed adequate accuracy. Thus, it is expected that utilizing other hard sphere models instead of CS, which is the most commonly used model, will not have a dramatic impact in the accuracy for the PVT calculation. However, it is not clear how the different hard sphere models could affect the solution behavior in the PVT calculation.

In this chapter, the role of the hard sphere term in a complete equation of state that contains chain and dispersion terms will be studied with the aid of the bifurcation diagrams. In order to accomplish this objective, different hard sphere models with different mathematical forms will be selected. The TPT1 hard-chain theory will be adopted in this chapter. To complete the equation of state, simple dispersion term such as the one that was proposed by Fu and Sandler (1995) will be utilized in this work in order to minimize the complexity of the equation.

The study of the PVT behavior in this chapter will first start with fixing the chain term to the one that is derived from CS model using TPT1 theory. Consequently, one could observe the effect of only changing the hard sphere term in the PVT calculation. After that, the corresponding chain term derived from TPT1 for each hard sphere model will be implemented in the equation to explore the effect in the solution behavior.

5.2. Mathematical formulas and derivations

Before shedding light on the bifurcation diagrams, it would be beneficial to represent the mathematical form of the complete equation of state. For non-associating fluid, the compressibility factor (Z) could be constructed by contributions from hard sphere (hs), chain and dispersion (disp) terms as the following equation:

$$Z = \frac{P\,V}{R\,T} = 1 + Z^{hs} + Z^{chain} + Z^{disp} = 1 + \eta\left(\frac{\frac{\partial A^{res}}{R\,T}}{\partial \eta}\right) \tag{5.1}$$

$$= 1 + \eta\left(\frac{\frac{\partial\left(A^{hs} + A^{chain} + A^{disp}\right)}{R\,T}}{\partial \eta}\right)$$

Alternatively, the above equation could be rewritten as:

$$\frac{A^{res}}{R\,T} = \frac{A^{hs} + A^{chain} + A^{disp}}{R\,T} = \int_0^{\eta} \frac{Z-1}{\eta}\,d\eta \tag{5.2}$$

$$= \int_0^{\eta} \frac{Z^{hs} + Z^{chain} + Z^{disp}}{\eta}\,d\eta$$

5.2.1. Hard Sphere Term

Any accurate hard sphere model, such as the models investigated in **Chapter 2**, could be utilized in the above equation after subtracting the ideal gas term since it is explicitly given in equation (5.1). Table 5.1 summarizes the hard sphere models that will be investigated in this study and their corresponding residual Helmholtz free energy (A^{hs})

are given in Table 5.2. The residual Helmholtz free energy could be calculated by equation (5.2).

Table 5.1: Selected hard sphere models from Chapter 2 to be substituted in equation (5.1)

Carnahan and Starling, (1969)	$Z^{hs} = m\left(\frac{1+\eta+\eta^2-\eta^3}{(1-\eta)^3}-1\right)$
Kolafa, (1986)	$Z^{hs} = m\left(\frac{1+\eta+\eta^2-\frac{2}{3}(\eta^3+\eta^4)}{(1-\eta)^3}-1\right)$
Khoshbarchi and Vera, (1997)	$Z^{hs} = m\left(\frac{1-\frac{1}{25}\xi-\frac{2}{5}\xi^2-\frac{5}{4}\xi^3+\frac{9}{50}\xi^5+\frac{71}{50}\xi^{12}}{(1-\xi)^3}-1\right)$
Yelash and Kraska, (2001)	$Z^{hs} = m\left(\frac{3+8\eta+14\eta^2+14\eta^3+\frac{40}{3}\eta^4}{3-4\eta}-1\right)$
Rambaldi et al., (2006)	$Z^{hs} = m\left(\frac{4\eta}{1-2.5\eta+1.658808\eta^2}\right)$

Table 5.2: Residual Helmholtz free energy of the selected hard sphere models

Carnahan and Starling, (1969)	$\frac{A^{hs}}{R\,T} = m\frac{(4-3\eta)\eta}{(-1+\eta)^2}$
Kolafa, (1986)	$\frac{A^{hs}}{R\,T} = m\frac{1}{6}\left(\frac{\eta\left(34+\eta(-33+4\eta)\right)}{(-1+\eta)^2} + 10\ln(1-\eta)\right)$
Khoshbarchi and Vera, (1997)	$\frac{A^{hs}}{R\,T} = -m\frac{1}{25200(-1+\xi)^2}(\xi(1914444 - 2903418\xi + 665112\xi^2 + 166278\xi^3 + 65604\xi^4 + 32802\xi^5 + 18744\xi^6 + 11715\xi^7 + 7810\xi^8 + 5467\xi^9 + 3976\xi^{10}) + 1989036(-1+\xi)^2\ln(1-\xi))$
Yelash and Kraska, (2001)	$\frac{A^{hs}}{R\,T} = m\frac{1}{9}\left(-\eta\left(72+\eta(27+10\eta)\right) - 162\,\mathrm{arctanh}\left(\frac{2\eta}{-3+2\eta}\right)\right)$
Rambaldi et al., (2006)	$\frac{A^{hs}}{R\,T} = m\left(20.2464 + 12.8892\arctan\left(4.0279 - \frac{3.2223}{\eta}\right)\right)$

5.2.2. Chain Term

The chain term could be obtained from one of the chain theories, such as the theories considered in **Chapter 3**. In this chapter, TPT1 will be utilized since it is the most commonly used theory. Table 5.3 displays the chain terms derived using TPT1 for each investigated hard sphere model and their corresponding residual Helmholtz free energy (A^{chain}) are given in table 5.4.

Table 5.3: Chain terms obtained from TPT1

Hard Sphere Models	Corresponding chain terms obtained from TPT1
Carnahan and Starling, (1969)	$Z^{chain} = (1-m)\frac{(5-2\eta)\eta}{2-3\eta+\eta^2}$
Kolafa, (1986)	$Z^{chain} = -(1-m)\frac{5\eta\left(-6+\eta(2+\eta)\right)}{(-1+\eta)\left(-12+\eta\left(6+\eta(-1+2\eta)\right)\right)}$
Khoshbarchi and Vera, (1997)	$Z^{chain} = (1-m)\left(8-\frac{3}{-1+\xi} + \frac{-3256+\xi(3400+225\xi-126\xi^3)}{296+\xi(-340-25\xi+18\xi^3+142\xi^{10})}\right)$
Yelash and Kraska, (2001)	$Z^{chain} = (1-m)\frac{\eta(-3+2\eta)\left(45+8\eta(9+10\eta)\right)}{-54+\eta\left(9+\eta\left(21+8\eta(3+10\eta)\right)\right)}$

Rambaldi et al., (2006)	$Z^{chain} = (1-m)\dfrac{(1.50711-2\eta)\eta}{0.602843+\eta(-1.50711+\eta)}$

Table 5.4: Residual Helmholtz free energy for the chain terms

Carnahan and Starling, (1969)	$\dfrac{A^{chain}}{R\,T} = (1-m)\ln\left(\dfrac{-2+\eta}{2(-1+\eta)^3}\right)$
Kolafa, (1986)	$\dfrac{A^{chain}}{R\,T} = (1-m)\ln\left(\dfrac{-12+\eta\left(6+\eta(-1+2\eta)\right)}{12(-1+\eta)^3}\right)$
Khoshbarchi and Vera, (1997)	$\dfrac{A^{chain}}{R\,T} = (1-m)\ln(((3(148\sqrt{2}\pi^{11} - 1020\pi^{10}\,\eta - 225\sqrt{2}\pi^{9}\,\eta^2 + 2916\sqrt{2}\pi^{7}\,\eta^4 + 804955968\eta^{11}\,)))$ / $((200\pi^{9}\left(\pi - 3\sqrt{2}\eta\right)^3\,))$
Yelash and Kraska, (2001)	$\dfrac{A^{chain}}{R\,T} = (1-m)\ln\left(-2+\dfrac{9}{3-4\eta}-\dfrac{1}{6}\eta(9+5\eta)\right)$
Rambaldi et al., (2006)	$\dfrac{A^{chain}}{R\,T} = (1-m)\ln\left(\dfrac{1}{1+\eta(-2.5+1.658808\eta)}\right)$

5.2.3. Dispersion Term

In order to minimize the complexity of equation (5.1) and to explore the effect of changing the hard sphere term, the dispersion term will be fixed. As indicated previously, the simple dispersion term of Fu and Sandler (1995) will be used:

$$Z^{disp} = -m\, Z_M \left(\frac{v^* Y}{v_s + v^* Y}\right) \tag{5.3}$$

In terms of the Helmholtz free energy, the dispersion term is given by:

$$\frac{A^{disp}}{R\,T} = m\, Z_M \ln\left(\frac{v_s}{v_s + v^* Y}\right) \tag{5.4}$$

where v_s is the molar volume of a segment, Z_M is the maximum coordination number that was taken to be equal 36 and v^* is the closed-packed molar volume of a segment which is defined as:

$$v^* = \frac{N_{Av} d^3}{\sqrt{2}} \tag{5.5}$$

N_{Av} is Avogadro's number and d is the effective hard sphere dimeter that is given by:

$$d = \sigma[1 - c\, \exp(-3u^0/kT)] \tag{5.6}$$

where σ is the temperature independent diameter of a segment, c is an adjustable parameter, u^0 is the temperature independent square-well depth and k is the Boltzmann's constant. The variable Y is defined as:

$$Y = \exp\left(\frac{u}{2kT}\right) - 1 \tag{5.7}$$

where u is the temperature dependence square-well depth that is given by:

$$u = u^0[1 + (e/kT)] \tag{5.8}$$

e/k is an adjustable parameter based on fitting experimental vapor-liquid equilibrium data.

To use this dispersion term with any hard sphere model, there are three adjustable parameters that need to be found: m, u^0 and σ. However, it is more convenient to use molar volume rather than the dimeter of a segment as an adjustable parameter. The temperature independent molar volume in a closed-packed arrangement (v^{00}) is given by:

$$v^{00} = (\pi N_{Av}/6\eta_c)\sigma^3 \tag{5.9}$$

where η_c is the maximum packing fraction that was taken to be equal to $\pi\sqrt{2}/6 \approx 0.74048$

In addition to the above three adjustable parameters there are additional two universal parameters: c and e/k that are based on adjusting the experimental values of the vapor pressure and the liquid density of a specific component. In this study, ethane was selected as the main component in the comparison between the models.

5.3. Parameters estimation

In this work, the experimental data for the vapor pressure and the liquid density were taken from Vargaftik (1975). In thus work, the adjustable parameters were obtained by simultaneously fitting vapor pressures and liquid densities using the simplex method. Table 5.5 summarizes the five adjustable parameters for ethane using different HS models while fixing the chain term to the one obtained from TPT1 based on CS model.

Alternatively, Table 5.6 represents the five adjustable parameters for ethane using different HS models with their corresponding chain terms obtained from TPT1.

Table 5.5: Ethane parameters for different HS models with same chain term

Hard Sphere Model	m	v^{00} (mL)	u^0/k (K)	c	e/k (K)
Carnahan and Starling, (1969)	2.4056	13.436	82.999	0.32946	-13.184
Kolafa, (1986)	2.4386	13.232	82.574	0.33157	-13.443
Khoshbarchi and Vera, (1997)	2.4353	13.254	82.469	0.32962	-13.318
Yelash and Kraska, (2001)	2.3868	13.574	83.341	0.33044	-13.154
Rambaldi et al., (2006)	2.5165	12.693	81.322	0.32903	-13.599

Table 5.6: Ethane parameters for different HS models with their corresponding chain terms obtained from TPT1

Hard Sphere Model	m	v^{00} (mL)	u^0/k (K)	c	e/k (K)
Carnahan and Starling, (1969)	2.4056	13.436	82.999	0.32946	-13.184
Kolafa, (1986)	2.4769	13.009	81.83	0.33089	-13.579
Khoshbarchi and Vera, (1997)	2.4247	13.302	82.586	0.32811	-13.169
Yelash and Kraska, (2001)	2.4143	13.418	82.913	0.3319	-13.389
Rambaldi et al., (2006)	2.5244	12.647	80.908	0.32532	-13.434

5.4. Comparison with molecular simulation data

This study will first investigate the effect of changing the hard sphere term while fixing the other terms in equation (5.1). Second, the effect of using the corresponding chain term of the various HS models will be explored. Therefore, it would be beneficial to test the accuracy of different combinations with the molecular simulation data of the hard chain. Table 5.7 summarizes the average absolute deviation (AAD) for the compressibility factor predicted by the various hard sphere models while fixing the chain term to CS. The simulation data for $m \leq 16$ and $m = 32$ were adopted from Chang and

Sandler (1994) and Denlinger and Hall (1990), respectively. The values for the 51-mer and 201-mer chains were obtained by Gao and Weiner (1989).

Table 5.7: Percentage Average Absolute Deviation (AAD) of the calculated compressibility of m-hard-sphere chains obtained by various HS models while fixing the chain term to CS

	AAD (%)				
m	**Carnahan and Starling**	**Kolafa**	**Khoshbarchi and Vera**	**Yelash and Kraska**	**Rambaldi et al.**
4	2.57	2.88	2.59	2.47	3.86
8	5.33	5.69	5.35	5.21	6.78
16	9.04	9.37	9.08	8.93	10.26
32	14.63	15.06	14.65	14.55	15.68
51	9.26	9.68	9.26	9.15	10.82
201	14.06	14.49	14.04	13.96	15.64
Overall	7.87	8.24	7.89	7.76	9.25

Likewise, the average absolute deviation (AAD) for the compressibility factor predicted by the various hard sphere models with their corresponding chain terms are illustrated in Table 5.8.

Table 5.8: Percentage Average Absolute Deviation (AAD) of the calculated compressibility of m-hard-sphere chains compared with molecular simulation data

	AAD (%)				
m	**Carnahan and Starling**	**Kolafa**	**Khoshbarchi and Vera**	**Yelash and Kraska**	**Rambaldi et al.**
4	2.57	2.84	2.61	2.49	3.51
8	5.33	5.62	5.37	5.19	6.27
16	9.04	9.19	8.99	9.05	9.46
32	14.63	14.71	14.48	14.71	14.51
51	9.26	9.51	9.25	9.13	10.02
201	14.06	14.29	14.03	13.93	14.78
Overall	7.87	8.10	7.86	7.79	8.58

From the results of both tables, one could conclude that there is a minor variation in the accuracy when utilizing the corresponding chain terms of the different HS models. However, it is not clear how the PVT behavior in a complete EOS will be influenced.

5.5. Bifurcation diagrams

Bifurcation diagrams that were discussed in **Chapter 4** will be utilized in this work to demonstrate the role of the hard sphere term in the complete EOS. This study will focus on the PVT behavior in the first quadrant only. Therefore, the branches on the other quadrants will not be displayed. In addition, the bifurcation diagram of PR EOS will be shown for comparison.

5.5.1. Bifurcation diagrams for short-chain compounds using CS model in the chain term: branches, turning points and number of roots

With the consideration of non-associating components, both PR and equation (5.1) are similar in terms of the associated interaction regardless of the accuracy. Figures (5.1 – 5.12) illustrate how the number of compressibility factor (Z) roots varies with temperature for ethane at 1 atm. Unlike PR EOS, the other equations exhibit more than one branch with multiple turning points as depicted in Figures 5.2-5.12. The upper branches in these figures are similar to the single branch resulted by PR EOS. However, there are two more turning points on this branch located at low temperature region in the region (13.79 – 13.89) K. This is an indication of liquid-liquid demixing which is an improper behavior for pure components. By exploring the bifurcation diagrams in Figures 5.2-5.12, one could conclude that CS model produces the least number of roots that is

four roots located in the temperature range (71.97 - 284.82) K. The additional branches on the other models may result because of the inconsistency of the chain term with the HS terms. For this reason, the bifurcation diagrams when the corresponding chain term is utilized will be investigated.

Peng & Robinson, (1976)	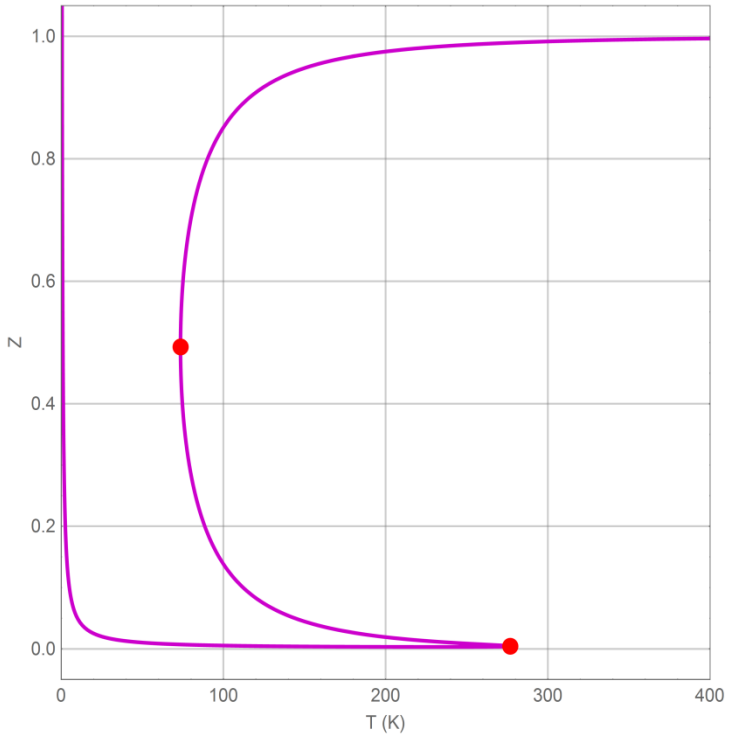 **Figure 5.1: Bifurcation diagram for ethane at 1 atm using PR EOS**

Carnahan and Starling, (1969)	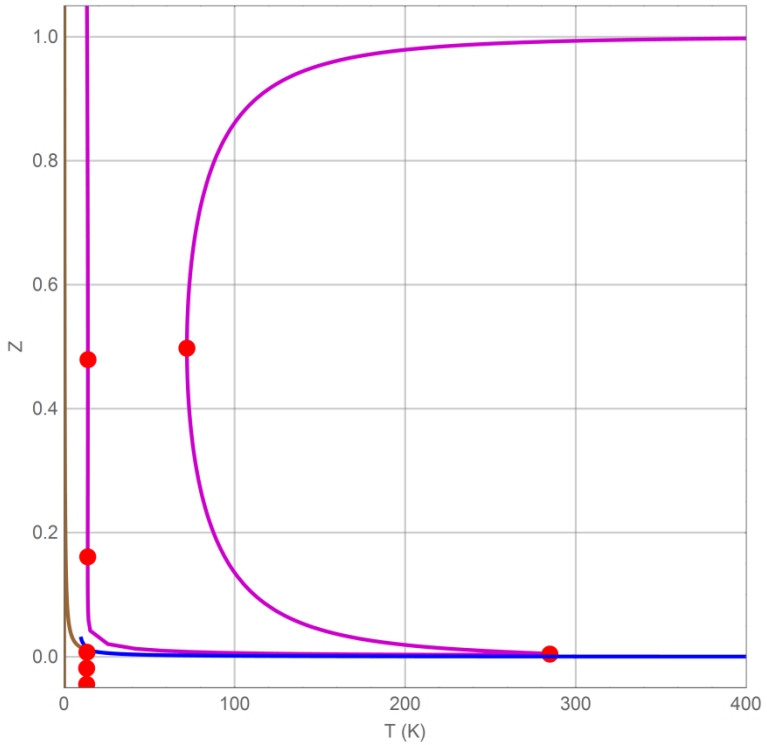 **Figure 5.2: Bifurcation diagram for ethane at 1 atm using CS HS model**	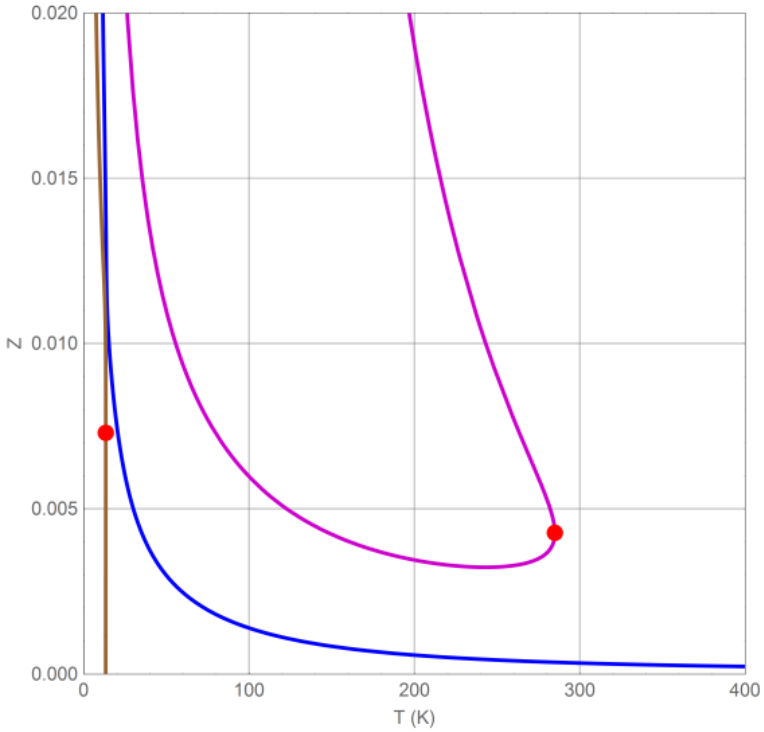 **Figure 5.3: Magnified range of the bifurcation diagram for ethane at 1 atm using CS HS model**

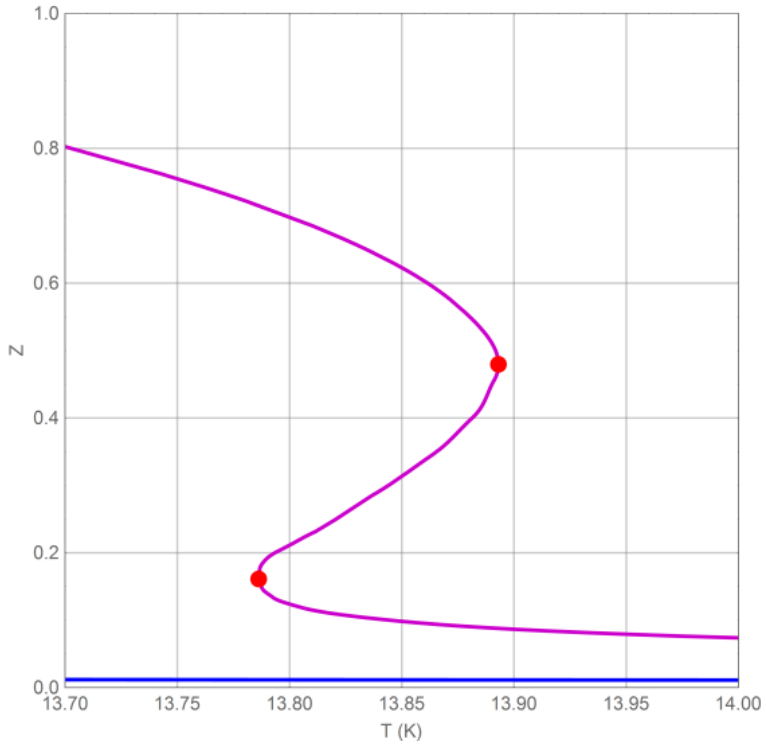

Figure 5.4: Magnified range of the bifurcation diagram for ethane at 1 atm using CS HS model showing the two turning points at low temperature

Kolafa, (1986)	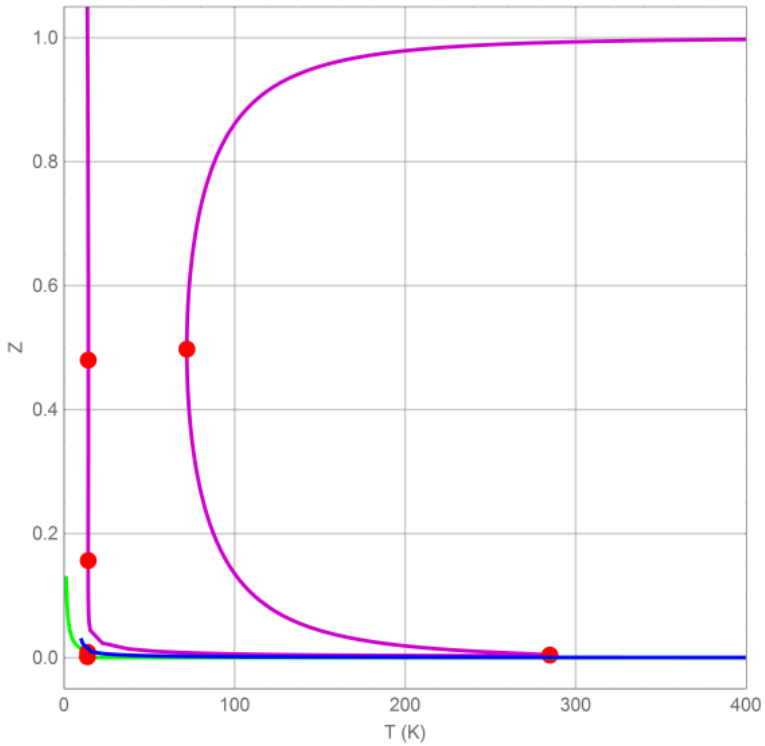 **Figure 5.5: Bifurcation diagram for ethane at 1 atm using Kolafa HS model**	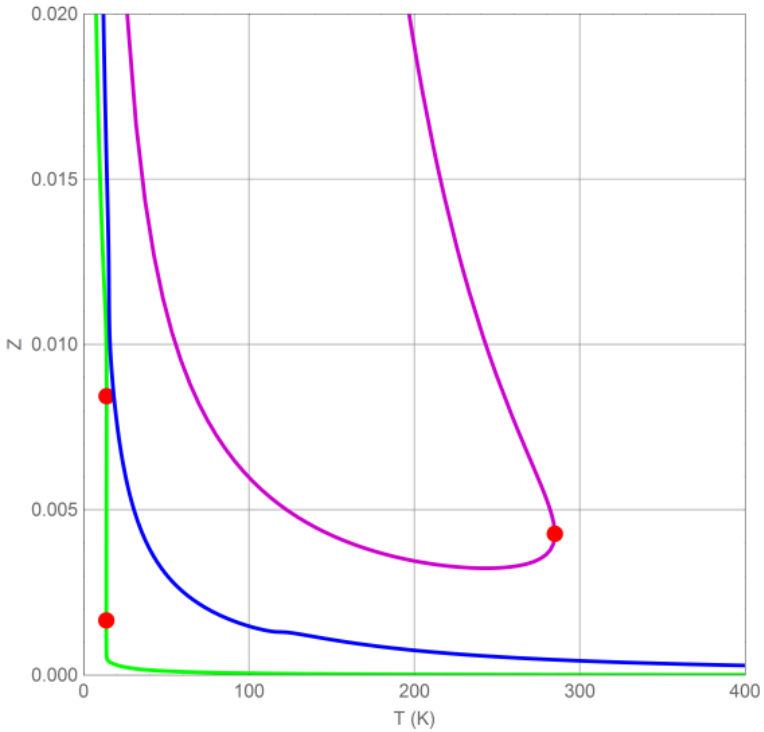 **Figure 5.6: Magnified range of the bifurcation diagram for ethane at 1 atm using Kolafa HS model**

Khoshbarchi and Vera, (1997)	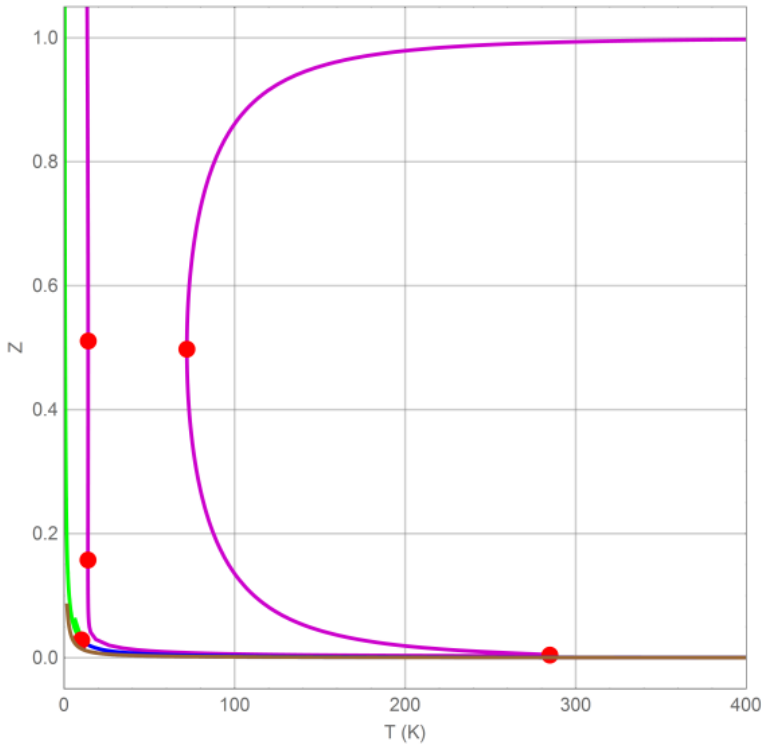 **Figure 5.7: Bifurcation diagram for ethane at 1 atm using Khoshbarchi and Vera HS model**	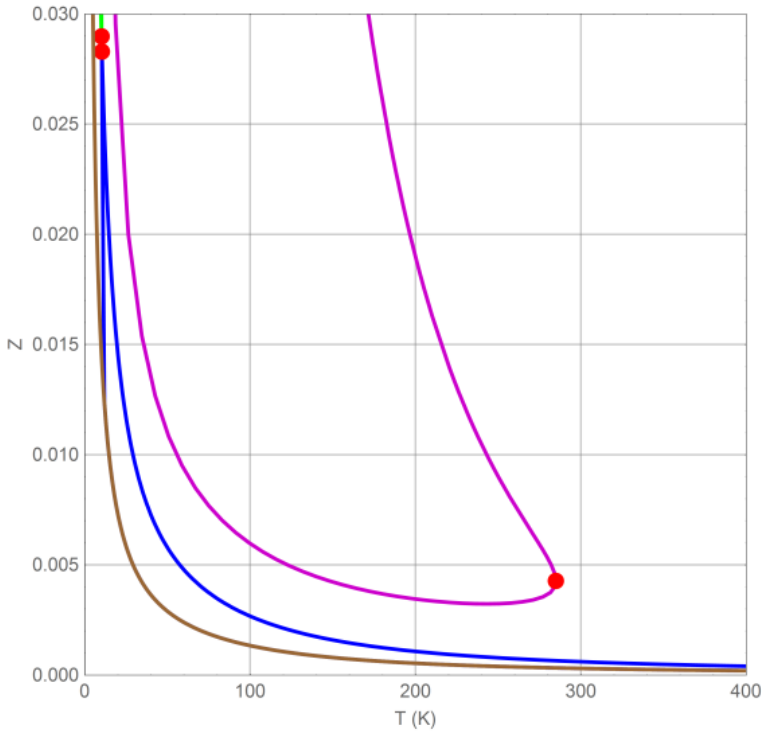 **Figure 5.8: Magnified range of the bifurcation diagram for ethane at 1 atm using Khoshbarchi and Vera HS model**

Yelash and Kraska, (2001)	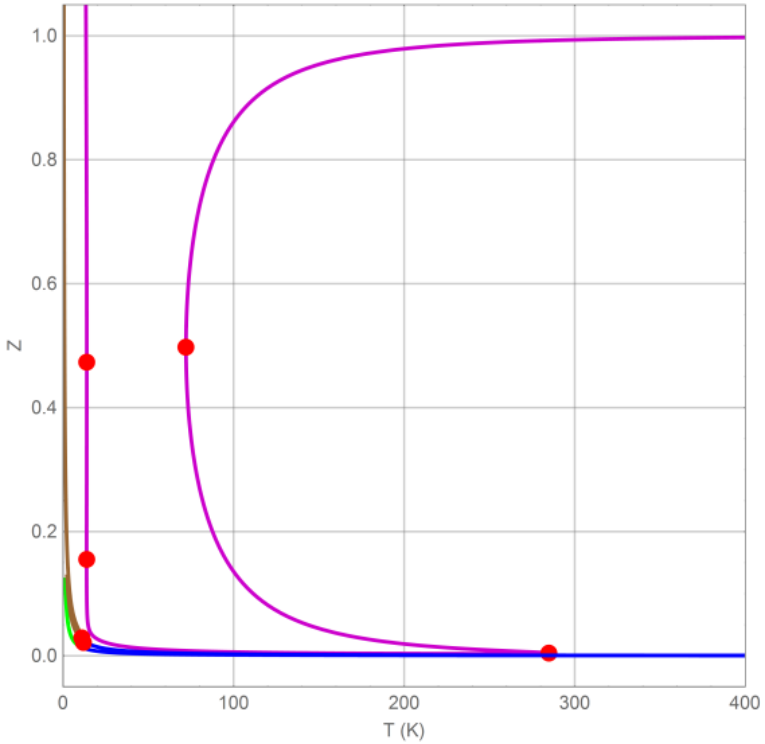 **Figure 5.9: Bifurcation diagram for ethane at 1 atm using Yelash and Kraska HS model**	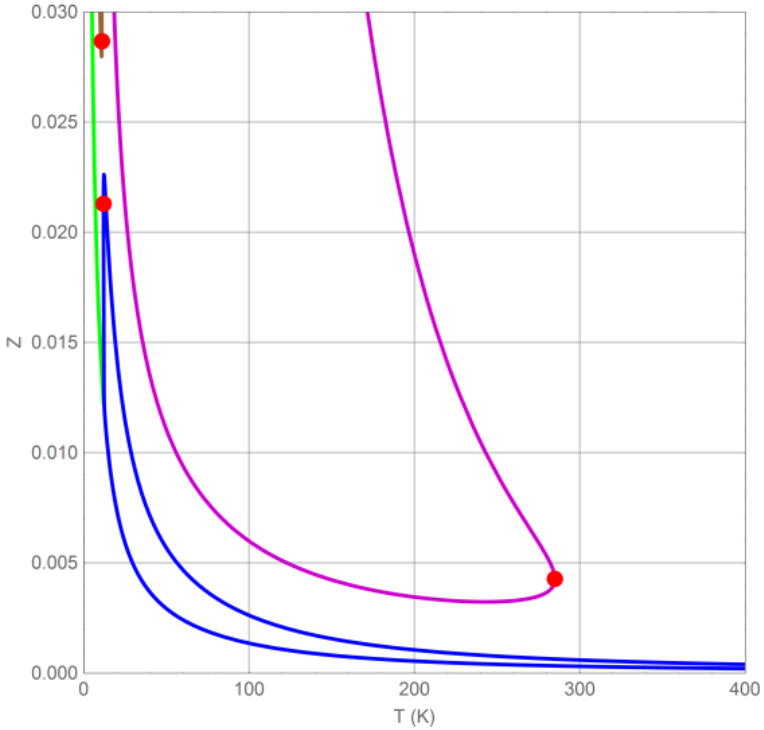 **Figure 5.10: Magnified range of the bifurcation diagram for ethane at 1 atm using Yelash and Kraska HS model**

Rambaldi et al., (2006)

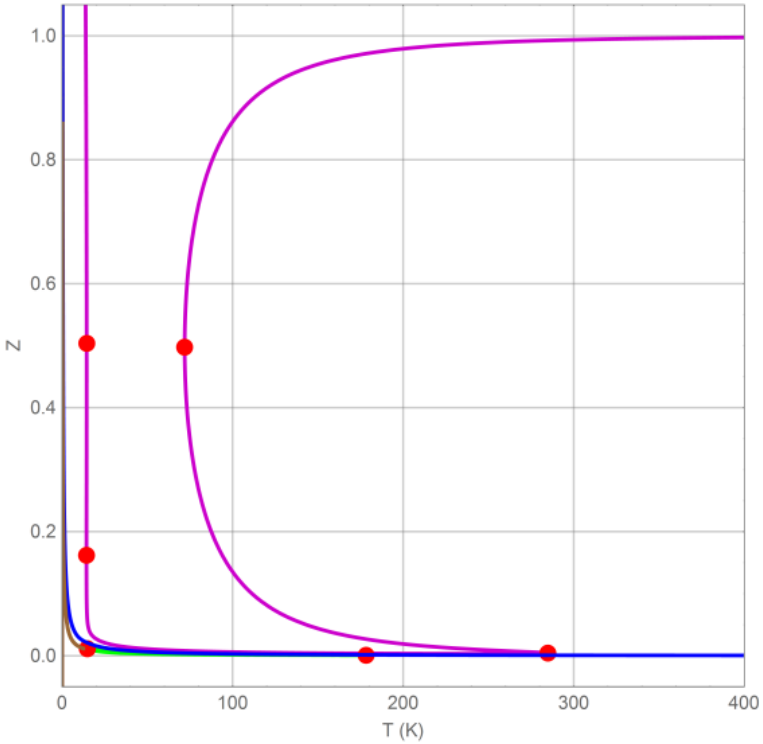

Figure 5.11: Bifurcation diagram for ethane at 1 atm using Rambaldi et al. HS model

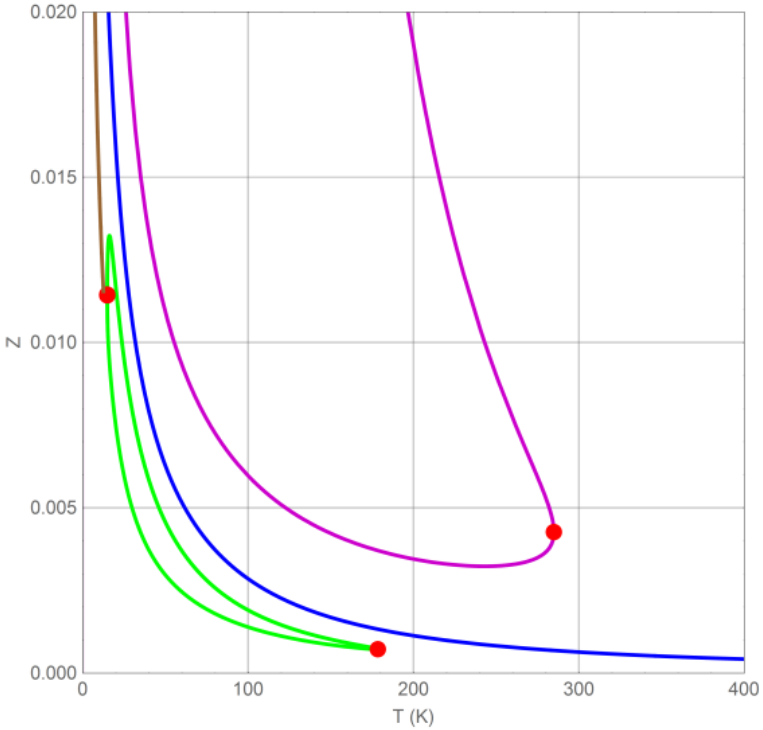

Figure 5.12: Magnified range of the bifurcation diagram for ethane at 1 atm using Rambaldi et al. HS model

5.5.2. Bifurcation diagrams for short-chain compounds using various hard sphere models in the chain term: branches, turning points and number of roots

By exploring the Figures 5.13-5.19, it is clear that the number of branches decreases when the corresponding chain term is used. However, this is not the case for Kolafa model that has same number of branches with more turning points in the lower branch leading to maximum of seven roots in temperature range of 273.26-284.85 K. The models of Khoshbarchi & Vera and Yelash & Kraska have only one branch in the first quadrant for temperatures above 15 K. Although the model of Khoshbarchi & Vera is mathematically complex, it has the least number of roots. Hence, it is not necessarily that the complex models will result in multiple roots.

From the previous diagrams, it is clear that all models suffer from predicting the two turning points at low temperature region. Furthermore, there is no completely a model without non-physical behavior like Peng & Robinson. Therefore, it would be beneficial to explore the role of changing the chain theory and dispersion term.

Kolafa, (1986)	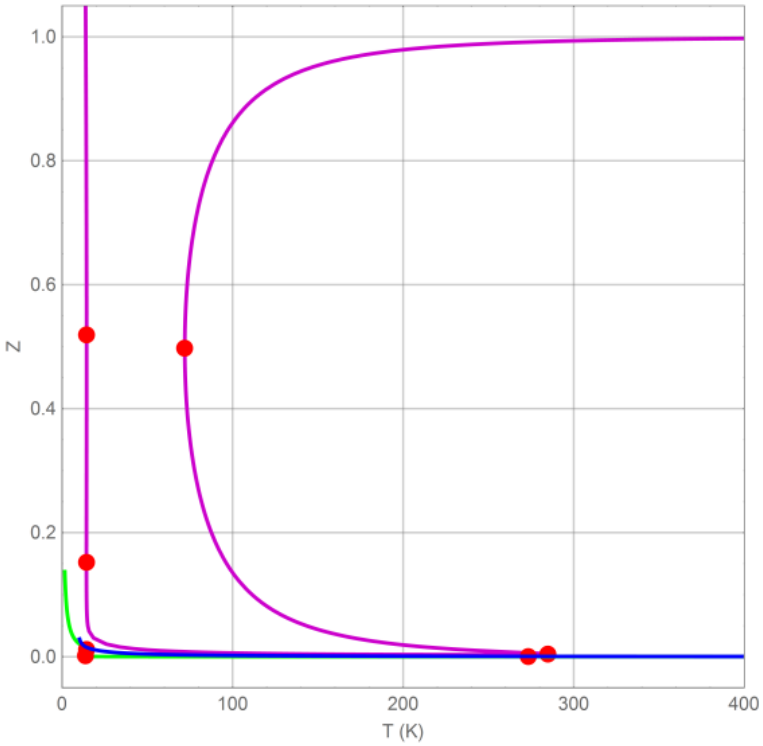 **Figure 5.13: Bifurcation diagram for ethane at 1 atm using Kolafa HS model and its corresponding chain term**	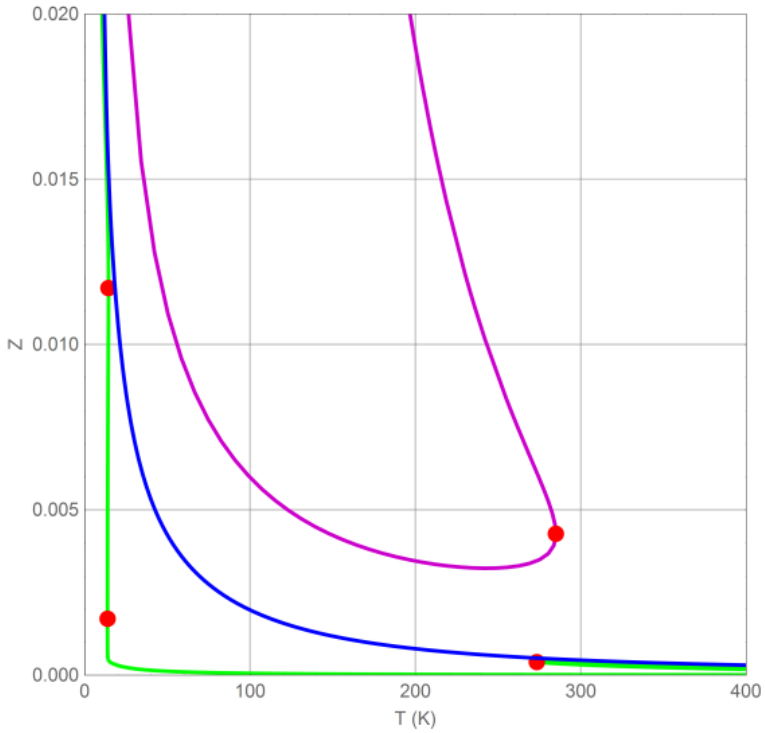 **Figure 5.14: Magnified range of the bifurcation diagram for ethane at 1 atm using Kolafa HS model and its corresponding chain term**

Khoshbarchi and Vera, (1997)	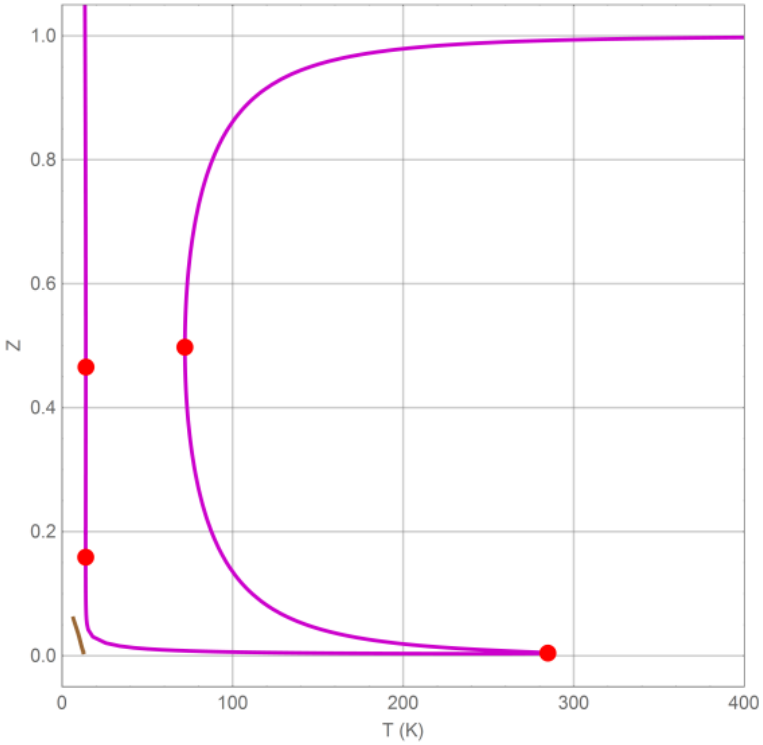 **Figure 5.15: Bifurcation diagram for ethane at 1 atm using Khoshbarchi and Vera HS model and its corresponding chain term**	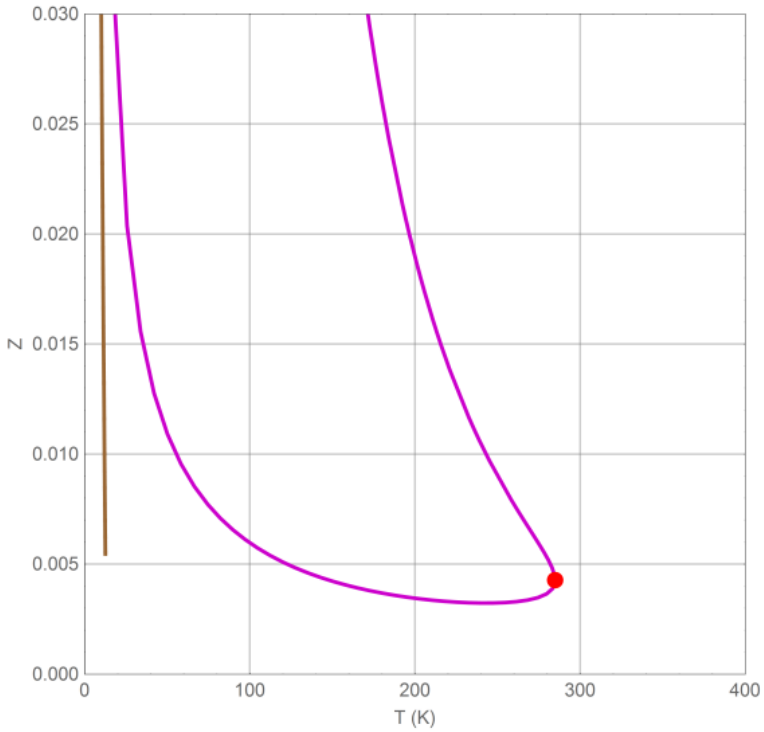 **Figure 5.16: Magnified range of the bifurcation diagram for ethane at 1 atm using Khoshbarchi and Vera HS model and its corresponding chain term**

Yelash and Kraska, (2001)	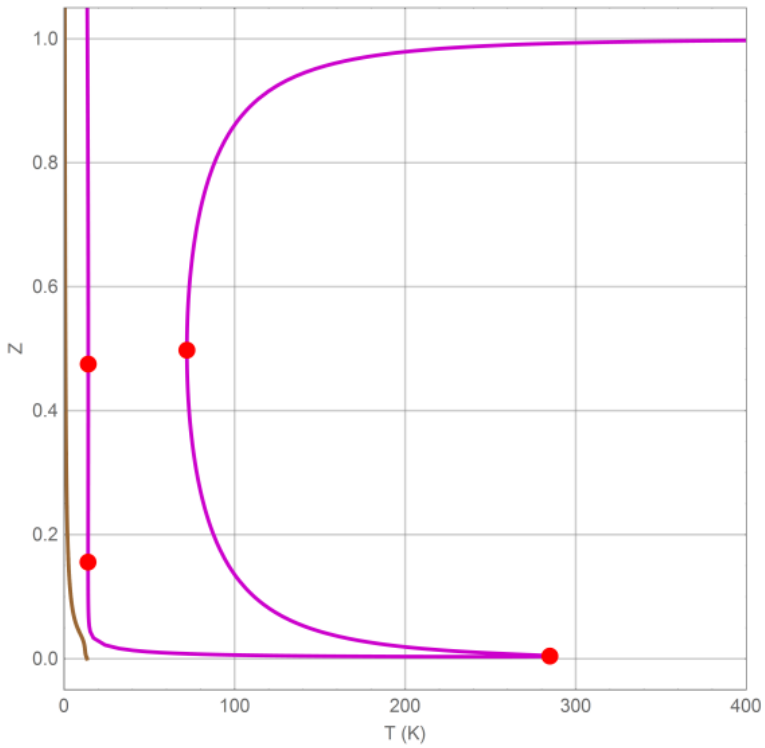 **Figure 5.17: Bifurcation diagram for ethane at 1 atm using Yelash and Kraska HS model and its corresponding chain term**	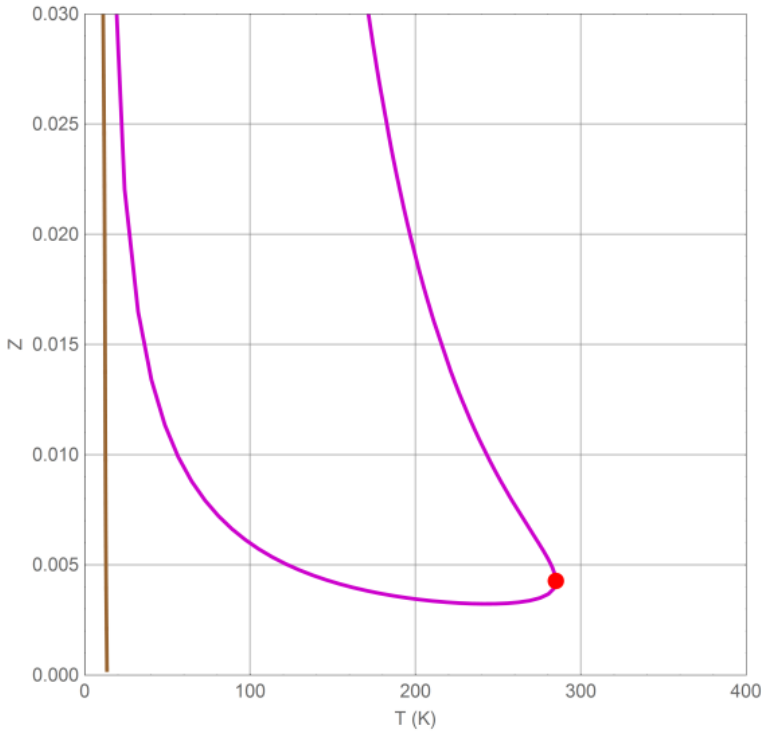 **Figure 5.18: Magnified range of the bifurcation diagram for ethane at 1 atm using Yelash and Kraska HS model and its corresponding chain term**

Rambaldi et al., (2006)	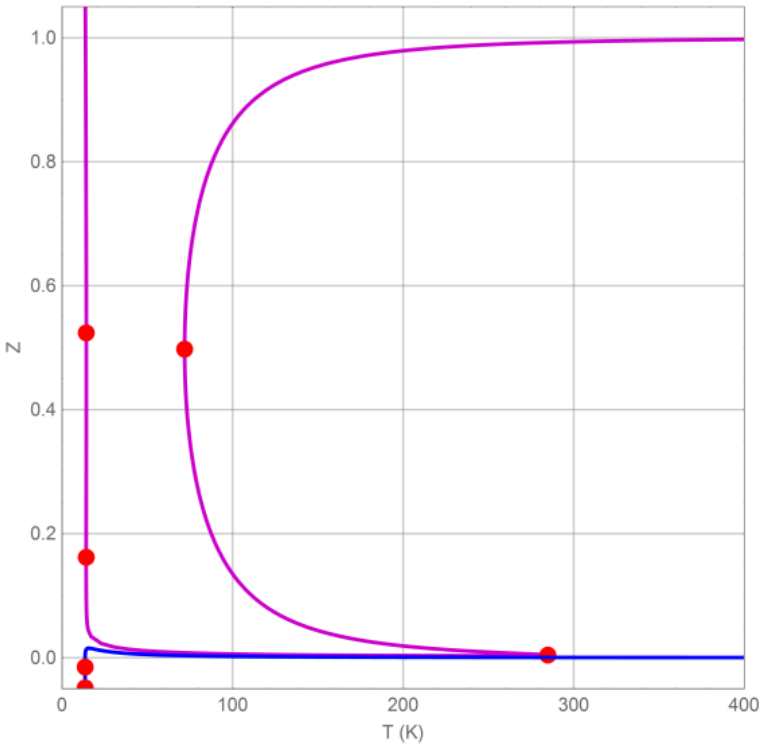 **Figure 5.19: Bifurcation diagram for ethane at 1 atm using Rambaldi et al. HS model and its corresponding chain term**	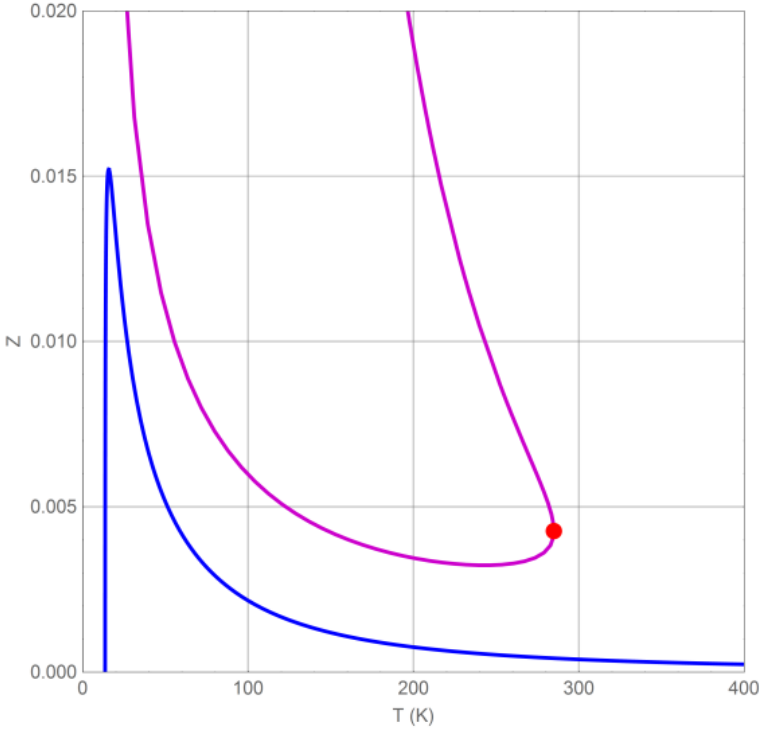 **Figure 5.20: Magnified range of the bifurcation diagram for ethane at 1 atm using Rambaldi et al. HS model EOS and its corresponding chain term**

CHAPTER 6

THE ROLE OF VARIOUS HARD CHAIN THEORIES ON PVT BEHAVIOR OF NON-ASSOCIATING FLUID: BIFURCATION ANALYSIS

6.1. Introduction

The hard chain theories along with their accuracies were discussed in **Chapter 3**. These theories differ in their mathematical forms and have shown different accuracy in comparison with the molecular simulation data. The difference in the mathematical form is expected to affect the PVT behaviour in a complete EOS.

In this chapter, the most common hard chain theories will be adopted in order to study their influence on the PVT behavior. The bifurcation diagrams will be utilized to accomplish this objective. The bifurcation analysis for TPT1 was considered in the previous chapter with various hard sphere models. The same hard sphere models will be used in this chapter but with different chain theories. The dispersion term will be fixed to the one that was proposed by Fu and Sandler (1995).

6.2. Mathematical formulas and derivations

As previously given in Chapter 5, the compressibility factor is given by:

$$Z = \frac{P\,V}{R\,T} = 1 + Z^{hs} + Z^{chain} + Z^{disp} = 1 + \eta\left(\frac{\frac{\partial A^{res}}{R\,T}}{\partial \eta}\right) \tag{5.1}$$

$$= 1 + \eta\left(\frac{\frac{\partial\left(A^{hs} + A^{chain} + A^{disp}\right)}{R\,T}}{\partial \eta}\right)$$

For more convenience in the GFD theory, the above equation could be rewritten as:

$$Z = \frac{P\,V}{R\,T} = Z^{GFD} + Z^{disp} = 1 + \eta\left(\frac{\frac{\partial A^{res}}{R\,T}}{\partial \eta}\right) \tag{6.1}$$

$$= 1 + \eta\left(\frac{\frac{\partial\left(A^{GFD} + A^{disp}\right)}{R\,T}}{\partial \eta}\right)$$

where Z^{GFD} is the compressibility factor calculated by equation (3.8).

In this chapter, the same five HS models will be used but with different theories for the chain term. Equations (3.1) to (3.10) in **Chapter 3** could be used to derive the chain terms from various hard sphere models. The results for TPT1 were shown in **Chapter 5**. The derivations for the other theories are represented in Tables 6.1-6.6.

Table 6.1: Chain terms obtained from HSC theory

Hard Sphere Models	**Corresponding chain terms obtained from HSC**
Carnahan and Starling, (1969)	$Z^{chain} = (m-1)\frac{\eta(5 + 2(-3+\eta)\eta)}{2(-1+\eta)^3}$
Kolafa, (1986)	$Z^{chain} = (m-1)\frac{5(-2+\eta)\eta(-3+2\eta)}{12(-1+\eta)^3}$

Khoshbarchi and Vera, (1997)	$Z^{chain} = (m-1)(400\pi(-1+\xi)^3 + 3\sqrt{2}(296 + \xi(-340 - 25\xi + 18\xi^3 + 142\xi^{10})))/(400\pi(-1+\xi)^3)$
Yelash and Kraska, (2001)	$Z^{chain} = (m-1)\frac{1}{6}\eta\left(9 + 5\eta + \frac{72}{-3+4\eta}\right)$
Rambaldi et al., (2006)	$Z^{chain} = (m-1)\left(1 - \frac{1}{1+\eta(-2.5+1.658808\eta)}\right)$

Table 6.2: Residual Helmholtz free energy for the chain terms obtained from HSC

Carnahan and Starling, (1969)	$\frac{A^{chain}}{R\,T} = (m-1)\left(\frac{\eta(-6+5\eta)}{4(-1+\eta)^2} + \ln(1-\eta)\right)$
Kolafa, (1986)	$\frac{A^{chain}}{R\,T} = (m-1)\frac{5}{24}\left(\frac{\eta(-8+7\eta)}{(-1+\eta)^2} + 4\ln(1-\eta)\right)$
Khoshbarchi and Vera, (1997) "approximated"	$\frac{A^{chain}}{R\,T} = (m-1)(3\sqrt{2}\,\xi(173376 + \xi(-262626 + \xi(60144 + 71\xi(210 + \xi(84 + \xi(42 + \xi(24 + \xi(15 + \xi(10 + 7\xi)))))))) + 112\left(4833\sqrt{2} + 100\pi\right)(-1+\xi)^2\ln(1-\xi))/(11200\pi(-1+\xi)^2)$

Yelash and Kraska, (2001)	$\frac{A^{chain}}{R\,T} = (m-1)\left(\frac{1}{12}\eta(18+5\eta) + 6\,\mathrm{arctanh}\left(\frac{2\eta}{-3+2\eta}\right)\right)$
Rambaldi et al., (2006)	$\frac{A^{chain}}{R\,T} = (m-1)(-5.0938 + 4.0279\arctan(4.0279 - 5.3452\eta) + 0.5\ln(0.6028 - 1.5071\,\eta + \eta^2))$

Table 6.3: Chain terms obtained from TPT-D theory

Hard Sphere Models	Corresponding chain terms obtained from TPT-D
Carnahan and Starling, (1969)	$Z^{chain} = \frac{(-1+m)\eta(-5+2\eta)}{(-2+\eta)(-1+\eta)} + \frac{(2-m)0.98505\eta}{2(0.73017+0.98505\eta)}$
Kolafa, (1986)	$Z^{chain} = \frac{(2-m)0.98544\eta}{2(0.72854+0.98544\eta)} + \frac{5(-1+m)\eta(-6+\eta(2+\eta))}{(-1+\eta)(-12+\eta(6+\eta(-1+2\eta)))}$
Khoshbarchi and Vera, (1997)	$Z^{chain} = (\pi\xi(-(6(-2+m)0.9777)/(60.73207 + \sqrt{2}\,\pi 0.9777\xi) - (6\sqrt{2}(-1+m)(-548 + \xi(730 + \xi(25 + 2\xi(-36 + \xi(9 + 71\xi^6\,(-11 + 8\xi)))))))/(\pi(-1+\xi)(296 + \xi(-340 - 25\xi + 18\xi^3 + 142\xi^{10}))))/(6\sqrt{2})$

Yelash and Kraska, (2001)	$Z^{chain} = \frac{(2-m)0.99303\eta}{2(0.73671+0.99303\eta)} - \frac{(-1+m)\eta(-3+2\eta)(45+8\eta(9+10\eta))}{-54+\eta(9+\eta(21+8\eta(3+10\eta)))}$
Rambaldi et al., (2006)	$Z^{chain} = \frac{(2-m)0.98239\eta}{2(0.72448+0.98239\eta)} + \frac{2(-1+m)\eta(-0.7536+\eta)}{0.6028+\eta(-1.5071+\eta)}$

Table 6.4: Residual Helmholtz free energy for the chain terms obtain from TPT-D

Carnahan and Starling, (1969)	$\frac{A^{chain}}{R\,T} = (-1+m)\left(3\ln(1-\eta) + \ln\left(-\frac{2}{-2+\eta}\right)\right) - \frac{1}{2}(-2+m)\ln\left(1+\frac{0.98505\eta}{0.73017}\right)$
Kolafa, (1986)	$\frac{A^{chain}}{R\,T} = -\frac{1}{2}(-2+m)\ln\left(1+\frac{0.98544\eta}{0.72854}\right) + (-1+m)\left(3\ln(1-\eta) + \ln\left(\frac{12}{12+\eta(-6+\eta-2\eta^2)}\right)\right)$

Khoshbarchi and Vera, (1997)	$$\frac{A^{chain}}{R\,T} = -\frac{1}{2}(-2+m)\ln\left(1+\frac{\pi 0.9777\xi}{3\sqrt{2}\,0.73207}\right) + \frac{1}{2}(-1+m)\left(\ln(43808)+16\ln(\pi)+6\ln(\pi-\pi\xi) - 2\ln\left(148\sqrt{2}\pi^{11} - 170\sqrt{2}\pi^{11}\xi - \frac{25\pi^{11}\xi^2}{\sqrt{2}} + 9\sqrt{2}\pi^{11}\xi^4 + 71\sqrt{2}\pi^{11}\xi^{11}\right)\right)$$
Yelash and Kraska, (2001)	$$\frac{A^{chain}}{R\,T} = -\frac{1}{2}(-2+m)\ln\left(1+\frac{0.99303\eta}{0.73671}\right) + (-1+m)\ln\left(\frac{18-24\eta}{18+\eta\left(21+\eta(21+20\eta)\right)}\right)$$
Rambaldi et al., (2006)	$$\frac{A^{chain}}{R\,T} = -\frac{1}{2}(-2+m)\ln\left(1+\frac{0.98239\eta}{0.72448}\right) + (-1+m)(0.5061+\ln(0.6028-1.5071\eta+\eta^2))$$

Table 6.5: Chain terms obtained from GFD theory

Hard Sphere Models	Corresponding chain terms obtained from GFD
Carnahan and Starling, (1969)	Z^{GFD} $= \frac{(1.95926 + 0.95926(-3+m))(1 + 2.45696\eta + 4.10386\eta^2 - 3.7550}{(1-\eta)^3}$ $- \frac{\big(0.95926 + 0.95926(-3+m)\big)(1+\eta+\eta^2-\eta^3)}{(1-\eta)^3}$
Kolafa, (1986)	Z^{GFD} $= \frac{(1.95926 + 0.95926(-3+m))(1 + 2.45696\eta + 4.10386\eta^2 - 3.7550}{(1-\eta)^3}$ $- \frac{\big(0.95926 + 0.95926(-3+m)\big)\left(1+\eta+\eta^2-\frac{2}{3}(\eta^3+\eta^4)\right)}{(1-\eta)^3}$
Khoshbarchi and Vera, (1997)	$Z^{GFD} = \big(1.95926 + 0.95926(-3+m)\big)(1 + 2.45696\eta + 4.10386\eta^2 - 3.75503\eta^3)(1-\eta)^3 - \big(0.95926 + 0.95926(-3+m)\big)\left(1 - \frac{3\sqrt{2}\eta}{25\pi} - \frac{36\eta^2}{5\pi^2} - \frac{135\eta^3}{\sqrt{2}\pi^3} + \frac{4374\sqrt{2}\eta^5}{25\pi^5} + \frac{1207433952\eta^{12}}{25\pi^{12}}\right)\left(1 - \frac{3\sqrt{2}\eta}{\pi}\right)^3$

Yelash and Kraska, (2001)	Z^{GFD} $= \frac{(1.95926 + 0.95926(-3+m))(1 + 2.45696\eta + 4.10386\eta^2 - 3.7550}{(1-\eta)^3}$ $- \frac{\big(0.95926 + 0.95926(-3+m)\big)\left(3 + 8\eta + 14\eta^2 + 14\eta^3 + \frac{40\eta^4}{3}\right)}{3 - 4\eta}$
Rambaldi et al., (2006)	Z^{GFD} $= \frac{(1.95926 + 0.95926(-3+m))(1 + 2.45696\eta + 4.10386\eta^2 - 3.7550}{(1-\eta)^3}$ $- \big(0.95926 + 0.95926(-3+m)\big)\left(1 + \frac{4\eta}{1 - 2.5\eta + 1.658808\eta^2}\right)$

Table 6.6: Residual Helmholtz free energy for the chain terms obtain from GFD

Carnahan and Starling, (1969)	$\frac{A^{GFD}}{R\,T} = \frac{1}{2(-1+\eta)^2}\Big(\eta\Big(0.16296 - 3.83704(-3+m)$ $- 2.45696\big(1.95926 + 0.95926(-3+m)\big)(-2+\eta)$ $+ 1.10386\eta$ $+ 7.10386\big(0.95926 + 0.95926(-3+m)\big)\eta$ $- 3.75503\big(1.95926 + 0.95926(-3+m)\big)(-2+3\eta)\Big)$ $+ 5.51006\big(1.95926$ $+ 0.95926(-3+m)\big)(-1+\eta)^2\ln(1-\eta)\Big)$

Kolafa, (1986)	$\frac{A^{GFD}}{R\,T} = \frac{1}{6(-1+\eta)^2}\Big(\eta\,\Big(-9.10372 - 21.10372(-3+m)$ $- 7.37088\big(1.95926 + 0.95926(-3+m)\big)(-2+\eta)$ $+ 3.31158\eta$ $+ 36.3116\big(0.95926 + 0.95926(-3+m)\big)\eta$ $- 4\big(0.95926 + 0.95926(-3+m)\big)\eta^2$ $- 11.26509\big(1.95926 + 0.95926(-3+m)\big)(-2+3\eta)\Big)$ $- 2\big(-11.3972$ $- 3.1321(-3+m)\big)(-1+\eta)^2\ln(1-\eta)\Big)$

Khoshbarchi and Vera, (1997)	$\frac{A^{GFD}}{R\,T}$ $= \frac{1}{175\pi^9(-1+\eta)^2\left(-\frac{\pi}{3\sqrt{2}}+\eta\right)^2} 2187\sqrt{2}\,(-189006.6284\,\eta$ $+ 98300.5606\,m\,\eta + 761081.5146\eta^2 - 393714.2685\,m\,\eta^2$ $- 1070204.3363\,\eta^3 + 549907.1086\,m\,\eta^3 + 574328.2337\eta^4$ $- 292484.7117\,m\,\eta^4 - 58205.3875\,\eta^5 + 29102.6938\,m\,\eta^5$ $- 11453.7336\,\eta^6 + 5726.8668\,m\,\eta^6 - 3539.7486\,\eta^7 + 1769.8743\,m\,\eta^7$ $- 1512.3827\,\eta^8 + 756.19134m\eta^8 - 776.4312\eta^9 + 388.2156m\eta^9$ $- 460.5136\eta^{10} + 230.2568m\eta^{10} - 310.6046\eta^{11} + 155.3023m\eta^{11}$ $+ 7489.5053\eta^{12} - 3744.7526m\eta^{12} - 7628.0355\eta^{13} + 3814.0178m\eta^{13}$ $- \frac{6139\left(0.95926 + 0.95926(-3+m)\right)\pi^9(-1+\eta)^2\left(-\frac{\pi}{3\sqrt{2}}+\eta\right)^2 \ln\left(\frac{\pi}{3\sqrt{2}}\right)}{972\sqrt{2}}$ $+ 4646.7516\left(1.95926 + 0.95926(-3+m)\right)(-1+\eta)^2\left(-\frac{\pi}{3\sqrt{2}}+\eta\right)^2 \ln(1$ $- \eta) - 140042.1585\ln\left(\frac{\pi}{3\sqrt{2}}-\eta\right) + 70021.0793m\ln\left(\frac{\pi}{3\sqrt{2}}-\eta\right)$ $+ 658331.0379\eta\ln\left(\frac{\pi}{3\sqrt{2}}-\eta\right) - 329165.51893m\eta\ln\left(\frac{\pi}{3\sqrt{2}}-\eta\right)$ $- 1151941.8709\eta^2\ln\left(\frac{\pi}{3\sqrt{2}}-\eta\right) + 575970.9354m\eta^2\ln\left(\frac{\pi}{3\sqrt{2}}-\eta\right)$ $+ 889059.2622\eta^3\ln\left(\frac{\pi}{3\sqrt{2}}-\eta\right) - 444529.6311m\eta^3\ln\left(\frac{\pi}{3\sqrt{2}}-\eta\right)$ $- 255406.2707\eta^4\ln\left(\frac{\pi}{3\sqrt{2}}-\eta\right) + 127703.1354m\eta^4\ln\left(\frac{\pi}{3\sqrt{2}}-\eta\right))$

Yelash and Kraska, (2001)	$\frac{A^{GFD}}{R\,T} = \frac{1}{18(-1+\eta)^2}(18(6.21199(1.95926 + 0.95926(-3+m)) + 2(15.2810 + 14.2810(-3+m)))\eta + 56(0.95926 + 0.95926(-3+m))\eta^3 + 14(0.95926 + 0.95926(-3+m))\eta^4 + 20(0.95926 + 0.95926(-3+m))\eta^5 - 162(0.95926 + 0.95926(-3+m))\ln(3) - 9\eta^2(-62.9843 - 1.6469(1.95926 + 0.95926(-3+m)) + 38.62469m + 18(0.95926 + 0.95926(-3+m))\ln(3)) + 162(0.95926 + 0.95926(-3+m))(-1+\eta)^2\ln(3-4\eta) + 49.5905(1.95926 + 0.95926(-3+m))(-1+\eta)^2\ln(1-\eta))$

Rambaldi et al., (2006)	$\frac{A^{GFD}}{R\,T} = \frac{1}{(-1+\eta)^2}(-16.4128 + 0.95926(51.3296 - 17.1099m) + (44.1012 + 2.45696(-0.9185 + 0.9593m) + 0.95926(-119.9242 + 4.10386(-1.433697605079942 \times 10^{-11} - 7.3719 \times 10^{-14}m) + 39.9747m))\eta + (39.3770 + 2.45696(0.4593 - 0.4796m) + 4.10386(-0.4593 + 0.4796m) - 23.2548m)\eta^2 + 12.8893(0.9593 + 0.95926(-3.0000 + 1.0000m))(1-\eta)^2\arctan(4.0279 - 5.3452\eta) - 1.0000(1.9593 - 3.75503(-0.9185 + 0.95926m) + 0.95926(-3.0000 + 1.0000m))(1-\eta)^2\ln(1-\eta) - 1.5183 \times 10^{-12}(0.7926 + 0.95926(7.8147 + m))(1-\eta)^2\ln(0.6028 + \eta(-1.5071 + \eta)))$

6.3. Parameters estimation

The experimental data for the vapor pressure and the liquid density were taken from Vargaftik (1975). The adjustable parameters were obtained by simultaneously fitting vapor pressures and liquid densities. **Tables** 6.7-6.9 summarize the five adjustable parameters using different HS models with their corresponding chain terms obtained from various theories. Different components were taken as reference as illustrated in the tables.

Table 6.7: Ethane parameters for different HS models with their corresponding chain terms obtained from HSC theory

Hard Sphere Model	m	v^{00} (mL)	u^0/k (K)	c	e/k (K)
Carnahan and Starling, (1969)	2.201	15.328	83.984	0.31001	-11.543
Kolafa, (1986)	2.2381	15.062	83.279	0.31125	-11.811
Khoshbarchi and Vera, (1997)	2.2132	15.241	83.705	0.31051	-11.586
Yelash and Kraska, (2001)	2.189	15.436	84.244	0.31087	-11.524
Rambaldi et al., (2006)	2.2936	14.588	82.148	0.30775	-11.874

Table 6.8: Propane parameters for different HS models with their corresponding chain terms obtained from TPT-D

Hard Sphere Model	m	v^{00} (mL)	u^0/k (K)	c	e/k (K)
Carnahan and Starling, (1969)	2.6888	16.000	91.263	0.2831	-7.82
Kolafa, (1986)	2.6861	16.000	91.316	0.28434	-7.6338

Khoshbarchi and Vera, (1997)	2.6847	16.000	91.257	0.28178	-7.6215
Yelash and Kraska, (2001)	2.6957	16.000	91.202	0.28556	-8.0323
Rambaldi et al., (2006)	2.6646	16.000	91.53	0.27836	-6.881

Table 6.9: Hexane parameters for different HS models with their corresponding chain terms obtained from GFD theory

Hard Sphere Model	**m**	**v^{00} (mL)**	**u^0/k (K)**	**c**	**e/k (K)**
Carnahan and Starling, (1969)	5.5499	16.000	91.012	0.4012	-17.633
Kolafa, (1986)	5.5581	16.000	90.941	0.40115	-17.931
Khoshbarchi and Vera, (1997)	5.5575	16.000	91.024	0.40195	-17.807
Yelash and Kraska, (2001)	5.5402	16.000	91.035	0.40016	-17.394
Rambaldi et al., (2006)	5.5985	16.000	90.812	0.4047	-19.022

6.4. Comparison with molecular simulation data

Before exploring the PVT behavior, it would be valuable to test the accuracy of the hard chain resulted from the various HS and chain theories using the molecular simulation data as a reference. Tables 6.10-6.12 summarize the average absolute deviation (AAD) for the compressibility factor predicted by the various hard sphere models with different chain theories. The same simulation data that were adopted in **Chapter 5** are used in the comparison.

Table 6.10: Percentage Average Absolute Deviation (AAD) of the Calculated Compressibility of m-Hard-Sphere Chains Obtained from HSC theory Compared with Molecular Simulation Data

	AAD (%)				
m	Carnahan and Starling	Kolafa	Khoshbarchi and Vera	Yelash and Kraska	Rambaldi et al.
4	9.00	8.87	9.00	9.05	8.39
8	11.65	11.52	11.67	11.69	11.08
16	13.32	13.19	13.35	13.37	12.88
32	9.85	9.79	9.89	9.86	9.72
51	13.42	13.30	13.44	13.44	12.93
201	16.32	16.19	16.36	16.34	15.81
Overall	12.17	12.04	12.19	12.20	11.66

Table 6.11: Percentage Average Absolute Deviation (AAD) of the Calculated Compressibility of m-Hard-Sphere Chains Obtained from TPT-D Compared with Molecular Simulation Data

	AAD (%)				
m	Carnahan and Starling	Kolafa	Khoshbarchi and Vera	Yelash and Kraska	Rambaldi et al.
4	0.58	0.47	0.53	0.70	0.90
8	0.65	0.46	0.58	0.79	0.80
16	1.39	1.03	1.30	1.48	0.79
32	0.56	0.49	0.53	0.61	0.47

51	3.13	3.14	3.16	2.99	3.61
201	4.30	4.15	4.33	4.15	4.52
Overall	1.66	1.50	1.62	1.69	1.75

Table 6.12: Percentage Average Absolute Deviation (AAD) of the Calculated Compressibility of m-Hard-Sphere Chains Obtained from GFD theory Compared with Molecular Simulation Data

	AAD (%)				
m	**Carnahan and Starling**	**Kolafa**	**Khoshbarchi and Vera**	**Yelash and Kraska**	**Rambaldi et al.**
4	1.71	1.66	1.69	1.73	1.86
8	3.60	3.50	3.56	3.65	3.75
16	6.71	6.51	6.69	6.75	6.60
32	10.60	10.21	10.59	10.67	9.66
51	5.45	5.41	5.56	5.39	5.57
201	9.49	9.31	9.55	9.56	9.26
Overall	5.35	5.22	5.36	5.38	5.32

As indicated in **Chapter 3**, TPT-D produces the best agreement with the simulation data. Among the same chain theory, there is a minor overall difference between the different HS models.

6.5. Bifurcation diagrams

6.5.1. Bifurcation diagrams for ethane using various hard sphere models with HSC theory in the chain term: branches, turning points and number of roots

Figures 6.1-6.10 demonstrate how the number of compressibility factor (Z) roots varies with temperature for ethane at 1 atm. All models exhibit more than one branch in the first quadrant with multiple turning points. Moreover, all models have the two turning points in the low temperature region. The models of Carnahan & Starling, Khoshbarchi &

Vera and Yelash & Kraska resulted in behavior without additional branches in the temperature range corresponding to most practical applications.

Carnahan and Starling, (1969)	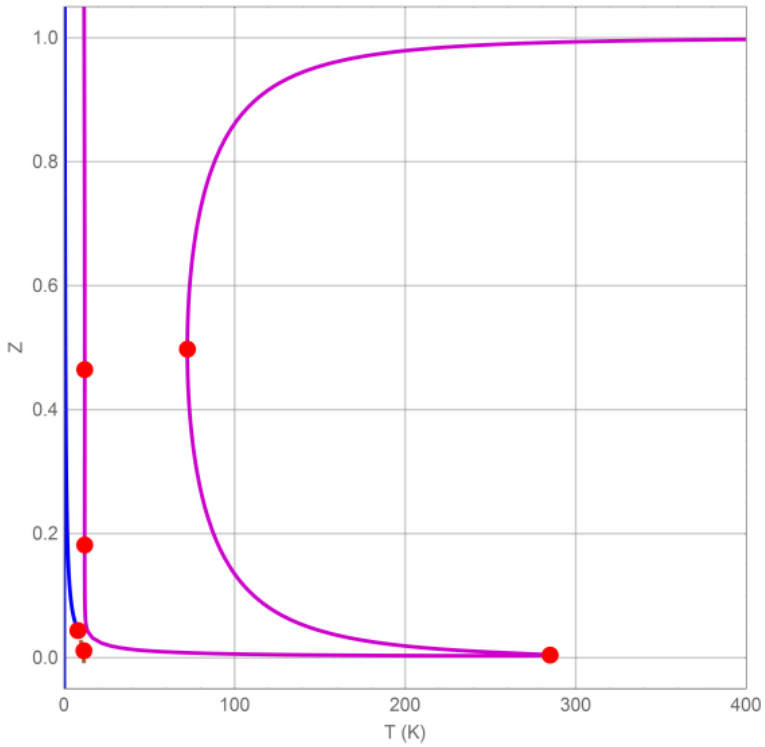 **Figure 6.1: Bifurcation diagram for ethane at 1 atm using CS HS model and its corresponding chain term obtained from HSC**	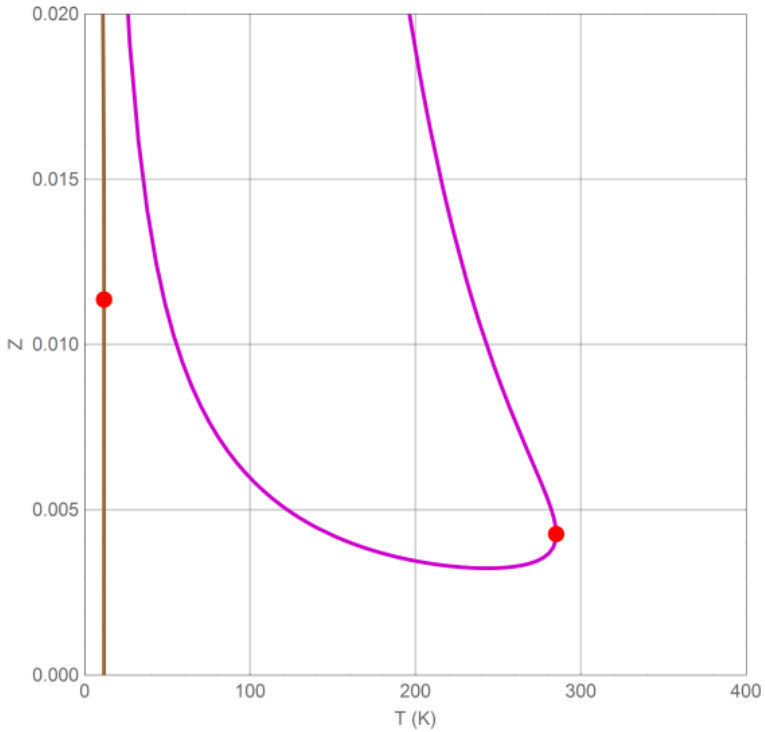 **Figure 6.2: Magnified range of the bifurcation diagram for ethane at 1 atm using CS HS model and its corresponding chain term obtained from HSC**

Kolafa, (1986)	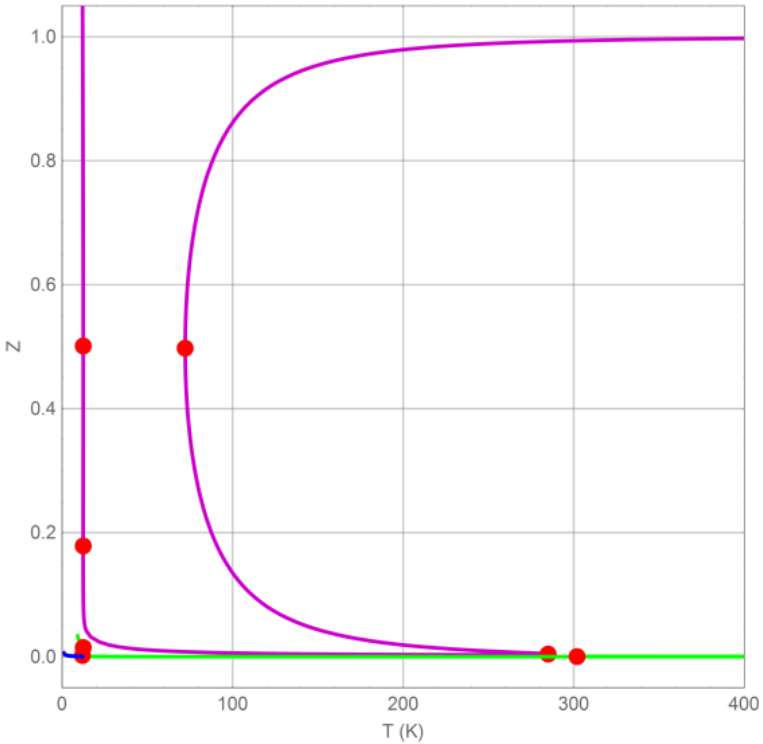 **Figure 6.3: Bifurcation diagram for ethane at 1 atm using Kolafa HS model and its corresponding chain term obtained from HSC**	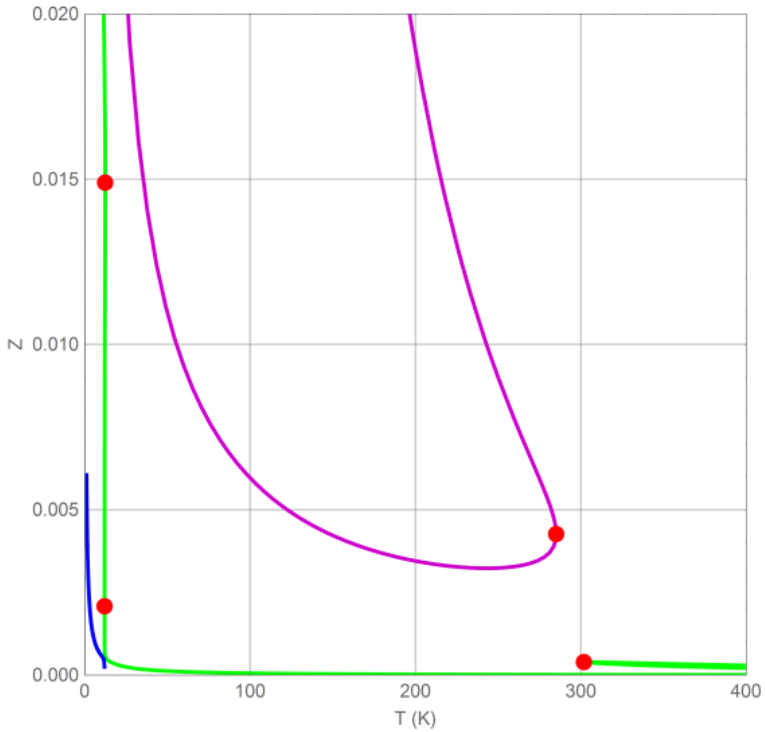 **Figure 6.4: Magnified range of the bifurcation diagram for ethane at 1 atm using Kolafa HS model and its corresponding chain term obtained from HSC**

Khoshbarchi and Vera, (1997)	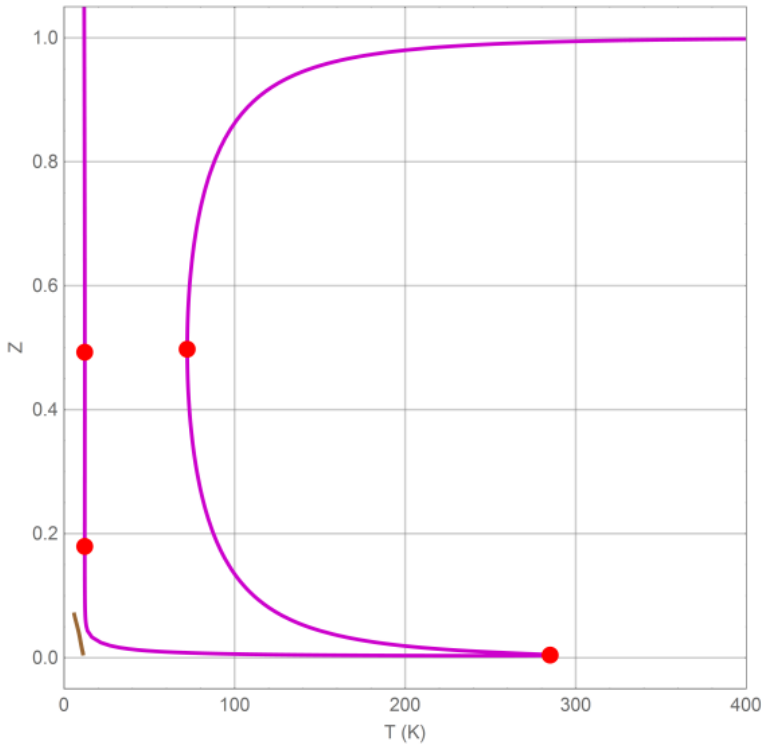 **Figure 6.5: Bifurcation diagram for ethane at 1 atm using Khoshbarchi and Vera HS model and its corresponding chain term obtained from HSC**	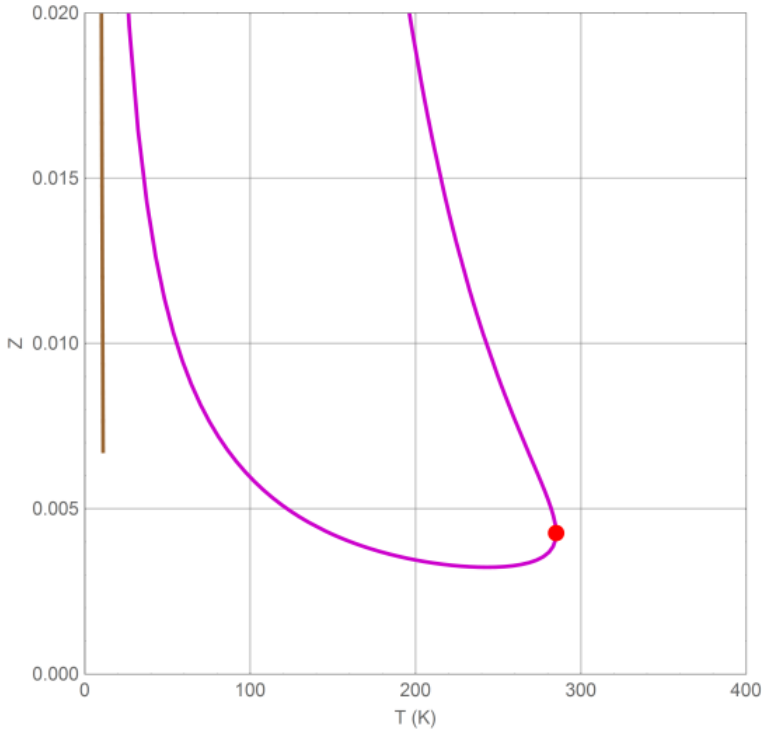 **Figure 6.6: Magnified range of the bifurcation diagram for ethane at 1 atm using Khoshbarchi and Vera HS model and its corresponding chain term obtained from HSC**

Yelash and Kraska, (2001)	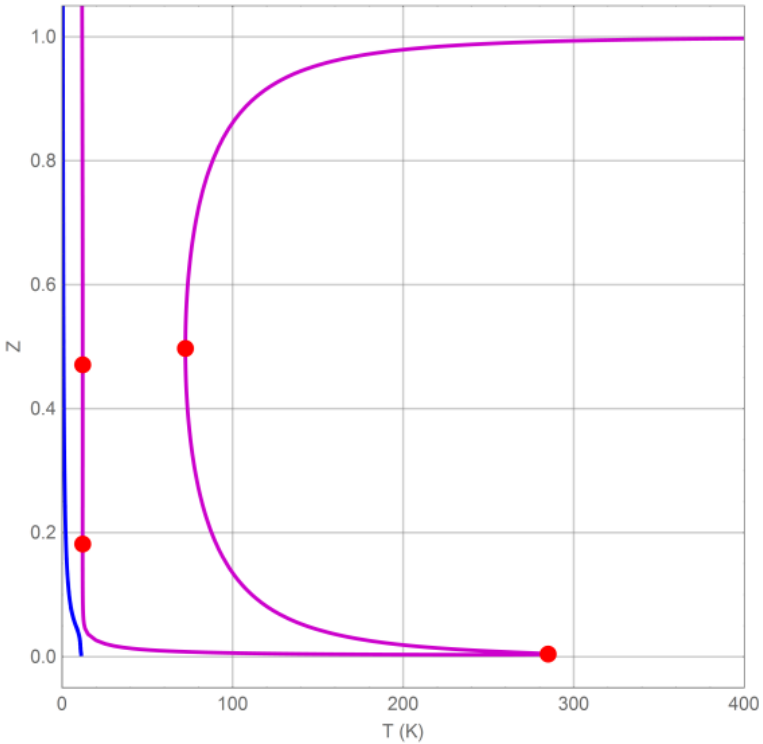 **Figure 6.7: Bifurcation diagram for ethane at 1 atm using Yelash and Kraska HS model and its corresponding chain term obtained from HSC**	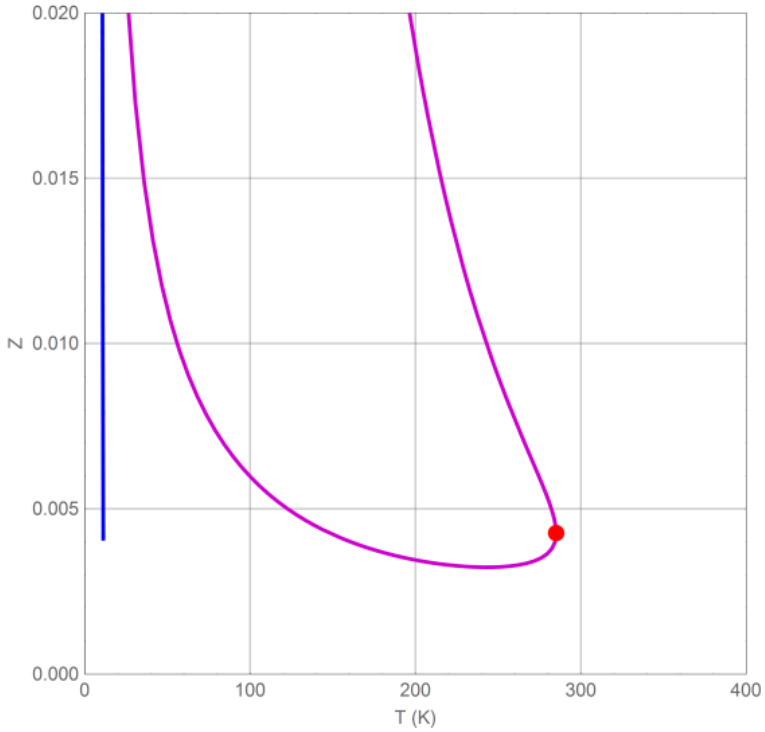 **Figure 6.8: Magnified range of the bifurcation diagram for ethane at 1 atm using Yelash and Kraska HS model and its corresponding chain term obtained from HSC**

Rambaldi et al., (2006)	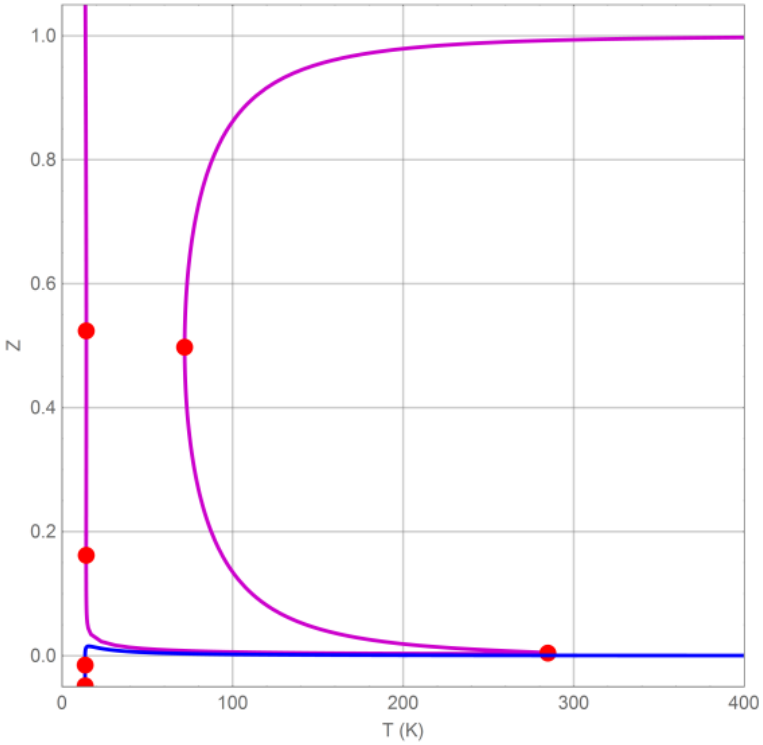 **Figure 6.9: Bifurcation diagram for ethane at 1 atm using Rambaldi et al. HS model and its corresponding chain term obtained from HSC**	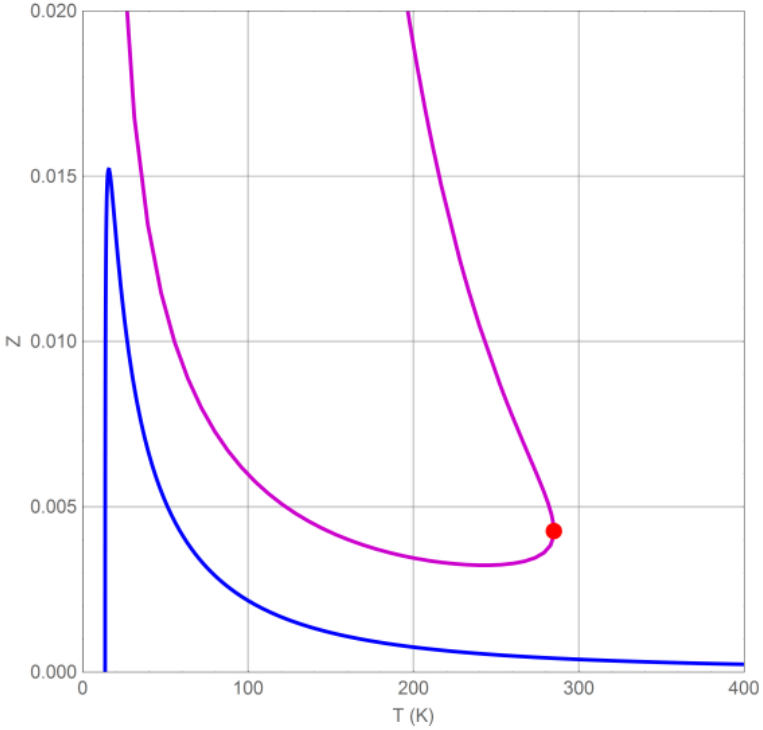 **Figure 6.10: Magnified range of the bifurcation diagram for ethane at 1 atm using Rambaldi et al. HS model EOS and its corresponding chain term obtained from HSC**

6.5.2. Bifurcation diagrams for propane using various hard sphere models with TPT-D in the chain term: branches, turning points and number of roots

When the bifurcation diagrams for propane were generated at 1 atm, the two turning points in the low temperature region disappeared. For this reason, the pressure was lowered to 0.6 atm.

By exploring **Figures** 6.11-6.20, it is clear that the PVT behavior in the first quadrant is similar to the one predicted by TPT1. Thus, the additional term in the TPT-D does not affect the solution behavior in the first quadrant.

Unlike the other hard sphere models, Rambaldi et al. model did not show the two turning points at 0.6 atm pressure. This is way the pressure was lowered a bit more to 0.58 atm. Hence, this non-physical phenomenon is affected by the hard sphere term in the complete EOS.

Carnahan and Starling, (1969)	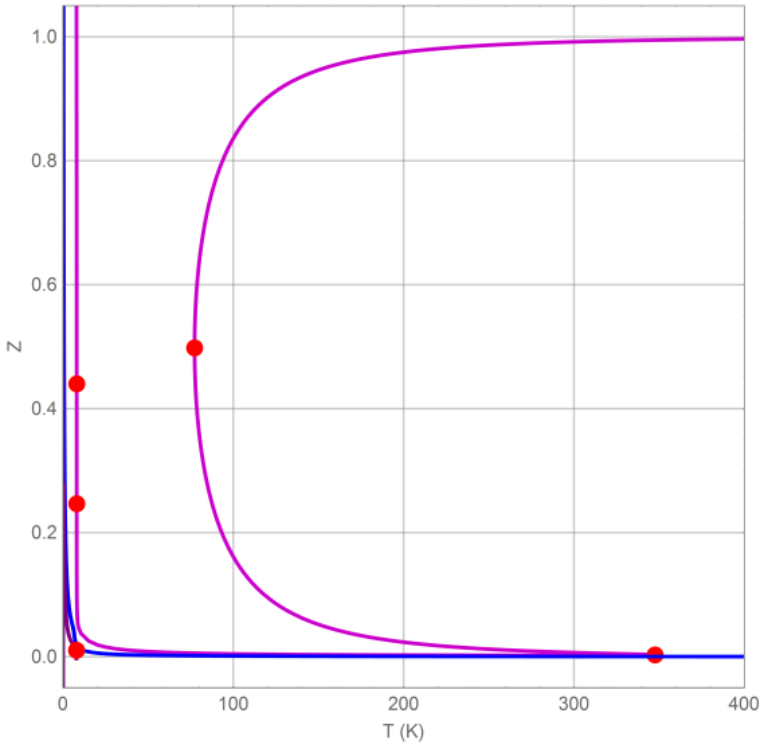 **Figure 6.11: Bifurcation diagram for propane at 0.6 atm using CS HS model and its corresponding chain term obtained from TPT-D**	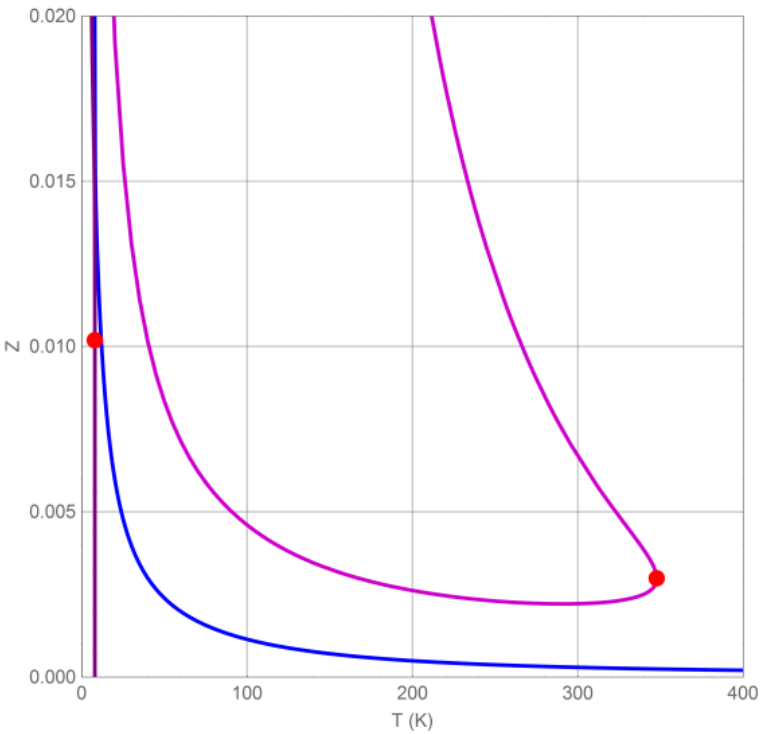 **Figure 6.12: Magnified range of the bifurcation diagram for propane at 0.6 atm using CS HS model and its corresponding chain term obtained from TPT-D**

Kolafa, (1986)	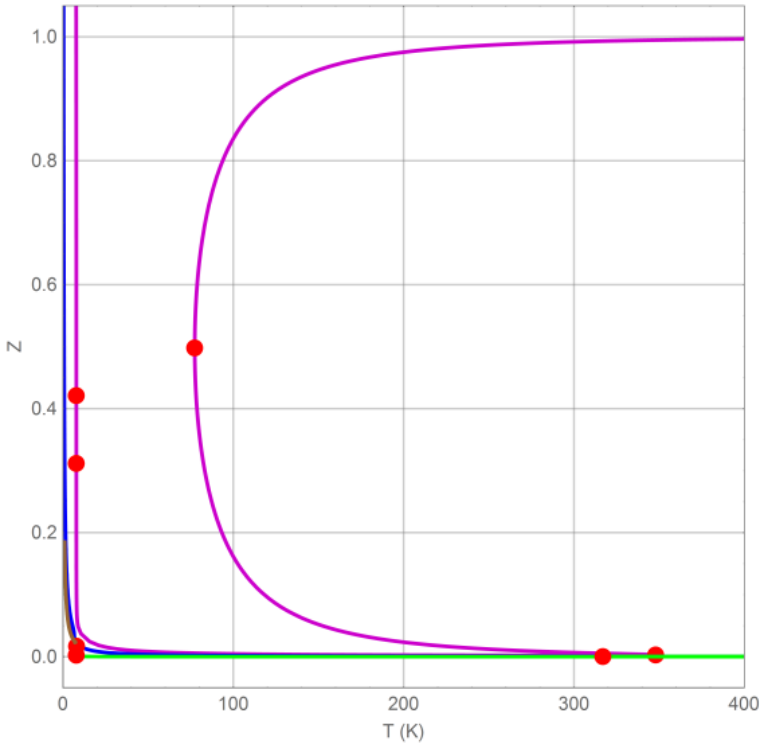 **Figure 6.13: Bifurcation diagram for propane at 0.6 atm using Kolafa HS model and its corresponding chain term obtained from TPT-D**	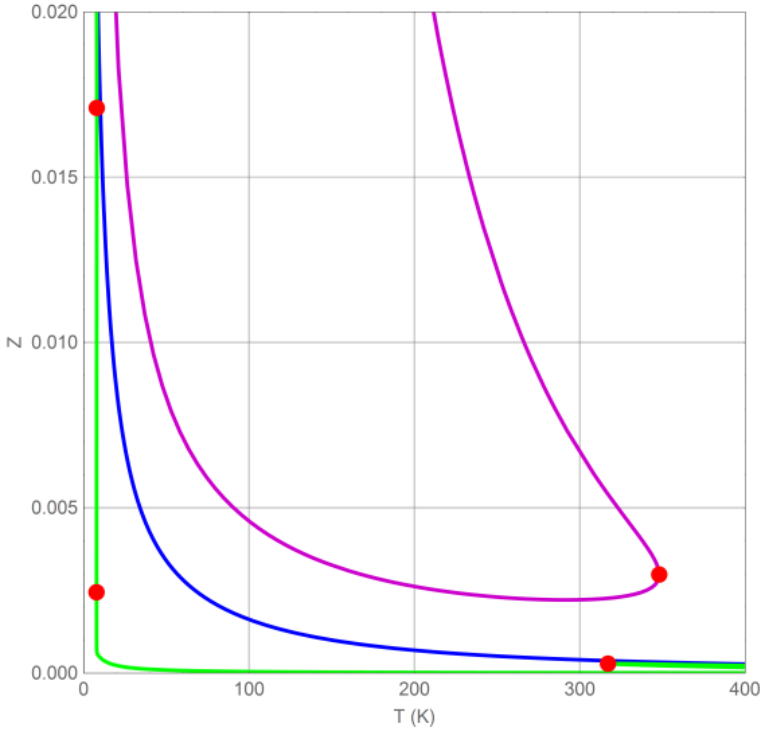 **Figure 6.14: Magnified range of the bifurcation diagram for propane at 0.6 atm using Kolafa HS model and its corresponding chain term obtained from TPT-D**

Khoshbarchi and Vera, (1997)	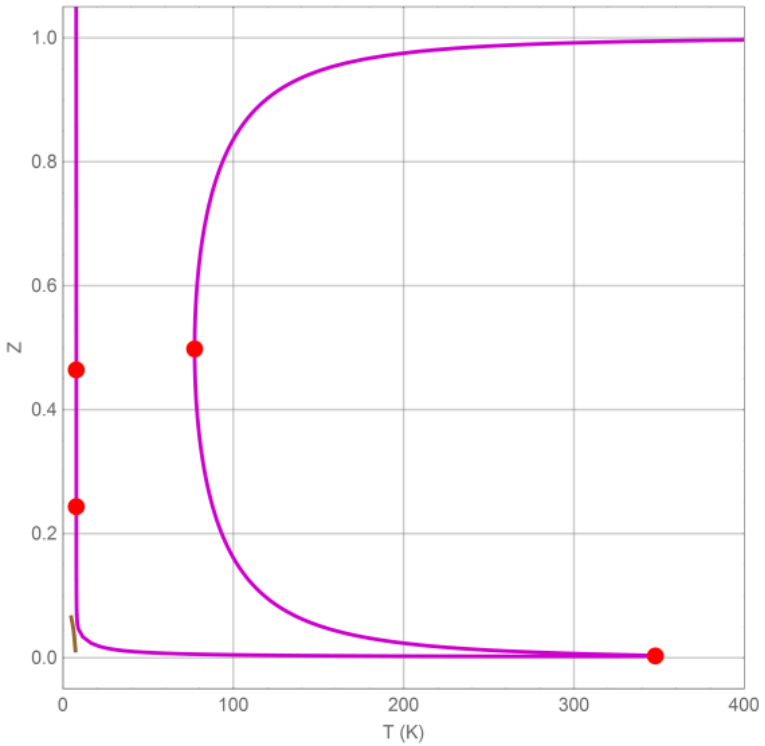 **Figure 6.15: Bifurcation diagram for propane at 0.6 atm using Khoshbarchi and Vera HS model and its corresponding chain term obtained from TPT-D**	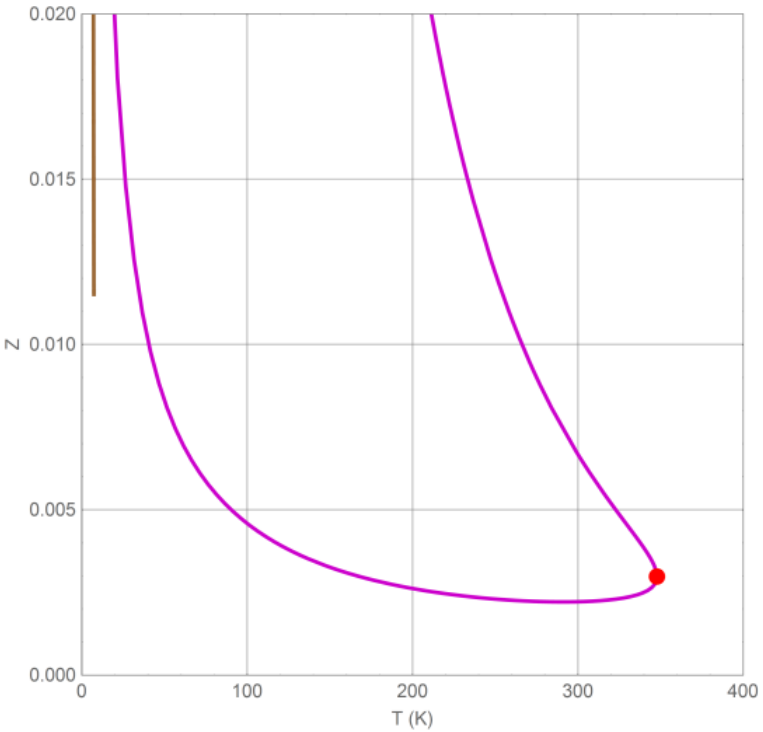 **Figure 6.16: Magnified range of the bifurcation diagram for propane at 0.6 atm using Khoshbarchi and Vera HS model and its corresponding chain term obtained from TPT-D**

Yelash and Kraska, (2001)	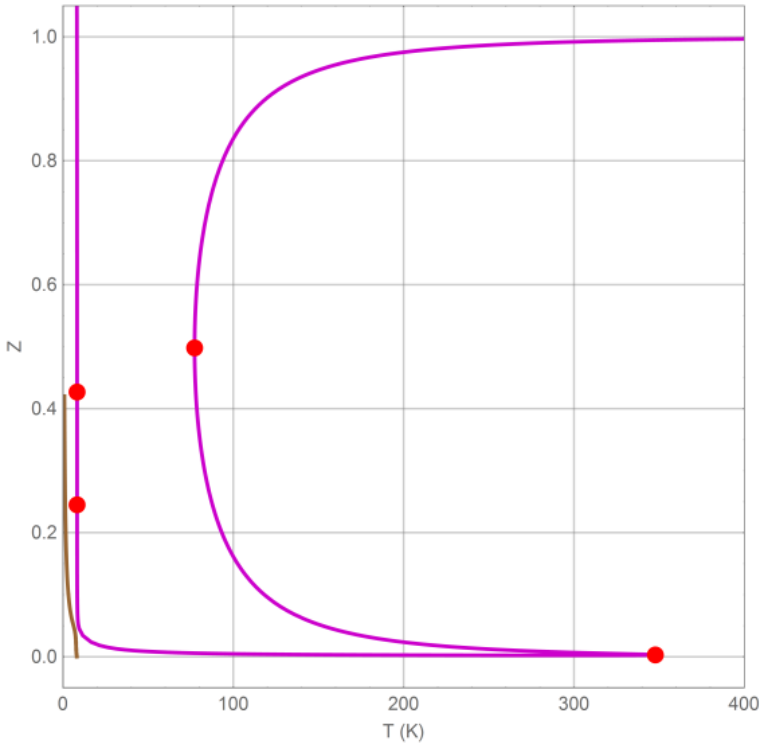 **Figure 6.17: Bifurcation diagram for propane at 0.6 atm using Yelash and Kraska HS model and its corresponding chain term obtained from TPT-D**	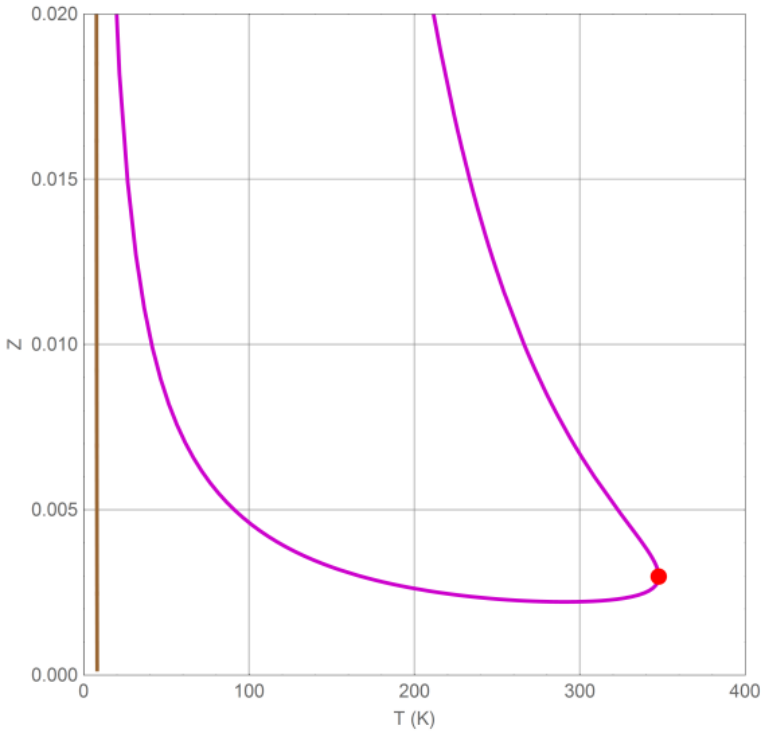 **Figure 6.18: Magnified range of the bifurcation diagram for propane at 0.6 atm using Yelash and Kraska HS model and its corresponding chain term obtained from**

Rambaldi et al., (2006)	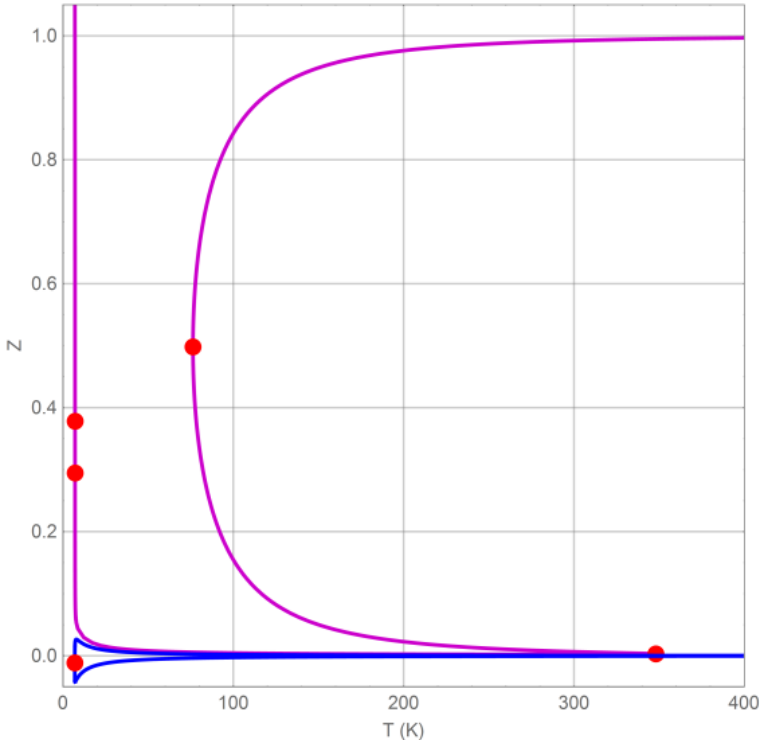 **Figure 6.19: Bifurcation diagram for propane at 0.58 atm using Rambaldi et al. HS model and its corresponding chain term obtained from TPT-D**	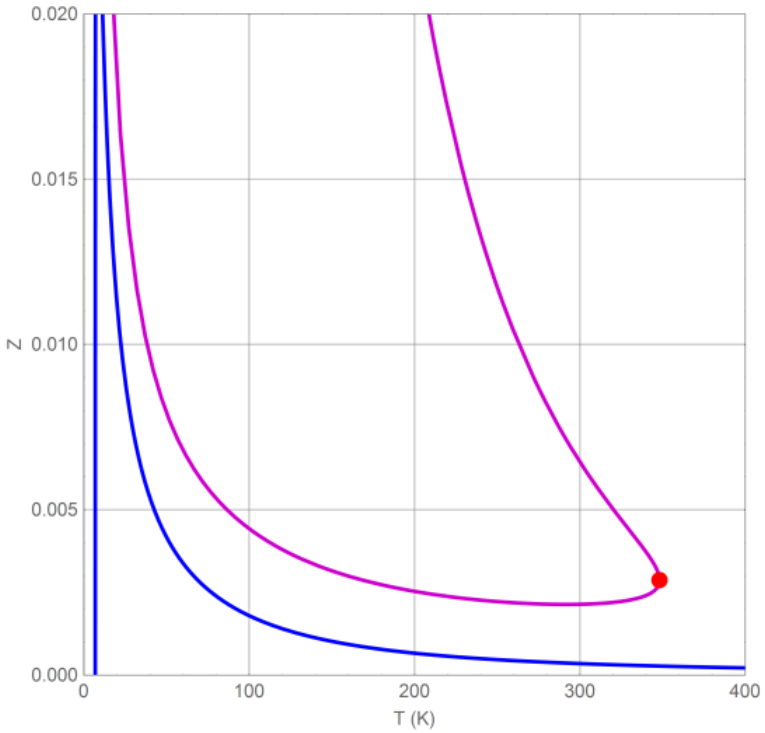 **Figure 6.20: Magnified range of the bifurcation diagram for propane at 0.58 atm using Rambaldi et al. HS model EOS and its corresponding chain term obtained from TPT-D**

6.5.3. Bifurcation diagrams for hexane using various hard sphere models with GFD theory in the chain term: branches, turning points and number of roots

For hexane, the pressure was lowered to 0.5 atm in order to explore the two turning points at the low temperature region. **Figures** 6.21-6.30 show that the models of Carnahan & Starling, Kolafa and Rambaldi et al. illustrated non-physical behavior in the temperature region of practical applications. It is clear that all models suffer from predicting the two turning points at the low temperature region.

Carnahan and Starling, (1969)	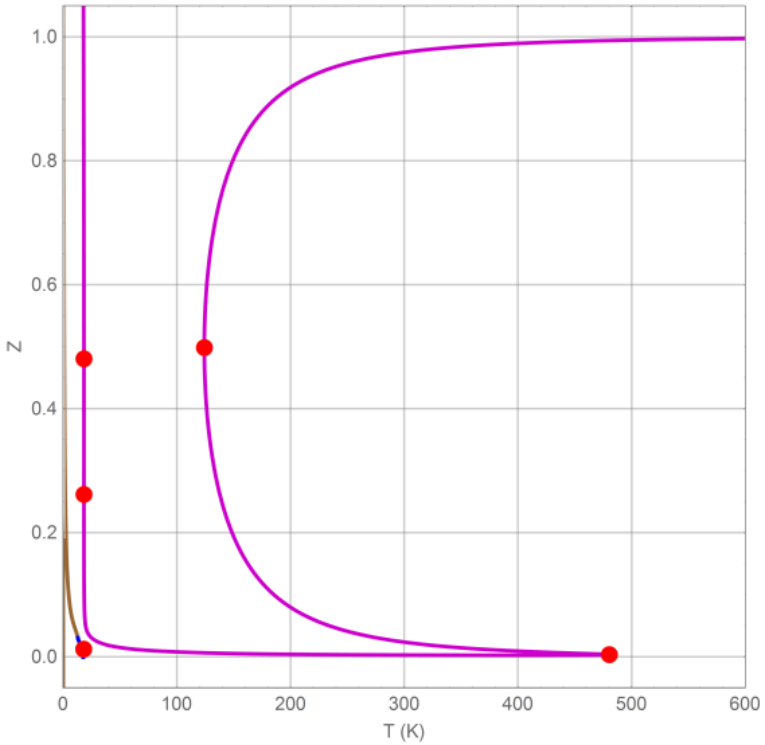 **Figure 6.21: Bifurcation diagram for hexane at 0.5 atm using CS HS model and its corresponding chain term obtained from GFD**	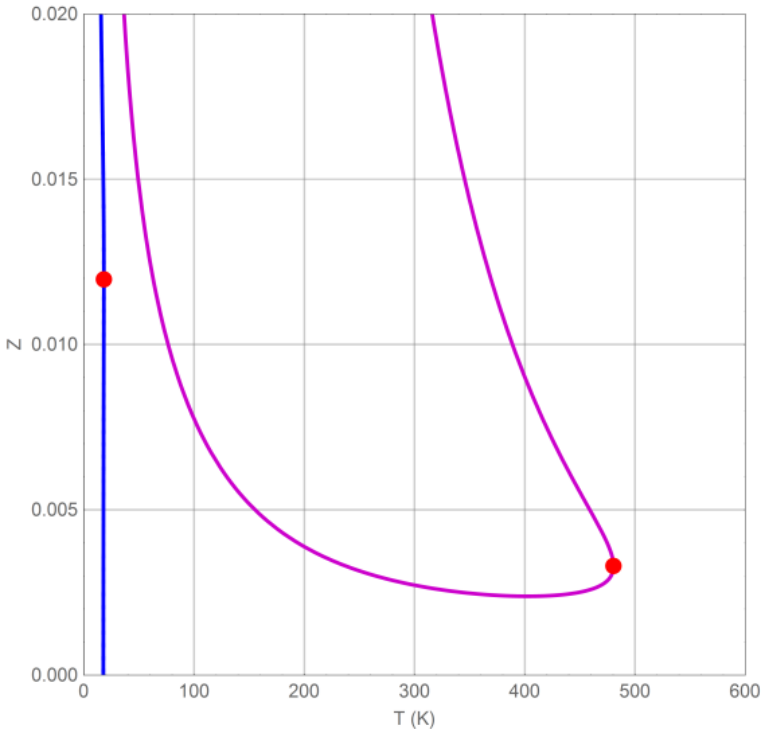 **Figure 6.22: Magnified range of the bifurcation diagram for hexane at 0.5 atm using CS HS model and its corresponding chain term obtained from GFD**

Kolafa, (1986)	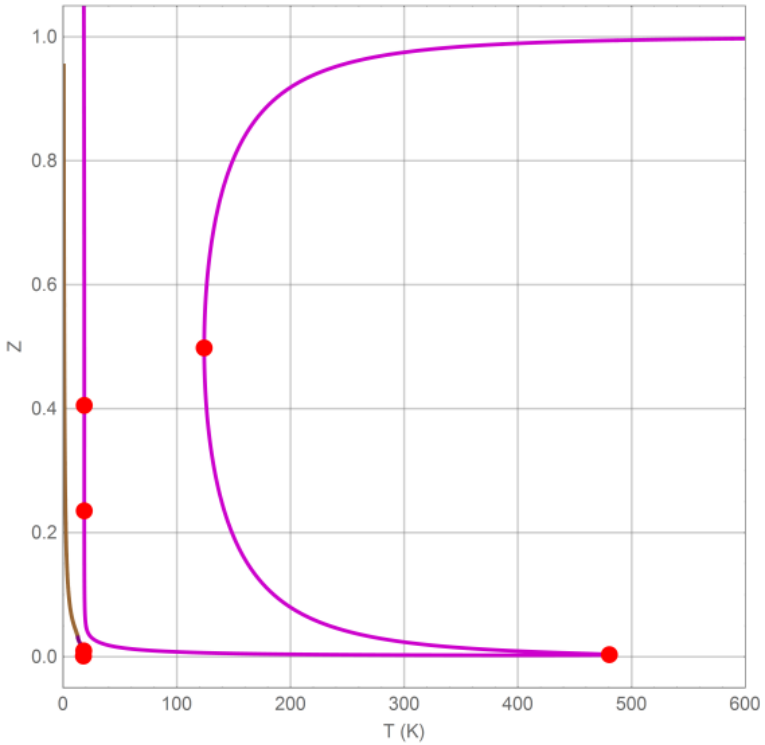 **Figure 6.23: Bifurcation diagram for hexane at 0.5 atm using Kolafa HS model and its corresponding chain term obtained from GFD**	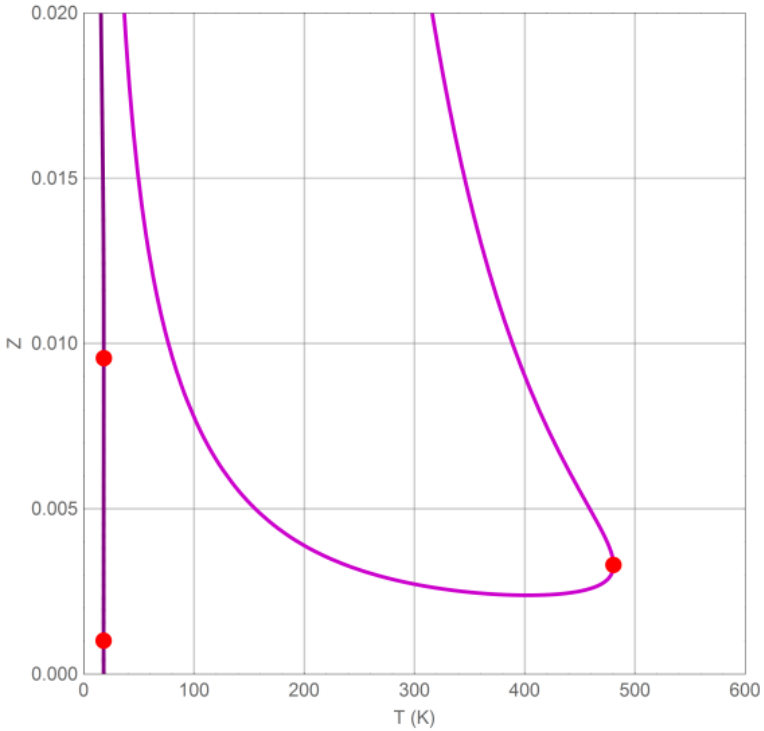 **Figure 6.24: Magnified range of the bifurcation diagram for hexane at 0.5 atm using Kolafa HS model and its corresponding chain term obtained from GFD**

Khoshbarchi and Vera, (1997)

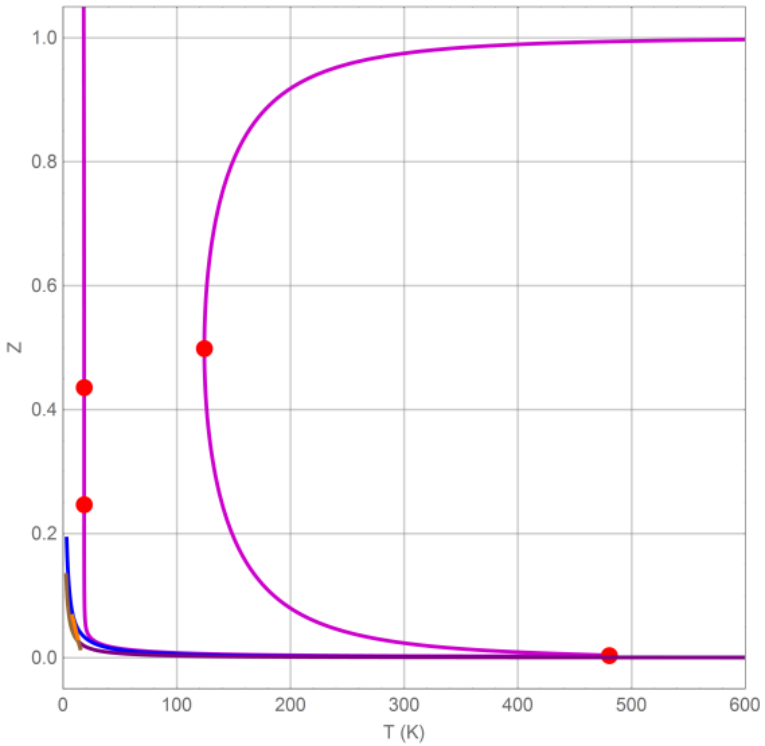

Figure 6.25: Bifurcation diagram for hexane at 0.5 atm using Khoshbarchi and Vera HS model and its corresponding chain term obtained from GFD

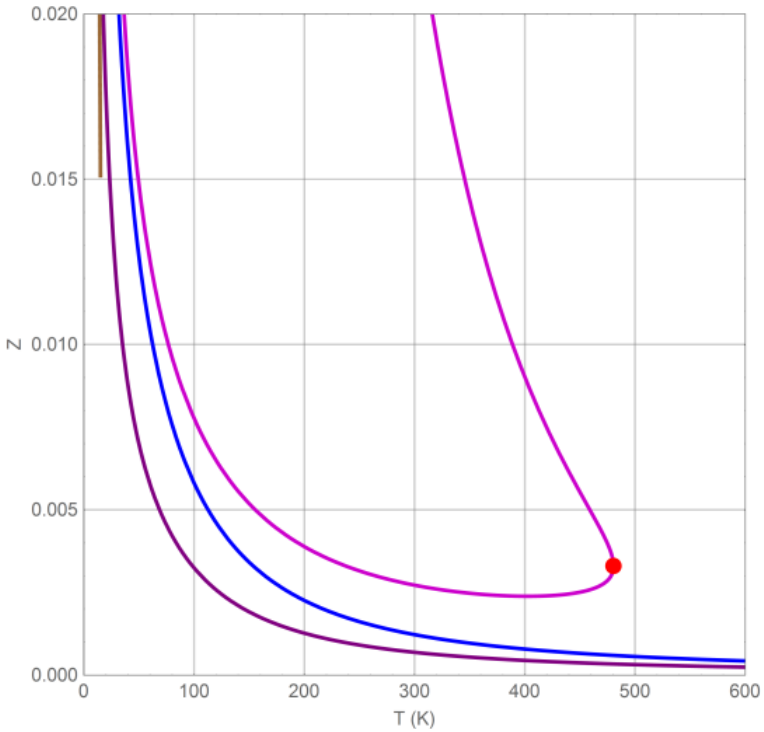

Figure 6.26: Magnified range of the bifurcation diagram for hexane at 0.5 atm using Khoshbarchi and Vera HS model and its corresponding chain term obtained from

Yelash and Kraska, (2001)

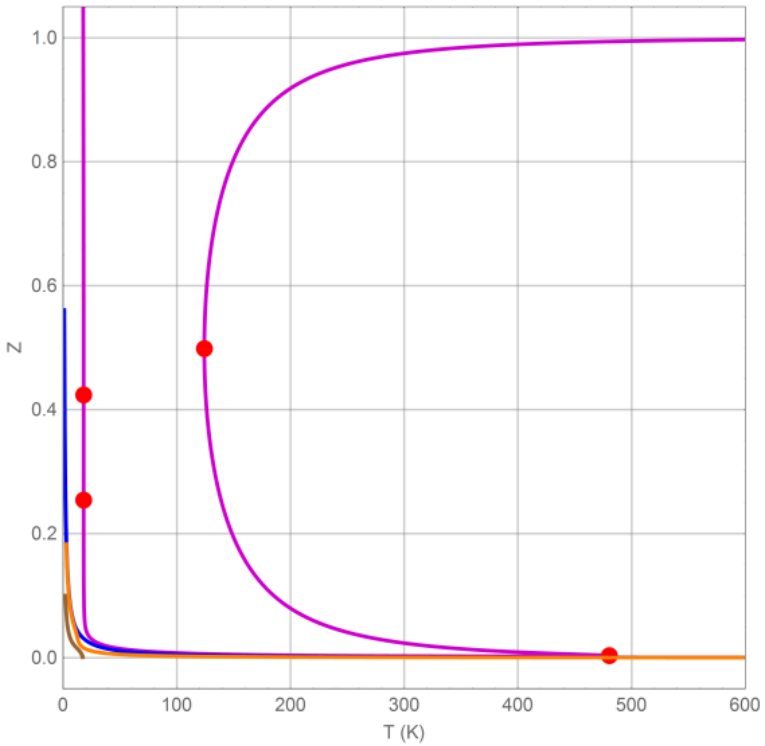

Figure 6.27: Bifurcation diagram for hexane at 0.5 atm using Yelash and Kraska HS model and its corresponding chain term obtained from GFD

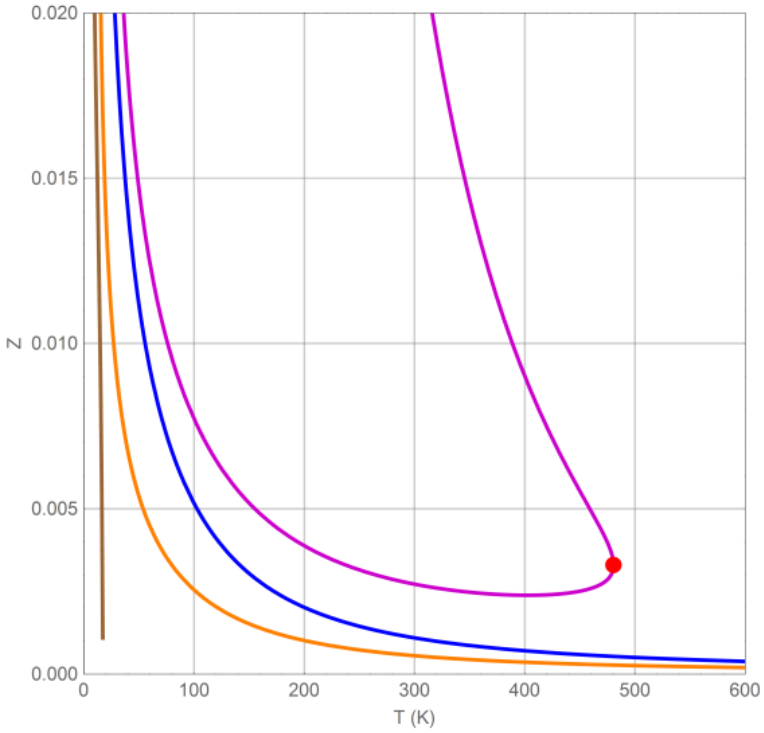

Figure 6.28: Magnified range of the bifurcation diagram for hexane at 0.5 atm using Yelash and Kraska HS model and its corresponding chain term obtained from GFD

Rambaldi et al., (2006)	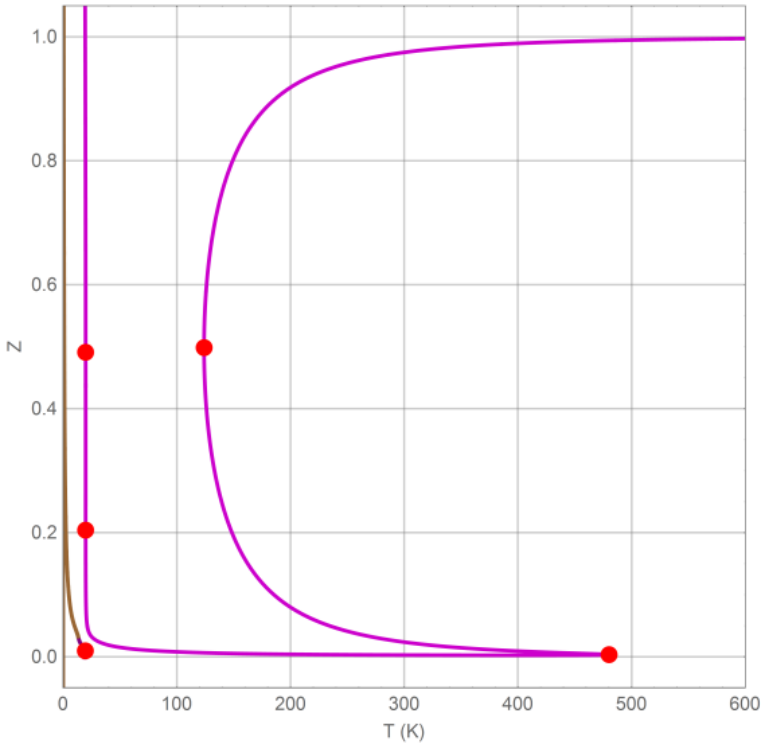 **Figure 6.29: Bifurcation diagram for hexane at 0.5 atm using Rambaldi et al. HS model and its corresponding chain term obtained from GFD**	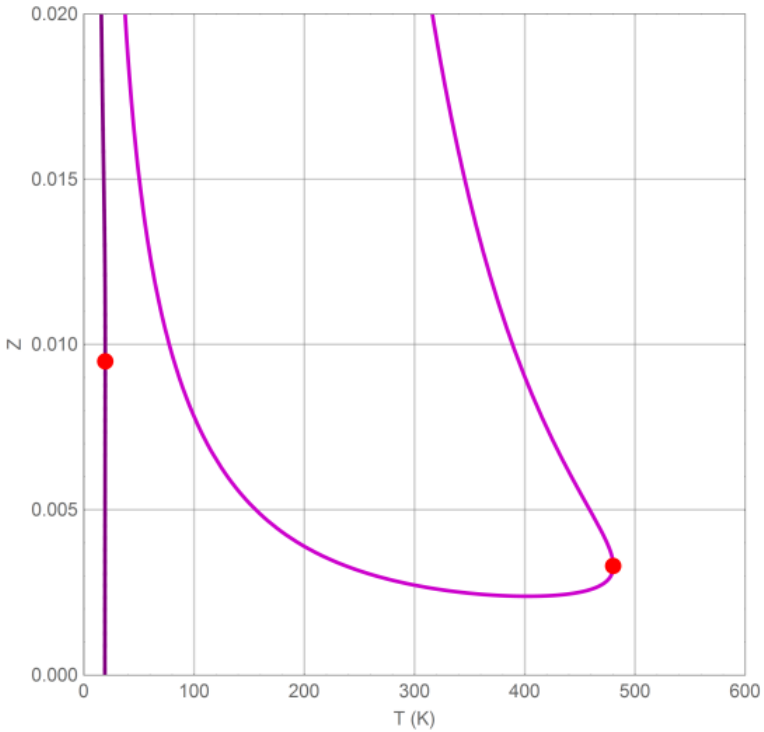 **Figure 6.30: Magnified range of the bifurcation diagram for hexane at 0.5 atm using Rambaldi et al. HS model EOS and its corresponding chain term obtained from GFD**

From the previous analysis, one could notice that there is no completely a single model without non-physical PVT behavior like cubic EOS. In addition, all investigated equations predict two more solutions in the low temperature region as if there are two immiscible liquid. Therefore, it would be useful to study the role of the dispersion term in the non-physical PVT behavior.

CHAPTER 7

THE ROLE OF DISPERSION AND ASSOCIATION TERMS ON PVT BEHAVIOR: BIFURCATION ANALYSIS

7.1. Introduction

The development of the dispersion term has received significant interest in constructing equations of state. Several equations have been proposed in order to describe the dispersion forces. These equations vary in their mathematical forms and accuracy. Thus, it is expected to have diverse solution behavior according to the dispersion term that is adopted.

In the previous chapters, the dispersion term was kept to the one proposed by Fu and Sandler (1995). In this chapter, Cotterman et al. (1986) dispersion term will be utilized. This dispersion term is more accurate than the previous one since it is based on Lennard-Jones interaction type. The chain term will be fixed to TPT1 since it has a satisfactory accuracy with a relatively simple mathematical form.

The previous work focused on the non-associating fluids. The effect of the association term on the complete equation of state was not studied. In this chapter, the role of adding the association term on the solution behavior will be explored.

7.2. Mathematical forms

7.2.1. Dispersion term

The dispersion term that will be adopted in this chapter was determined as a correlation of molecular simulation data for Lennard-Jones (LJ) fluids. Cotterman et al. (1986) proposed a dispersion term of the form:

$$\frac{A^{disp}}{R\,T} = m\frac{1}{T}\,\frac{\epsilon}{k}\left(a_{o1}^{disp} + \frac{a_{o2}^{disp}}{T_R}\right) \tag{7.1}$$

where

$$a_{o1}^{disp} = \xi[-8.5959 - 4.5424\,\xi - 2.1268\,\xi^2 + 10.285\,\xi^3] \tag{7.2}$$

$$a_{o2}^{disp} = \xi[-1.9075 + 9.9724\,\xi - 22.216\,\xi^2 + 15.904\,\xi^3] \tag{7.3}$$

T_R is a reduced temperature:

$$T_R = \frac{k}{\epsilon}\,T \tag{7.4}$$

ϵ is defined as Lennard-Jones intermolecular energy.

The compressibility factor of the dispersion term could be written as:

$$\begin{aligned} Z^{disp} = (m\xi\,\epsilon/k(-8.5959T - 1.9075\,\epsilon/k + \xi(-9.0848T \\ + 19.9448\,\epsilon/k + \xi(-6.3804T + 41.14T\xi \\ - 66.648\,\epsilon/k + 63.616\xi\,\epsilon/k))))/T^2 \end{aligned} \tag{7.5}$$

The effective diameter (d) is defined as:

$$d = \sigma \left(\frac{1 + 0.2977\, kT/\epsilon}{1 + 0.33163\, kT/\epsilon + f(m)(kT/\epsilon)^2} \right) \tag{7.6}$$

where

$$f(m) = 0.0010477 + 0.025337 \frac{m-1}{m} \tag{7.7}$$

7.2.2. Association term

The association term was developed by Wertheim (1984a; 1984b; 1986a; 1986b) and it has been utilized in the statistical association fluid theory (SAFT) (Chapman, et al., 1990; Huang & Radosz, 1990; Huang & Radosz, 1991; Fu & Sandler, 1995). The association term could be written as:

$$\frac{A^{assoc}}{R\,T} = \sum_A \left[\left(\ln(X^A) - \frac{X^A}{2} \right) + \frac{1}{2} M \right] \tag{7.8}$$

where M is the number of association sites and X^A is the fraction of association sites A that are not bonded. The summation is over association sites and X^A is defined as:

$$X^A = \left[1 + N_{Av} \sum_B \rho\, X^B\, \Delta^{AB} \right]^{-1} \tag{7.9}$$

where ρ is the molar density and Δ^{AB} is the association strength that is given by:

$$\Delta^{AB} = g_{HS}(d) \left[\exp\left(\frac{\epsilon^{AB}}{kT} \right) - 1 \right] d^3 \kappa^{AB} \tag{7.10}$$

ϵ^{AB} and κ^{AB} are the association energy and volume of interaction between association sites A and B, respectively. $g_{HS}(d)$ is the pair correlation function at contact that was

explained in **Chapter 3**. Hence, the association term depends on the selected hard sphere model.

The association term could be written as:

$$Z^{assoc} = \rho \sum_{A} \left[\frac{1}{X^A} - \frac{1}{2}\right] \frac{\partial X^A}{\partial \rho} \tag{7.11}$$

7.3. Bifurcation diagrams for non-associating components

7.3.1. Parameters estimation

With Cotterman et al. (Cotterman, et al., 1986) dispersion term, there are three adjustable parameters for non-associating compounds: m, σ and ϵ. Ethane parameters are illustrated in **Table 7.1.**

Table 7.1: Ethane parameters for different HS models with TPT1 and Cotterman et al. dispersion term

Hard Sphere Model	m	σ (Å)	ϵ/k (K)
Carnahan and Starling, (1969)	1.6194	3.5553	177.97
Kolafa, (1986)	1.6216	3.5514	178.02
Khoshbarchi and Vera, (1997)	1.6263	3.5492	177.49
Yelash and Kraska, (2001)	1.6138	3.5604	178.32
Rambaldi et al., (2006)	1.6431	3.5306	176.81

7.3.2. Bifurcation diagrams using various hard sphere models with TPT1 and Cotterman et al. dispersion term: branches, turning points and number of roots

Figures 7.1-7.10 (7.1 – 7.10) illustrate how the compressibility factor of ethane varies with temperature at 1 atm. Unlike Fu and Sandler (1995) dispersion term, the dispersion term proposed by Cotterman et al. (Cotterman, et al., 1986) is free from exhibiting the two turning points at the low temperature region. In general, Cotterman et al. (1986) dispersion term added more solutions over the displayed temperature region for several HS models. However, a completely physical behavior was obtained when this dispersion term was combined with Rambaldi et al. (Rambaldi, et al., 2006) hard sphere model. Hence, any hard sphere model that has similar mathematical form as Rambaldi et al. (Rambaldi, et al., 2006) is expected to be free from non-physical behavior for non-associating components.

Carnahan and Starling, (1969)	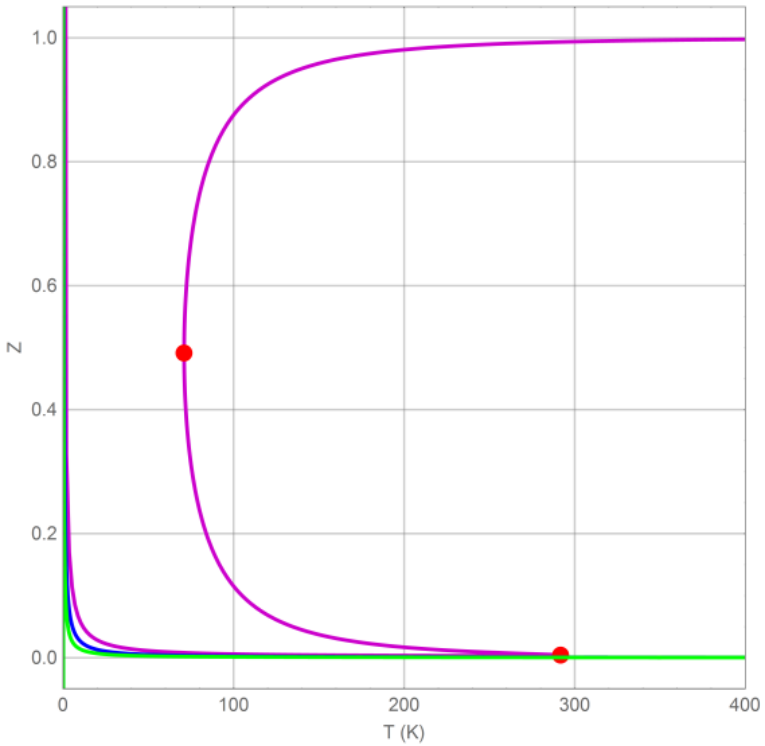 **Figure 7.1: Bifurcation diagram for ethane at 1 atm using CS HS model, TPT1 and Cotterman et al. dispersion**	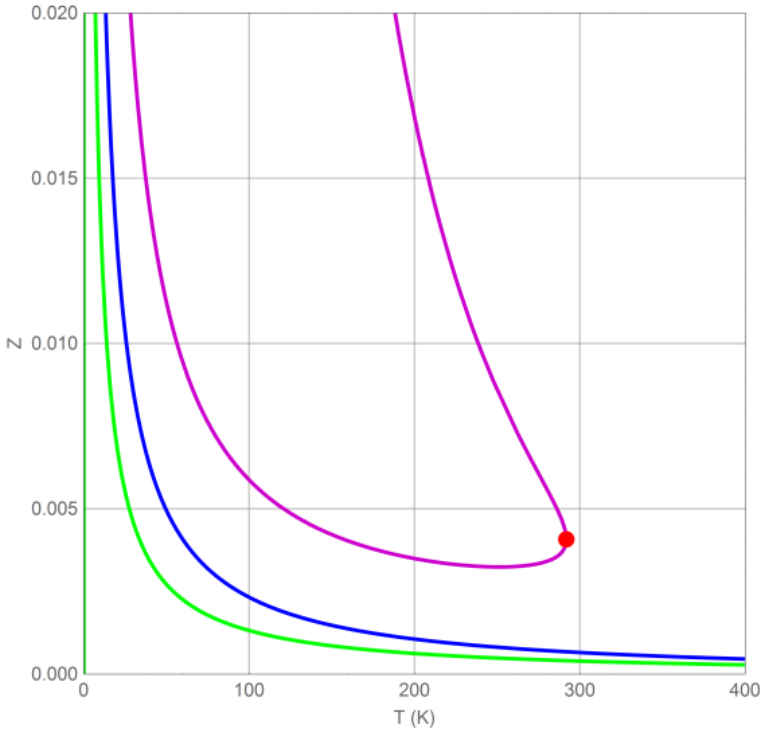 **Figure 7.2: Magnified range of the bifurcation diagram for ethane at 1 atm using CS HS model, TPT1 and Cotterman et al. dispersion**

Kolafa, (1986)	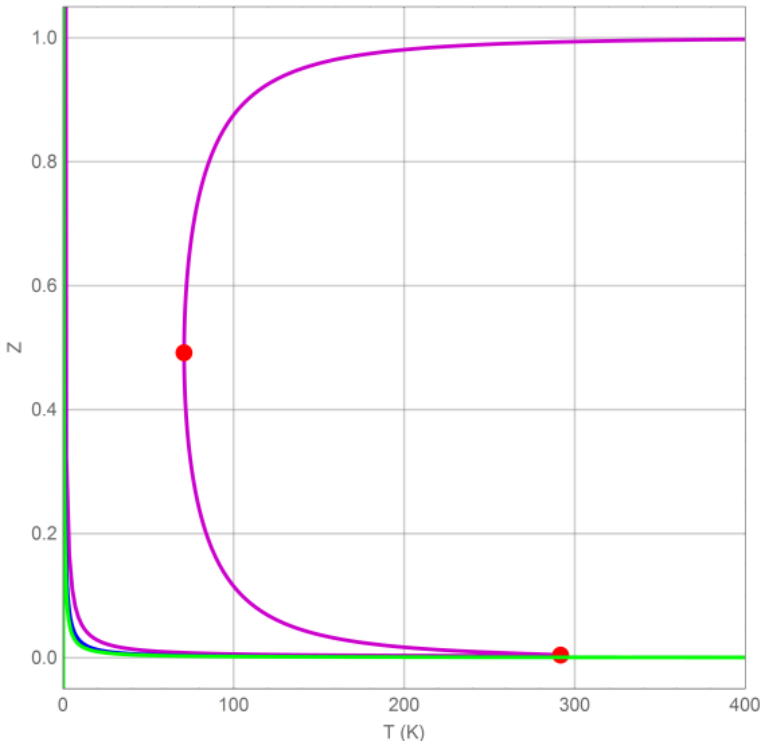 **Figure 7.3: Bifurcation diagram for ethane at 1 atm using Kolafa HS model, TPT1 and Cotterman et al. dispersion**	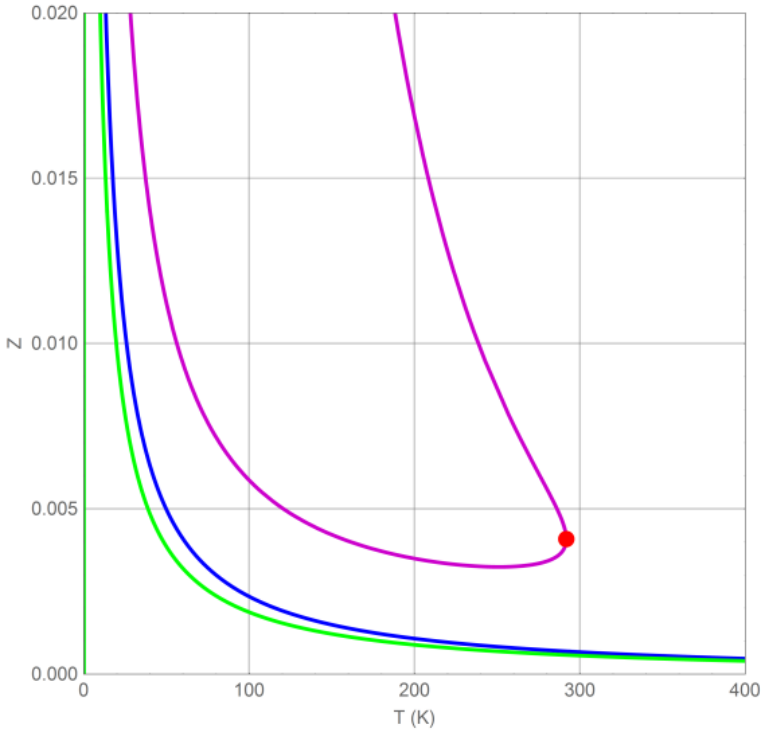 **Figure 7.4: Magnified range of the bifurcation diagram for ethane at 1 atm using Kolafa HS model, TPT1 and Cotterman et al. dispersion**

Khoshbarchi and Vera, (1997)	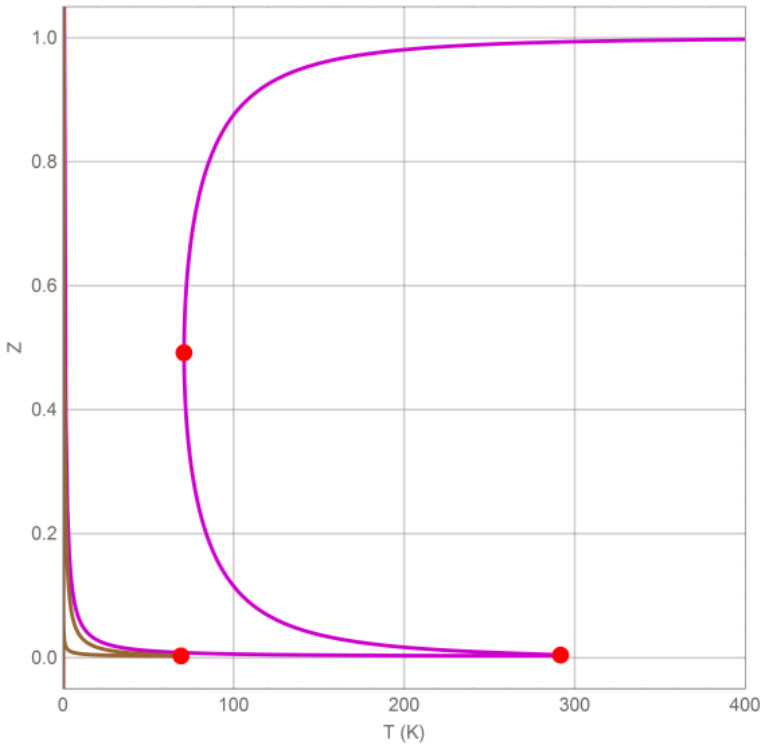 **Figure 7.5: Bifurcation diagram for ethane at 1 atm using Khoshbarchi and Vera HS model, TPT1 and Cotterman et al. dispersion**	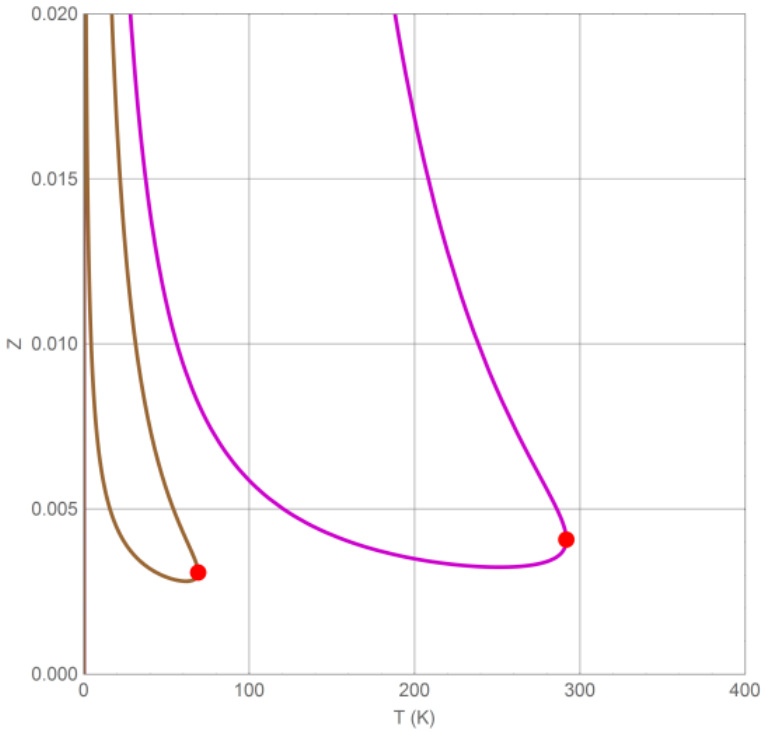 **Figure 7.6: Magnified range of the bifurcation diagram for ethane at 1 atm using Khoshbarchi and Vera HS model, TPT1 and Cotterman et al. dispersion**

Yelash and Kraska, (2001)	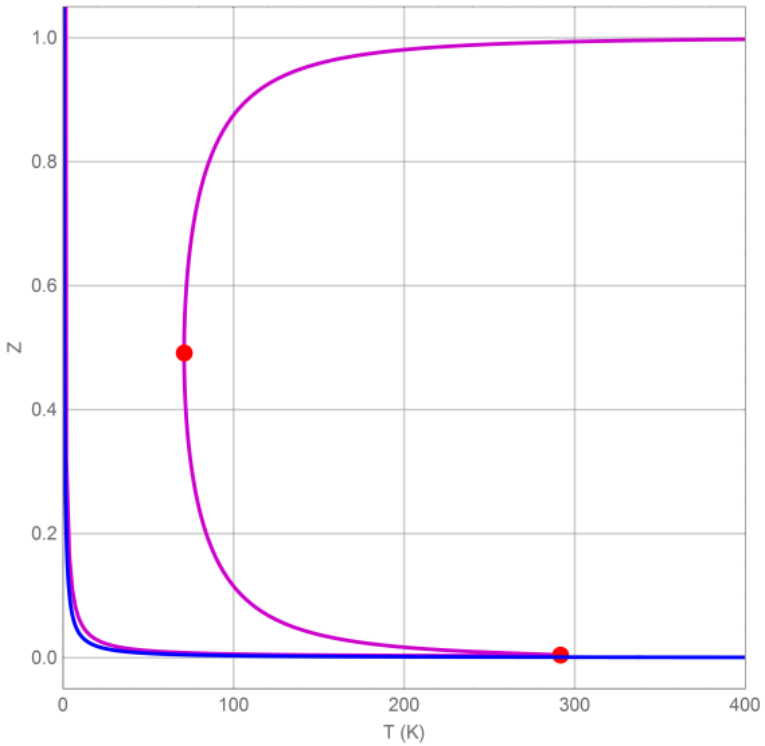 **Figure 7.7: Bifurcation diagram for ethane at 1 atm using Yelash and Kraska HS model, TPT1 and Cotterman et al. dispersion**	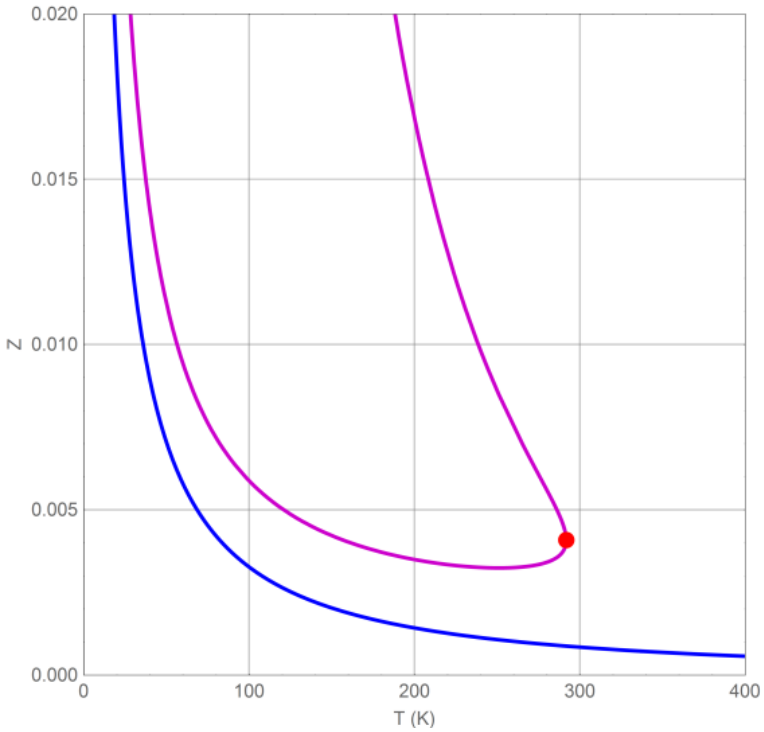 **Figure 7.8: Magnified range of the bifurcation diagram for ethane at 1 atm using Yelash and Kraska HS model, TPT1 and Cotterman et al. dispersion**

Rambaldi et al., (2006)	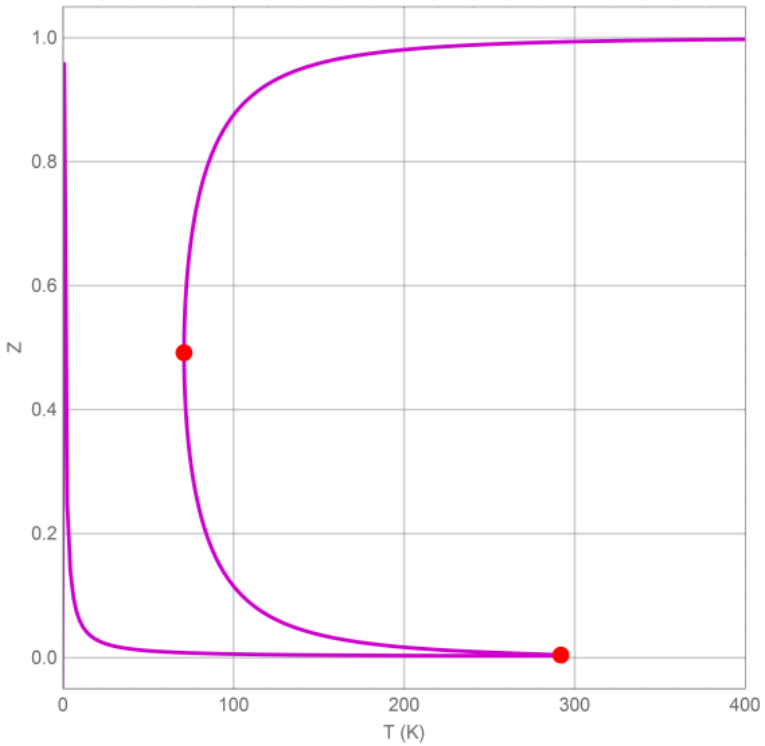 **Figure 7.9: Bifurcation diagram for ethane at 1 atm using Rambaldi et al. HS model, TPT1 and Cotterman et al. dispersion**	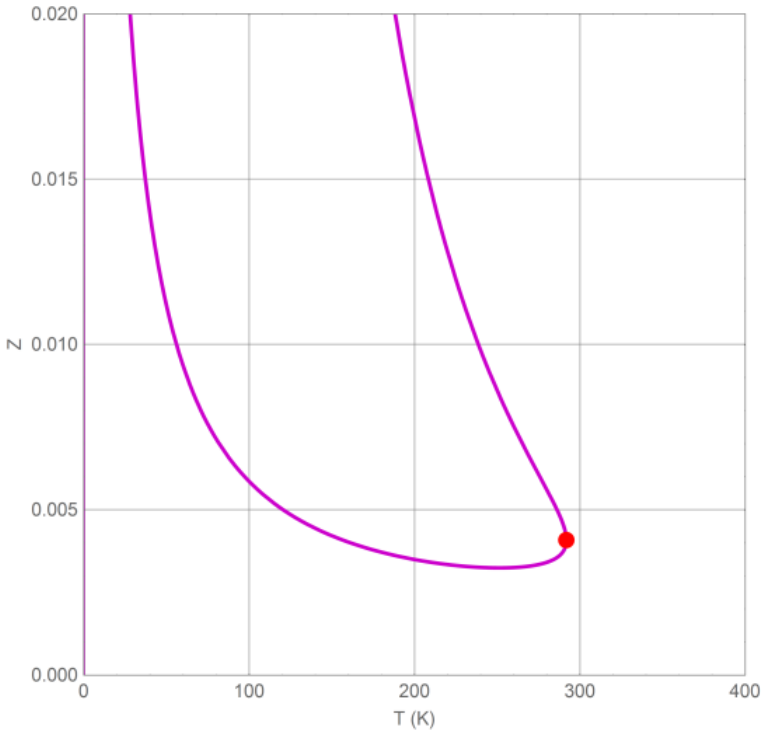 **Figure 7.10: Magnified range of the bifurcation diagram for ethane at 1 atm using Rambaldi et al. HS model, TPT1 and Cotterman et al. dispersion**

7.4. Bifurcation diagrams for associating components

7.4.1. Parameters estimation

For associating components, there are two more adjustable parameters: κ^{AB} and ϵ^{AB}. **Table 7.2** shows the five adjustable parameters for propanol.

Table 7.2: Propanol parameters for Rambaldi et al. HS model with TPT1 chain and Cotterman et al. dispersion term

m	σ (Å)	ϵ/k (K)	ϵ^{AB}/k (K)	κ^{AB}
2.5602	3.5000	225.26	2484.3	0.014062

7.4.2. Bifurcation diagram using Rambaldi et al. hard sphere model with TPT1 and Cotterman et al. dispersion term: branches, turning points and number of roots

In order to explore the effect of the association interaction, the association term is added to TPT1 using Rambaldi et al., which was obtained for the non-associating fluid. **Figures** 7.11-7.12 clearly illustrate that adding the association term do not produce more solution at any temperature.

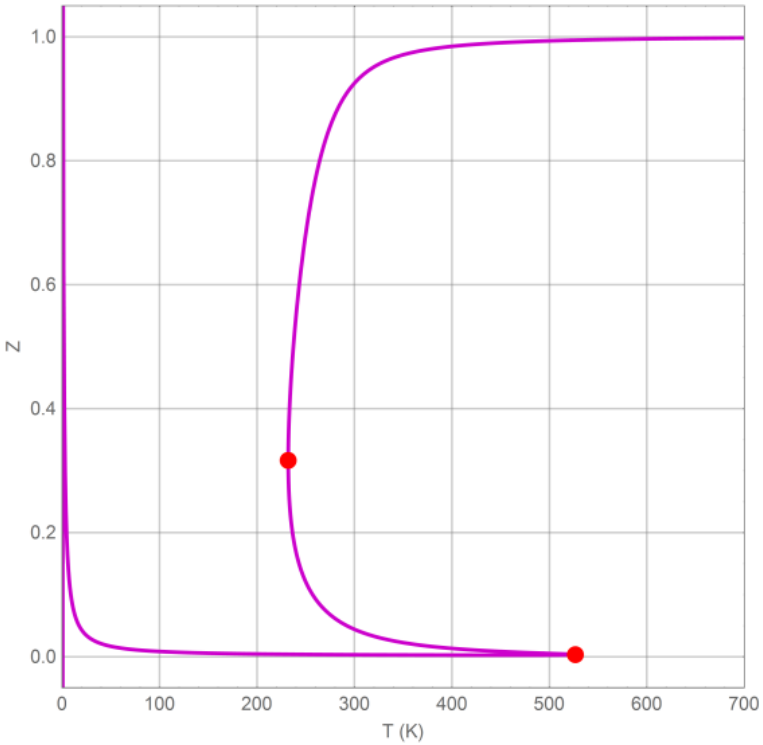

Figure 7.11: Bifurcation diagram for propanol at 1 atm using Rambaldi et al. HS model, TPT1, Cotterman et al. dispersion term and Wertheim association

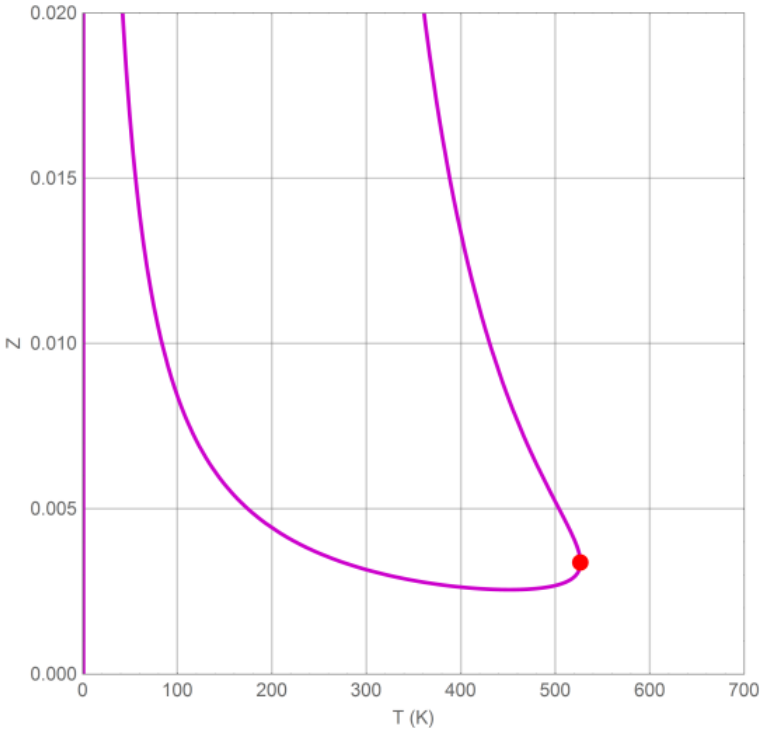

Figure 7.12: Magnified range of the bifurcation diagram for propanol at 1 atm using Rambaldi et al. HS model, TPT1, Cotterman et al. dispersion term and Wertheim association

7.5. PVT behavior without non-physical branches

From the previous analysis, it was found that the problem of volume root multiplicities could be resolved by utilizing Rambaldi et al. (2006) hard sphere model with TPT1 and Cotterman et al. (1986) dispersion term. When the association term was added to the EOS, no additional volume roots were found. The following subsections will explore the proposed terms that are free from non-physical branches.

7.5.1. Hard sphere term

To obtain a physical solution behavior, the HS term should have the same mathematical form as Rambaldi et al. (2006). **Chapter 2** showed that %AAD for Rambaldi et al. (2006) hard sphere model was 0.646% while the %AAD for Carnahan and Starling (1969) model was 0.157%. Thus, it would be advantageous to develop a hard sphere model with the same mathematical form as Rambaldi et al. (2006) but with better accuracy.

7.5.1.1. Developing a new hard sphere model

By reviewing the EOS literature, Rambaldi et al. (2006) model has the form of non-factorable quadratic (NFQ) equation. In order to develop an accurate NFQ hard sphere model satisfying the ideal gas limit and the second virial coefficient, the following platform equation would be suggested:

$$Z = 1 + \frac{4\eta}{1 - c_1\,\eta + c_2\,\eta^2} \tag{7.12}$$

where c_1 and c_2 are adjustable parameters. If the same simulation data that where represented in **Chapter 2** are utilized in order to find proper values for c_1 and c_2 the following model could be obtained:

$$Z = 1 + \frac{4\eta}{1 - 2.47094\,\eta + 1.60901\,\eta^2} \tag{7.13}$$

The residual Helmholtz free energy of the proposed hard sphere model is given by:

$$\frac{A^{hs}}{R\,T} = 18.67741 - 13.91553\arctan(4.29805 - 5.59756\,\eta) \tag{7.14}$$

7.5.1.2. Accuracy of the new hard sphere model

Several properties were tested to ensure the reliability of the suggested model. Table 7.3 compares the compressibility of the suggested model with Carnahan and Starling (1969) model. The simulation data were obtained from Erpenbeck & Wood (1984) except the last three values that were taken from Henderson & Barker (1971). As illustrated in **Table 7.3**, the new model better predicts the compressibility factor especially at high densities.

Table 7.3: Comparison of the new model with CS model

η	z_{sim}	Carnahan and Starling	New Model
0.02962	1.1278	1.1277	1.1276
0.04114	1.1828	1.1828	1.1826
0.07405	1.3594	1.3593	1.3586
0.14809	1.8884	1.8872	1.8850
0.18512	2.2436	2.2418	2.2388
0.24682	3.0316	3.0256	3.0226
0.37024	5.8502	5.8319	5.8443
0.41138	7.4304	7.4088	7.4326
0.43558	8.6003	8.5794	8.6087

0.46280	10.195	10.1779	10.2065
0.47124	10.79	10.7461	10.7715
0.48435	11.72	11.7084	11.7237
%AAD		**0.157%**	**0.110%**

Another measure of hard sphere model performance is the virial coefficient series. The n^{th} virial coefficient for pure hard-spheres is defined as:

$$B_n = \frac{1}{(n-1)!}\left(\frac{\partial^{n-1} Z}{\partial \eta^{n-1}}\right)_{\eta \to 0} \tag{7.15}$$

Molecular simulation data for the virial coefficients is available from Clisby and McCoy (MC) (2006). Simulation data and comparison with CS are shown in **Table 7.4**. The results in the table show that the new model has a satisfactory agreement with the simulation data of the virial coefficients. Carnahan and Starling model has better agreement than the new model since it was developed by approximating the virial coefficients.

Table 7.4: Hard sphere virial coefficients for suggested new HS model compared to molecular simulation values and values calculated from Carnahan and Starling model

	B_n		
n	**MC**	**Carnahan and Starling**	**New Model**
2	4	4	4.00
3	10	10	9.88
4	18.36	18	17.99
5	28.22	28	28.54
6	39.82	40	41.58
7	53.34	54	56.82
8	68.53	70	73.50
9	85.81	88	90.18
10	105.78	108	104.58
	%AAD	**1.25**	**3.19**

7.5.2. Chain term

The chain term in the proposed model that is free from non-physical branches was obtained from TPT1. The same behavior in the first quadrant for non-associating components was found when utilizing TPT-D. However, there is additional branch in the fourth quadrant i.e. negative volume root, which is clearly non-physical and beyond the application of all thermodynamic models.

The HSC theory showed the same behavior as TPT1. However, the low accuracy of the HSC theory makes it non-attractive to use.

The GFD theory, on the other hand, added one more branch, which influences the clarity of the solution behavior.

7.5.2.1. Mathematical form

From the previous discussion, it is recommended to utilize TPT1 in the chain term. The chain term of the proposed hard sphere term would have the following form:

$$Z^{chain} = (1-m)\left(\frac{(1.53569 - 2\,\eta)\eta}{0.62150 + \eta(-1.53569 + \eta)}\right) \tag{7.16}$$

Its corresponding Helmholtz free energy is given by:

$$\frac{A^{chain}}{R\,T} = (1-m)\ln\left(\frac{1}{1 + \eta(-2.47094 + 1.60901\,\eta)}\right) \tag{7.17}$$

7.5.2.2. Accuracy of the hard chain

The resulted equation for the hard chain will be compared with molecular simulation data for hard chains containing 4, 8, 16, 32, 51 and 201 hard sphere segments. The simulation data for $m \leq 16$ and $m = 32$ were taken from Chang and Sandler (1994) and Denlinger and Hall (1990), respectively. The values for the 51-mer and 201-mer chains were compared with the

molecular dynamics data developed by Gao and Weiner (1989). The calculated values of Carnahan and Starling model will be given for comparison. **Table 7.5** represents the compressibility factors of the proposed hard sphere chain model obtained based on molecular simulation and Carnahan and Starling. From the data in the table, it is evident that both models tend to overpredict the compressibility at all densities with almost similar deviation.

Table 7.5: Comparison of molecular simulation data with TPT1 hard chain obtained from CS and the new model as a function of reduced density (ρ*= 6 η/π)

	Z		
ρ*	**simulation**	**Carnahan and Starling**	**New Model**
		m = 4	
0.1	1.49	1.54	1.54
0.2	2.22	2.33	2.32
0.3	3.28	3.45	3.44
0.4	4.84	5.04	5.02
0.5	7.09	7.31	7.28
0.55	8.56	8.79	8.76
0.6	10.26	10.57	10.54
0.65	12.49	12.71	12.70
0.7	15	15.31	15.31
0.75	18.26	18.46	18.50
0.8	22.1	22.31	22.40
0.85	27.02	27.04	27.18
0.9	32.49	32.89	33.09
		m = 8	

0.1	1.76	1.95	1.95
0.2	2.99	3.36	3.35
0.3	4.91	5.42	5.40
0.4	7.75	8.40	8.35
0.5	11.95	12.71	12.64
0.55	14.83	15.54	15.47
0.6	18.26	18.95	18.89
0.65	22.32	23.08	23.04
0.7	27.14	28.10	28.10
0.75	33.34	34.22	34.29
0.8	40.85	41.71	41.89
0.85	50.64	50.95	51.26
0.9	62.03	62.41	62.85
		m = 16	
0.1	2.25	2.75	2.76
0.2	4.47	5.42	5.41
0.3	8.09	9.36	9.32
0.4	13.59	15.12	15.03
0.5	21.96	23.50	23.36
0.55	27.13	29.03	28.88
0.6	34.05	35.72	35.58
0.65	41.9	43.83	43.73
0.7	51.8	53.69	53.68
0.75	65.15	65.74	65.87
0.8	81.28	80.53	80.87
		m = 32	
0.191	7.08	8.98	8.98
0.382	23	26.20	26.03
0.478	37	40.90	40.62
0.573	57.6	61.78	61.47
		m = 51	
0.2	11.46	14.43	14.43
0.3	23.04	26.61	26.49
0.372	34.87	38.81	38.56
0.464	56.56	60.13	59.71
0.59	101.04	104.53	104.04
0.649	130.17	134.01	133.66

0.7	160.56	165.65	165.58
0.8	238.12	250.36	251.44
0.9	346.51	379.78	382.76
		m = 201	
0.2	36.8	53.06	53.05
0.3	79.44	100.54	100.06
0.4	152.11	170.56	169.37
0.5	256.2	273.08	271.23
0.6	407.16	423.40	421.49
0.7	621.54	645.48	645.15
0.8	927.79	978.19	982.43
0.9	1354.76	1486.89	1498.73

In order to quantify the agreement with simulation data, **Table 7.6** represents the percentage average absolute deviation (%AAD) for the compressibility factor predicted by Carnahan and Starling and the new model. The results in **Table 7.6** indicate that the new model is slightly better than Carnahan and Starling in predicting the compressibility factor for all chain

lengths. The discrepancy with the simulation data increases with the chain length. The results of 32-mer chain are inconsistent with the others because the comparison for 32-mer chain is limited to moderate density values.

Table 7.6: Percentage average absolute deviation (AAD) of the calculated compressibility of m-hard-sphere chains compared with molecular simulation data

	AAD (%)	
m	**Carnahan and Starling**	**New Model**
4	2.57	2.57
8	5.33	5.30
16	9.04	8.78
32	14.63	14.14
51	9.26	9.09
201	14.06	13.90
Overall	7.87	7.73

7.5.3. Dispersion and association terms

The dispersion and the association terms in the new model were utilized as in section 7.2 where the dispersion term was taken according to Cotterman et al. (1986) and the association term according to Wertheim (1984a; 1984b; 1986a; 1986b). The pair correlation function at contact $g_{HS}(d)$ is given by:

$$g_{HS}(d) = \frac{1}{1 - 2.47094\,\eta + 1.609010\,\eta^2} \tag{7.18}$$

7.5.4. Parameters estimation for some compounds

Once the previous terms have been established, the total equation of state could be adopted to optimize the adjustable parameters. **Table 7.7** represents the adjustable parameters for some components. Using these parameters, the bifurcation diagrams for ethane and propanol are generated and shown in **Figures 7.13** and **7.14**.

Table 7.7: Parameters for some compounds

compound	m	σ (Å)	ϵ/k (K)	ϵ^{AB}/k (K)	κ^{AB}
Ethane	1.6379	3.5408	176.57		
Propane	2.2000	3.5555	180.88		
Butane	2.8026	3.5532	184.22		
Pentane	3.0638	3.6633	196.57		
Hexane	3.8538	3.5827	190.31		
Heptane	4.2256	3.6452	195.74		
Octane	4.5097	3.6919	202.32		
Nonane	5.1846	3.6739	199.29		
Decane	5.8568	3.6594	197.13		
Benzene	2.8475	3.5470	242.16		
Propanol	2.5746	3.5000	224.78	0.014285	2466.5

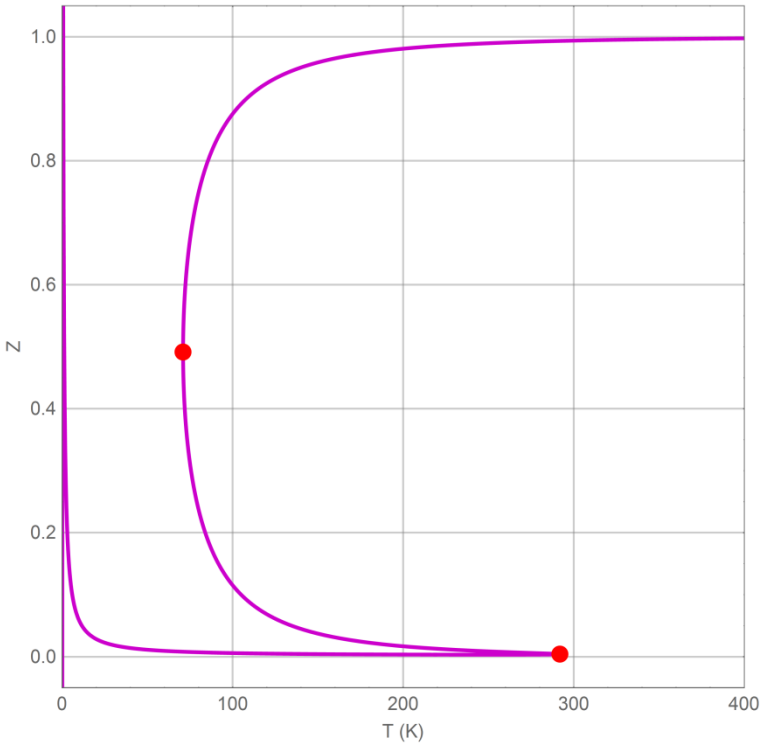

Figure 7.13: Bifurcation diagram for ethane at 1 atm using the new HS model, TPT1 and Cotterman et al. dispersion term

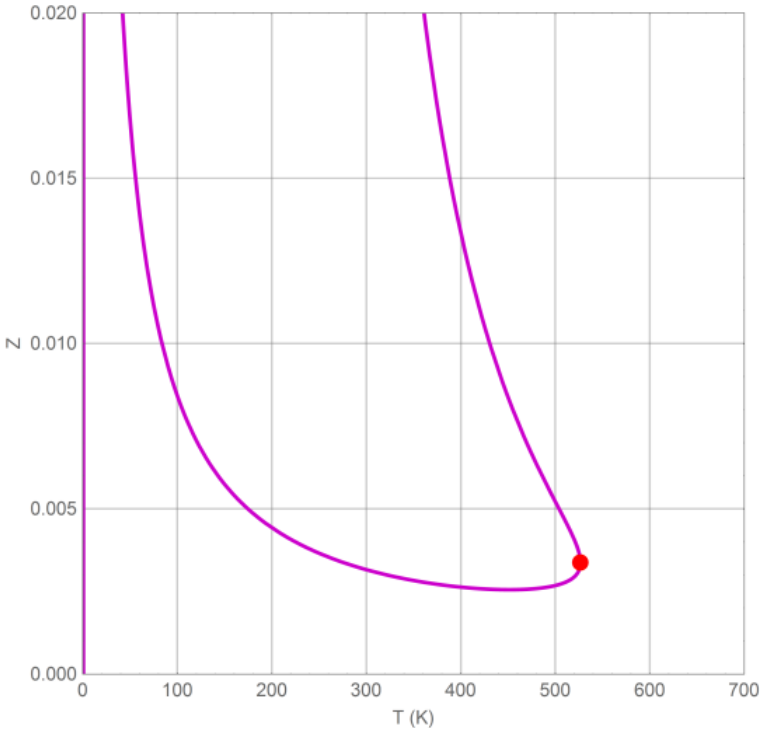

Figure 7.14: Bifurcation diagram for propanol at 1 atm using the new HS model, TPT1, Cotterman et al. dispersion term and Wertheim association

CHAPTER 8

CONCLUSIONS AND RECOMMENDATIONS

8.1. Conclusions

The hard-sphere chain theories play a major role in the development of theoretical models, which are not cubic in volume. Although most hard-sphere chain theories compare well with molecule simulation data, the accuracy is not the only factor that matter in the final proposed models. The mathematical formulations of the proposed models might indeed cause some unexpected pitfalls in the prediction of pressure-volume-temperature behavior. Some theory-based models like PC-SAFT EOS accommodate non-physical behavior such as artificial two-phase separation regions and multiple non-physical volume roots because of the constructed mathematical formulations.

In this thesis, the final constructed mathematical forms of hard sphere chain theory (HSC), the first order thermodynamic perturbation theory (TPT1), the thermodynamic perturbation dimer theory (TPT-D) and the generalized Flory dimer theory (GFD) were critically studied to explore their role on the generation of non-physical behavior. To do so, two dispersion terms were adopted to complete the equations of state; namely, Fu & Sandler (1995) and Cotterman et al. (1986) dispersion terms. Extensive evaluation to hard sphere models were made since the hard sphere model is the main component in all hard-sphere chain theories. Various hard sphere models were investigated including Carnahan and Starling (CS) (1969) , Kolafa (Boublík, 1986), Khoshbarchi and Vera (1997), Yelash and Kraska (2001) and Rambaldi et al.

(2006) hard-sphere models. The ultimate target was to select a complete model with a potential hard sphere model and hard-sphere chain theory that is free from non-physical behavior including the multiplicity of volume roots that exist in all current theory-based models. The association term was added into the final selected model. Due to the need of an accurate hard sphere model with a simple mathematical form, a new hard sphere model was introduced by adjusting molecular simulation data.

The arc-length continuation method was utilized in order to generate the bifurcation diagrams, which illustrate how the number of compressibility factor (Z) roots varies with temperature at a specified pressure. Thus, the bifurcation diagrams were employed as powerful tools to explore how the PVT behavior could be affected by the various terms of the theory-based EOS including hard sphere, chain, dispersion, and association terms.

This study was approached through utilizing various hard sphere terms that have different mathematical forms. TPT1 was adopted to derive the chain term that was fixed based on Carnahan & Starling. It was found that using inconsistent terms in the EOS introduces more non-physical roots although the accuracies of the physical roots are similar. After that, the corresponding chain terms of the various hard sphere models were derived and utilized in the EOS. This approach caused a reduction in the number of the non-physical volume roots but it did not entirely resolve the problem. In addition, the resulted PVT behavior exhibited an artificial two-phase separation region at low temperature.

In order to explore the role of the chain term, various chain theories were used to derive the chain term, namely HSC, TPT1, TPT-D and GFD. The dispersion term was fixed to Fu & Sandler's (1995) dispersion term. It was found that TPT1 and TPT-D produce the same PVT behavior at the first quadrant while HSC could produce less non-physical roots for some hard sphere models. The GFD theory may produce more or less non-physical roots depending on the form of the hard sphere model. The problem of getting non-physical roots was not resolved by utilizing different chain theories. In addition, the resulted bifurcation diagrams illustrated the existence of artificial two-phase separation region at low temperature. Since TPT1 theory has a relatively simple mathematical form and good accuracy, it was reasonable to utilize TPT1 theory to derive the chain terms and then study the role of the dispersion term.

Another dispersion term, which was proposed by Cotterman et al. (1986), was utilized in order to explore the influence on the PVT behavior. It was found that the hard sphere models that have the form of non-factorable quadratic (NFQ) equation resulted in PVT behavior similar to cubic EOSs. In other words, the model is free from exhibiting multiple volume roots and artificial two-phase separation region. Thus, one could develop theory-based EOS for non-associating components and having PVT behavior similar to cubic EOSs by adopting the following conditions:

- The hard sphere term has the form of NFQ
- The chain term is derived from TPT1
- The dispersion term is taken from Cotterman et al. (1986)

Although TPT-D chain theory produces the same PVT behavior in the first quadrant, it predicted negative volume root, which is clearly non-physical and beyond the application of all thermodynamic models. The HSC theory showed the same behavior as TPT1, but its low accuracy makes it non-attractive to use. Moreover, the PVT behavior was not affected when the proper association term, which is derived from the NFQ hard sphere model, was added to the equation. Therefore, the proposed model could be utilized for both associating and non-associating components.

8.2. Recommendations

This thesis employed five different hard sphere models while there are many models available in the literature. Thus, it would be recommended to expand the study to investigate more models with different mathematical forms. In addition, only two different dispersion terms were studied. Hence, the work could be extended to account for various dispersion terms.

Because it is more important to calculate the properties of mixtures, it is recommended to extend this study to account for mixtures and to study the influence of various mixing rules on the PVT behavior.

The theory-based EOSs have been utilized in the polymer field. Thus, it is recommended to explore the performance of the proposed model with large molecules such as polymers. Moreover, this study was limited to associating components with only two association sites, the role of considering more association sites could also be investigated.

REFERENCES

Seydel, R., 2009. *Practical Bifurcation and Stability Analysis.* s.l.:Springer Science & Business Media.

Alder, B. J. & Wainwright, T. E., 1960. Studies in Molecular Dynamics. II. Behavior of a Small Number of Elastic Spheres. *The Journal of Chemical Physics* , 33(5), p. 1439 .

Allgower, E. L. & Georg, . K., 1990. *Numerical Continuation Methods: An Introduction.* 1st Edition ed. Springer-Verlag: Berlin Heidelberg.

Alsaifi, N. M. & Englezos, P., 2011. Prediction of multiphase equilibrium using the PC-SAFT equation of state and simultaneous testing of phase stability. *Fluid Phase Equilibria,* 302(1–2), p. 169–178.

Aslam, N. & Sunol, A., 2006a. Reliable Computation of All the Density Roots of the Statistical Associating Fluid Theory Equation of State through Global Fixed-Point Homotopy. *Industrial & Engineering Chemistry Research,* 45(9), pp. 3303-3310.

Barosova, M., 1996. *Statistical thermodynamic study of binary mixtures of hard spheres, PhD Thesis.* Czech Republic: Institute of Chemical Technology.

Baus, M. & Colot, J. L., 1987. Thermodynamics and structure of a fluid of hard rods, disks, spheres, or hyperspheres from rescaled virial expansions. *PHYSICAL REVIEW A,* 36(8), p. 3912.

Behme, S., Sadowski, G. & Arlt, W., 1999. Modeling of the separation of polydisperse polymer systems by compressed gases. *Fluid Phase Equilibria,* Volume 158-160, p. 869–877.

Binous, H. & Shaikh, A. A., 2015. Introduction of the Arc-Length Continuation Technique in the Chemical Engineering Graduate Program at KFUPM. *Computer Applications in Engineering Education,* 23(3), pp. 344-351.

Blas, F. J. & Vega, L. F., 1998. Critical behavior and partial miscibility phenomena in binary mixtures of hydrocarbons by the statistical associating fluid theory. *Chemical Physics,* Volume 109, p. 7405.

Bolaños, G. & Thies, M. C., 1996. Suppercritical toluene-petroleum pitch mixtures: liquid-liquid equilibria and SAFT modeling. *Fluid Phase Equilibria,* 117(1-2), p. 273–280.

Boublík, T., 1986. Equations of state of hard body fluids. *Molecular Physics,* 59(2), pp. 371-380.

Button, J. K. & Gubbins, K. E., 1999. SAFT prediction of vapour-liquid equilibria of mixtures containing carbon dioxide and aqueous monoethanolamine or diethanolamine. *Fluid Phase Equilibria,* Volume 158-160, p. 175–181.

Byun, H. S., Hasch, B. M. & McHugh, M. A., 1996. Phase behavior and modeling of the systems CO2-acetonitrile and CO2-acrylic acid. *Fluid Phase Equilibria,* 115(1-2), p. 179–192.

Carnahan, N. F. & Starling, K. E., 1969. Equation of State for N onattracting Rigid Spheres. *THE JOURNAL OF CHEMICAL PHYSICS,* Volume 51.

Chang, J. & Sandler, S. I., 1994. An equation of state for the hard-sphere chain fluid: theory and Monte Carlo simulation. *Chemical Engineering Science,* 49(17), pp. 2777-2791.

Chapman, W. G., Gubbins, K. E., Jackson, G. & Radosz, M., 1990. New reference equation of state for associating liquids. *Industrial and Enginering Chemistry Research,* Volume 29, p. 1709.

Chapman, W. G., Jackson, G. & Gubbins, K. E., 1988. Phase equilibria of associating fluids. *Molecular Physics,* 65(5), pp. 1057-1079.

Chen, C.-k., Banaszak, M. & Radosz , M., 1998. Statistical Associating Fluid Theory Equation of State with Lennard-Jones Reference Applied to Pure and Binary n-Alkane Systems. *Physical Chemistry,* Volume 102, p. 2427–2431.

Chiew, Y. C., 1990. Percus-Yevick integral-equation theory for athermal hard-sphere chains. *Molecular Physics,* 70(1), pp. 129-143.

Chiew, Y. C., 1991. Percus-Yevick integral equation theory for athermal hard-sphere chains. II. Average intermolecular correlation functions. *Molecular Physics,* 73(2), pp. 359-373.

Clements, P. J. et al., 1997. Thermodynamics of ternary mixtures exhibiting tunnel phase behaviour. *Chemical Society, Faraday Transactions,* 93(7), pp. 1331-1339.

Clisby, N. & McCoy, B. M., 2006. Ninth and Tenth Order Virial Coefficients for Hard Spheres in D Dimensions. *Statistical Physics,* 122(1), pp. 15-57.

Cotterman, R. L., Schwarz, B. J. & Prausnitz, J. M., 1986. Molecular thermodynamics for fluids at low and high densities. Part I: Pure fluids containing small or large molecules. *AlChE,* 32(11), p. 1787–1798.

Denlinger, M. A. & Hall, C. K., 1990. Molecular-dynamics simulation results for the pressure of hard-chain fluids. *Molecular Physics,* 71(3), pp. 541-559.

Dickman, R. & Hall, C. K., 1986. Equation of state for chain molecules: Continuous-space analog of Flory theory. *Chemical Physics,* 85(7), p. 4108.

Economou, I. G. & Donohue, M. D., 1992. Equation of state with multiple associating sites for water and water-hydrocarbon mixtures. *Industrial & engineering chemistry,* Volume 31, p. 2388–2394.

Economou, I. G., Gregg, C. J. & Radosz, M., 1992. Solubilities of solid polynuclear aromatics (PNA's) in supercritical ethylene and ethane from statistical associating fluid theory (SAFT): toward separating PNA's by size and structure. *Industrial & Engineering Chemistry Research,* Volume 31, p. 2620–2624.

Erpenbeck, J. J. & Wood, W. W., 1984. Molecular dynamics calculations of the hard-sphere equation of state. *Journal of Statistical Physics,* 35(3), pp. 321-340.

Fu, Y. H. & Sandler, S. I., 1995. A simplified SAFT equation of state for associating compounds and mixtures. *Industrial and Engineering Chemistry Research,* Volume 34, pp. 1897-1909.

Fu, Y.-H. & Sandler, S. I., 1995. A Simplified SAFT Equation of State for Associating. *Ind. Eng. Chem. Res.*, Volume 13, pp. 1897-1909.

Galindo, A., Gil-Villegas, A., Whitehead, P. J. & Jackson, G., 1998. Prediction of Phase Equilibria for Refrigerant Mixtures of Difluoromethane (HFC-32), 1,1,1,2-Tetrafluoroethane (HFC-134a), and Pentafluoroethane (HFC-125a) Using SAFT-VR. *Physical Chemistry,* Volume 102, p. 7632–7639.

Galindo, A., Whitehead, P. J. & Jackson, G., 1997. Predicting the Phase Equilibria of Mixtures of Hydrogen Fluoride with Water, Difluoromethane (HFC-32), and 1,1,1,2-Tetrafluoroethane (HFC-134a) Using a Simplified SAFT Approach. *Physical Chemistry,* Volume 101, p. 2082–2091.

Galindo, A., Whitehead, P. J., Jackson, G. & Burgess, A. N., 1996. Predicting the High-Pressure Phase Equilibria of Water + n-Alkanes Using a Simplified SAFT Theory with Transferable Intermolecular Interaction Parameters. *Physical Chemistry,* Volume 100, p. 6781–6792.

Gao, J. & Weiner, J. H., 1989. Contribution of covalent bond force to pressure in polymer melts. *The Journal of Chemical Physics* , 91(5), p. 3168 .

Garcia-Lisbona, M. N., Galindo, A., Jackson, G. & Burguess, A. N., 1998. Predicting the high-pressure phase equilibria of binary aqueous solutions of 1-butanol, n-butoxyethanol and n-decylpentaoxyethylene ether (C10E5) using the SAFT-HS approach. *Molecular Physics,* 93(1), pp. 57-72.

Ghonasgi, D. & Chapman, W. G., 1994. A new equation of state for hard chain molecules. *Chemical Physics,* 100(9), p. 6633 .

Ghotbi, C. & Vera, J. H., 2001. Extension to mixtures of two robust hard-sphere equations of state satisfying the ordered close-packed limit. *The Canadian Journal of Chemical Engineering,* 79(4), p. 678–686.

Goldman, J. I. & White, J. A., 1988. Equation of state for the hard-sphere gas. *Chemical Physics,* 89(10), p. 6403.

Gregg, C. J. & Radosz, M., 1993. Vapor-liquid equilibria for carbon dioxide and 1-methylnaphthalene: experiment and correlation. *Fluid Phase Equilibria,* Volume 86, pp. 211-223.

Gregg, C. J., Stein, F. P., Chen, S. J. & Radosz, M., 1993. Phase equilibria of binary and ternary n-alkane solutions in supercritical ethylene, 1-butene, and ethylene + 1-butene. Transition from type A through LCST to U-LCST behavior predicted and confirmed experimentally. *Industrial & Engineering Chemistry Research,* Volume 32, p. 1442–1448.

Gulati, H. S. & Hall, C. K., 1998. Generalized Flory equations of state for copolymers modeled as square-well chain fluids. *Chemical Physics,* 108(17), p. 7478 .

Han, S. J., Gregg, C. J. & Radosz, M., 1997. How the Solute Polydispersity Affects the Cloud-Point and Coexistence Pressures in Propylene and Ethylene Solutions of Alternating Poly(ethylene-co-propylene). *Industrial & Engineering Chemistry Research,* Volume 36, p. 5520–5525.

Hasch, B. M., Maurer, E. J., Ansanelli, L. F. & McHugh, M. A., 1994. (Methanol + ethene): phase behavior and modeling with the SAFT equation of state. *Chemical Thermodynamics,* 26(6), pp. 625-640.

Hasch, B. M. & McHugh, M. A., 1995. Calculating poly(ethylene-co-acrylic acid)-solvent phase behavior with the SAFT equation of state. *Polymer Science Part B,* 33(4), p. 715–723.

Henderson, D. & Barker, J. A., 1971. Monte Carlo values for the radial distribution function of a system of fluid hard spheres. *Molecular Physics,* 21(1), pp. 187-191.

Honnell, K. G. & Hall, C. K., 1989. A new equation of state for athermal chains. *Chemical Physics,* 90(3), p. 1841.

Huang, S. H. & Radosz, M., 1990. Equation of State for Small, Large, Polydisperse and Associating Molecules. *Industrial and Engineering Chemistry Research,* Volume 29, p. 2284.

Huang, S. H. & Radosz, M., 1991a. Equation of state for small, large, polydisperse, and associating molecules: extension to fluid mixtures. *Industrial and Engineering Chemistry Research,* 30(8), pp. 1994-2005.

Huang, S. H. & Radosz, M., 1991b. Phase behavior of reservoir fluids V: SAFT model of CO2 and bitumen systems. *Fluid Phase Equilibria,* 70(1), pp. 33-54.

Huang, S. H. & Radosz, M., 1991. Equation of state for small, large, polydisperse, and associating molecules: extension to fluid mixtures. *Industrial and Engineering Chemistry Research,* 30(8), pp. 1994-2005.

Khoshkbarchi, M. K. & Vera, J. H., 1997. A simplified hard-sphere equation of state meeting the high and low density limits. *Fluid Phase Equilibria,* 130(1-2), p. 189–194.

Koak, N., de Loos, T. W. & Heidemann, R. A., 1999a. Effect of the Power Series Dispersion Term on the Pressure−Volume Behavior of Statistical Associating Fluid Theory. *Industrial & Engineering Chemistry Research,* 38(4), pp. 1718-1722.

Koak, N., de Loos, T. W. & Heidemann, R. A., 1999. Effect of the Power Series Dispersion Term on the Pressure−Volume Behavior of Statistical Associating Fluid Theory. *Industrial & Engineering Chemistry Research,* 38(4), pp. 1718-1722.

Koak, N., Visser, R. M. & de Loos, T. W., 1999b. High-pressure phase behavior of the systems polyethylene+ethylene and polybutene+1-butene. *Fluid Phase Equilibria,* Volume 158-160, p. 835–846.

Kraska, T. & Gubbins, K. E., 1996a. Phase Equilibria Calculations with a Modified SAFT Equation of State. 1. Pure Alkanes, Alkanols, and Water. *Industrial & Engineering Chemistry,* Volume 35, p. 4727–4737.

Kraska, T. & Gubbins, K. E., 1996b. Phase Equilibria Calculations with a Modified SAFT Equation of State. 2. Binary Mixtures of n-Alkanes, 1-Alkanols, and Water. *Industrial & Engineering Chemistry,* Volume 35, p. 4738–4746.

Kratky, K. W., 1977. Fifth to tenth virial coefficients of a hard-sphere fluid. *Physica A: Statistical Mechanics and its Applications,* 87(3), pp. 584-600.

Kuespert, D. R. & Donohue, M. D., 1993. Local ordering in asymmetric chain fluids. *Chemical Physics,* Volume 98, p. 9782.

Lee, S. H., LoStracco, M. A. & McHugh, M. A., 1996. Cosolvent Effect on the Phase Behavior of Poly(ethylene-co-acrylic acid)−Butane Mixtures. *Macromolecules,* Volume 29, p. 1349–1358.

Li , X. S., Lu, J. F., Li, Y. G. & Liu, J. C., 1998. Studies on UNIQUAC and SAFT equations for nonionic surfactant solutions. *Fluid Phase Equilibria,* 153(2), p. 215–229.

Liu, W. B., Li, Y. G. & Lu, J. F., 1999. A new equation of state for real aqueous ionic fluids based on electrolyte perturbation theory, mean spherical approximation and statistical associating fluid theory. *Fluid Phase Equilibria,* Volume 158-160, p. 595–606.

Lucia, A. & Luo, Q., 2002. Binary refrigerant–oil phase equilibrium using the simplified SAFT equation. *Advances in Environmental Research,* 6(2), pp. 123-134.

Malijevsky, A. & Veverka, J., 1999. New equations of state for pure and binary hard-sphere fluids. *Physical Chemistry Chemical Physics,* Volume 1, pp. 4267-4270.

Mangold , M. & Gilles , E. D., 2012. Analysis of Unsteady State Chemical Reactors by continuatioin Methods. In: K. Frerich , M. Wolfgang & J. Heinrich Voß, eds. *Scientific Computing in Chemical Engineering.* s.l.:Springer Science & Business Media, p. 149.

McCabe, C., Galindo, A., Gil-Villegas, A. & Jackson, G., 1998b. Predicting the High-Pressure Phase Equilibria of Binary Mixtures of Perfluoro-n-alkanes + n-Alkanes Using the SAFT-VR Approach. *Physical Chemistry,* Volume 102, p. 8060–8069.

McCabe, C., Gil-Villegas , A. & Jackson, G., 1998a. Predicting the High-Pressure Phase Equilibria of Methane + n-Hexane Using the SAFT-VR Approach. *Physical Chemistry,* Volume 102, p. 4183–4188.

Miandehy, M., Modarress, H. & Dehghani, M. R., 2006. Equation of state for hard-spheres and excess function calculations of binary liquid mixtures. *Fluid phase equilibria,* 239(1), pp. 91-99.

Mie, Z., 2013. *Numerical Bifurcation Analysis for Reaction-Diffusion Equations.* s.l.:Springer Science & Business Media.

Mulero, A., Galan, C. A., Parra, M. I. & Cuadros, F., 2008. Equations of State for Hard Spheres and Hard Disks. In: *Theory and Simulation of Hard-Sphere Fluids and Related Systems.* Badajoz: s.n., pp. 37-109.

Pan, C. & Radosz, M., 1998. Copolymer SAFT Modeling of Phase Behavior in Hydrocarbon-Chain Solutions: Alkane Oligomers, Polyethylene, Poly(ethylene-co-olefin-1), Polystyrene, and Poly(ethylene-co-styrene). *Industrial & Engineering Chemistry Research,* Volume 37, p. 3169–3179.

Pan, C. & Radosz, M., 1999. Modeling of solid–liquid equilibria in naphthalene, normal-alkane and polyethylene solutions. *Fluid Phase Equilibria*, 155(1), p. 57–73.

Peng, D. Y. & Robinson, D. B., 1976. A New Two-constant Equation of State. *Industrial & Engineering Chemistry Fundamentals ,* Volume 15, pp. 58-64.

Pfohl, O. & Brunner, G., 1998. 2. Use of BACK To Modify SAFT in Order To Enable Density and Phase Equilibrium Calculations Connected to Gas-Extraction Processes. *Industrial & Engineering Chemistry Research,* Volume 37, p. 2966–2976.

Polishuk, I., 2011. Addressing the issue of numerical pitfalls characteristic for SAFT EOS models. *Fluid Phase Equilibria ,* 301(1), p. 123–129.

Polishuk, I. & Mulero, A., 2011. The numerical challenges of SAFT EOS models. *Reviews in Chemical Engineering*, Volume 27, pp. 241-251.

Privat, R., Gani, R. & Jaubert, J.-N., 2010. Are safe results obtained when the PC-SAFT equation of state is applied to ordinary pure chemicals?. *Fluid Phase Equilibria*, 295(1), p. 76–92.

Rambaldi, S., Salustri, G. & Benedetti, C., 2006. Hard sphere gas state equation. *Physica A*, 361(1), p. 180–194.

Sadowski, G., Mokrushina, L. V. & Arlt, W., 1997. Finite and infinite dilution activity coefficients in polycarbonate systems. *Fluid Phase Equilibria*, 139(1-2), p. 391–403.

Sadus, R. J., 1995. Equations of State for Hard-Sphere Chains. *Physical Chemistry*, 99(32), pp. 12363-12366.

Sadus, R. J., 1999. Simple equation of state for hard-sphere chains. *AlChE*, 45(11), p. 2454–2457.

Song, Y., Lambert, S. M. & Prausnitz, J. M., 1994a. A Perturbed Hard-Sphere-Chain Equation of State for Normal Fluids and Polymers. *Industrial & Engineering Chemistry Research*, Volume 33, p. 1047–1057.

Song, Y., Lambert, S. M. & Prausnitz, J. M., 1994a. Equation of state for mixtures of hard-sphere chains including copolymers. *Macromolecules*, 27(2), p. 441–448.

Song, Y., Lambert, S. M. & Prausnitz, J. M., 1994b. A Perturbed Hard-Sphere-Chain Equation of State for Normal Fluids and Polymers. *Industrial & Engineering Chemistry Research*, Volume 33, p. 1047–1057.

Song, Y., Lambert, S. M. & Prausnitz, J. M., 1994b. Equation of state for mixtures of hard-sphere chains including copolymers. *Macromolecules,* 27(2), p. 441–448.

Suresh, J. & Beckman, E. J., 1994. Prediction of liquid-liquid equilibria in ternary mixtures from binary data. *Fluid Phase Equilibria,* Volume 99, pp. 219-240.

Suresh, S. J. & ElliottJr., J. R., 1992. Multiphase equilibrium analysis via a generalized equation of state for associating mixtures. *Industrial & Engineering Chemistry,* Volume 31, p. 2783–2794.

Suresh, S. J., Enick, R. M. & Beckman, E. J., 1994. Phase behavior of nylon 6/trifluoroethanol/carbon dioxide mixtures. *Macromolecules,* Volume 27, p. 348–356.

Tildesley, D. J. & Streett, W. B., 1980. An equation of state for hard dumbell fluids. *Molecular Physics,* 41(1), pp. 85-94.

Vargaftik, N. B., 1975. *Tale on the Thermophysical properties of Liquids and Gases, and. E d.* s.l.:John willey & son.

Verlet, L., 1968. Computer "Experiments" on Classical Fluids. II. Equilibrium Correlation Functions. *Physical Review,* 165(1), pp. 201-214.

Walsh, J. M., Guedes, H. J. R. & Gubbins, K. E., 1992. Physical theory for fluids of small associating molecules. *Physical Chemistry,* Volume 96, p. 10995–11004.

Wang, X. Z., 2002. van der Waals–Tonks-type equations of state for hard-disk and hard-sphere fluids. *Physical Review E,* 66(3), p. 31203 .

Weeks, J. . D., Chandler, D. & Andersen, H. C., 1971. Role of Repulsive Forces in Determining the Equilibrium Structure of Simple Liquids. *Chemical Physics,* 54(12), p. 5237 .

Wertheim, M. S., 1984a. Fluids with Highly Directional Attractive Forces. I. Statistical Thermodynamics. *Journal of statistical physics,* Volume 35, p. 19.

Wertheim, M. S., 1984b. Fluids with Highly Directional Attractive Forces. II. Thermodynamic Perturbation Theory and Integral Equations. *journal of statistical physics,* Volume 35, p. 35.

Wertheim, M. S., 1986a. Fluids with Highly Directional Attractive Forces. III. Multiple Attraction Sites. *journal of statistical physics,* Volume 42, p. 459.

Wertheim, M. S., 1986b. Fluids with Highly Directional Attractive Forces. IV. Equilibrium Polymerization. *journal of statistical physics,* Volume 42, p. 477.

Wu, C. S. & Chen, Y. P., 1994. Calculation of vapor-liquid equilibria of polymer solutions using the SAFT equation of state. *Fluid Phase Equilibria,* Volume 100, pp. 103-119.

Wu, J., Prausnitz, J. M. & Firoozabadi, A., 1998. Molecular-thermodynamic framework for asphaltene-oil equilibria. *AIChE,* Volume 44, p. 1188.

Xiong, Y. & Kiran, E., 1995. Comparison of Sanchez–Lacombe and SAFT model in predicting solubility of polyethylene in high-pressure fluids. *Applied Polymer Science,* 55(13), p. 1805–1818.

Xu, G., Brennecke, J. F. & Stadtherr, M. A., 2002. Reliable Computation of Phase Stability and Equilibrium from the SAFT Equation of State. *Industrial and Engineering Chemistry Research,* Volume 41, pp. 938-952.

Yelash, L., Muller, M., Paul, W. & Binder, K., 2005. A global investigation of phase equilibria using the perturbed-chain statistical-associating fluid theory approach. *The Journal of Chemical Physics,* Volume 123, pp. 14908-.

Yelash, L. V. & Kraska, T., 2001. A generic equation of state for the hard-sphere fluid incorporating the high density limit. *Physical Chemistry Chemical Physics,* 3(15), pp. 3114-3118.

Yethiraj, A. & Hall, C. K., 1990. Local structure of fluids containing chain-like molecules: Polymer reference interaction site model with a Yukawa closure. *Chemical Physics,* 93(7), p. 5315.

Yu, J. M., Huang, S. H. & Radosz, M., 1994. Phase behavior of reservoir fluids: VI. Cosolvent effects on bitumen fractionation with supercritical CO2. *Fluid Phase Equilibria,* Volume 93, pp. 353-362.

Yu, M. -L. & Chen, Y. -P., 1994. Correlation of liquid-liquid phase equilibria using the SAFT equation of state. *Fluid Phase Equilibria,* Volume 94, pp. 149-165.

Vitae

Name	Yousef A. Al-Sunni
Nationality	Saudi
Date of Birth	3rd July, 1990
Email	ys.7717@gmail.com
Address	Alkhobar, Eastern Province, Saudi Arabia
Academic Background	BSc Chemical Engineering, King Fahd University of Petroleum & Minerals, Dhahran, Saudi Arabia
Graduate Seminar	The role of various hard sphere theories on PVT behavior: Bifurcation and stability analysis, 11th November 2015